SIMULATING CHEMICAL REACTIONS OF GLASS POWDER IN CEMENT USING SILICA, CALCIUM HYDROXIDE AND SODIUM HYDROXIDE

SIMULATING CHEMICAL REACTIONS OF GLASS POWDER IN CEMENT USING SILICA, CALCIUM HYDROXIDE AND SODIUM HYDROXIDE

By SARAH YOUNG, B.ENG.

A Thesis Submitted to the School of Graduate Studies in Partial Fulfillment of the Requirements for the Degree Master of Applied Science

McMaster University

MASTER OF APPLIED SCIENCE (2013) McMaster University

(Civil Engineering) Hamilton, Ontario

TITLE: Simulating chemical reactions of glass powder in cement using silica, calcium hydroxide and sodium hydroxide

AUTHOR: Sarah Young, B.Eng. (McMaster University)

SUPERVISOR: Dr. Samir E. Chidiac, Ph.D., P.Eng

NUMBER OF PAGES: x, 100

Abstract

The use of supplementary cementitious materials (SCM) decreases the environmental impact of the cement industry. SCMs are commercial by-products that possess pozzolanic properties. Recycled glass powder, classified as a SCM, when added as a cement replacement reacts with the available lime in the cement to form calcium silicate hydrate (C-S-H) products. In contrast with other SCMs, glass is siliceous and thus the reaction can also cause alkali silica reaction (ASR) which causes expansion and cracking. This study was completed in order to characterize the chemical reactions and their rate using a simplified system that mimics glass particles in hardened cement paste.

Silica powder was added to solutions containing calcium hydroxide and/or sodium hydroxide. The rate of dissolution of the silica was monitored as well as the composition of the reaction products. Dissolution rates of silica with varying concentrations of silica, calcium hydroxide and sodium hydroxide, were fitted to the Hixson-Crowell cubic root law. The precipitate composition of the reaction product was represented by means of triaxial plots. It was found that silicate ions enter the solutions containing sodium hydroxide and containing both sodium hydroxide and calcium hydroxide. The rate is proportional to the quantity of sodium ions in the solution and to the pH. Also, higher concentrations of silica generally cause higher dissolution rates. The solutions with a pH of 13.48 and with lower silica concentrations created reaction products that were similar to C-S-H while the solutions with higher pH levels formed ASR after thirty days. The C-S-H prevented further dissolution of the silica. The formation of the ASR reaction products did not prevent further dissolution of the silica and they continued to dissolve until most of the silica had entered the solution.

Acknowledgements

First, I would like to thank my supervisor Dr. Samir Chidiac. His support encouraged me to continuously strive for excellence in my graduate student career.

Thank you to Lisa Federico who started me off on the right path and who provided a wealth of knowledge concerning glass in concrete. I also wish to thank the technicians with the Department of Civil Engineering, Kent Wheeler, Anna Robertson, Paul Heerema, and Peter Koudys. Their help and guidance helped make my experimental program possible. Thank you to the technicians with the Department of Materials Science and Engineering who helped me with my ICP-AES testing, Xiaogang Li and Doug Culley. Thank you to my fellow graduate students for their encouragement during my testing and writing. I would also like to thank the faculty and staff of the Civil Engineering Department at McMaster University.

I would like to thank the National Sciences and Engineering Research Council of Canada, the Ontario Graduate Scholarship Program and the Department of Civil Engineering at McMaster University for their funding.

Finally I would like to thank my friends and family for their continual encouragement. A very special thank you is extended to my parents, Anne and Doug Young, for their loving support and editing expertise.

Table of Contents

List of Figures

1 Introduction

1.1 Objective

The use of supplementary cementitious materials in concrete can add their beneficial properties to Portland cement. It is possible to use glass as an additive to cement, however adverse chemical reactions can occur. There have been numerous studies that have added ground recycled glass to concrete to monitor its expansion and to study its strength gain. These studies have provided recommendations for the particle size required to prevent deleterious expansion and to maximize strength. Noticeably, these recommendations vary greatly, partly due to different chemical compositions of the glasses used. These studies have not identified what is occurring on a chemical level.

The objective of this work is to study the chemical reactions that occur when glass reacts with concrete pore solution. The dissolution rate of silica particles will be quantified for varying pH and ion levels that mimic those found in concrete. Additionally, the reaction products from these different scenarios will be identified. This work will provide insight into the possible reactions that could occur when adding recycled glass particles into a concrete mix.

1.2 Outline

This work consists of six chapters, the first being this introduction.

The second chapter presents relevant literature. In this section, previous work is examined. The included earlier work encapsulates the following topics: the use of glass in concrete, the chemical reactions that occur in cement and finally the reactions that occur between glass and cement pore solution. This experimental work is placed in context of the previous research.

Chapter three covers the experimental method that was used in this study. The materials for the samples are detailed and the concentrations for each sample are listed. The procedure used for each portion of the experimental work conducted is outlined.

Chapter four presents the results obtained from testing the samples. The results are plotted against time and as a comparison between the samples for each testing time.

Chapter five is the discussion and analysis of these results. First, the dissolution of silica is modeled and discussed. Second, the compositions of the reaction products are presented.

Chapter six consists of the conclusions, where the results are summarized and recommendations are made for future work.

2 Literature Review

2.1 Introduction

Worldwide, the cement industry is known to have a massive environmental impact. The energy usage from cement production has been approximated to be from $8x10^{18}$ to $10x10^{18}$J per year (International Energy Agency, 2006). Additionally, the cement industry produces approximately 3% of all the world wide greenhouse gas emissions (World Business Council for Sustainable Development, 2002). The sources of the CO_2 are from the energy used to create cement and from the calcination of limestone (Romeo, Catalina, Lisbona, Lara, & Martínez, 2011). In 2010, it was found that for the production of clinker, the equivalent of 0.75kg of CO_2 was created for every kg of cement produced (Chen, Habert, Bouzidi, & Jullien). Large quantities of natural resources are also consumed in production. It takes approximately 1.53 kg of limestone and clay to make 1 kg of cement (Chen, Habert, Bouzidi, & Jullien, 2010). The substitution of a portion of the cement with an industrial by-product decreases the amount of new natural resources required as well as the quantity of greenhouse gasses released.

2.2 Cement Chemical Reactions

2.2.1 Portland Cement Hydration

Portland cement is formed from predominately limestone and clay as a source of silica and calcium. The raw materials are ground and heated in a kiln to produce cement clinker. Gypsum is added to the mix after heat treatment. The resulting Portland cement mix contains tricalcium silicate, beta-dicalcium silicate, calcium aluminate and ferroaluminate (Mehta & Monteiro, 2006). Portland cement is a hydraulic cement, meaning that only water needs to be added to the mix to form a hardened cement paste.

Once the cement has been mixed with water, the hydration reaction starts and multiple products are formed. The components in hardened Portland cement paste include calcium-silicate-hydrate, calcium hydroxide, ettringite and monosulfate. Calcium-silicate-hydrate (C-S-H) makes up approximately half of the material in the hardened cement paste. Its structure is irregular and the composition is approximately $C_3S_2H_3$, however it varies significantly (Mehta & Monteiro, 2006). The calcium hydroxide makes up around one fifth to one quarter of the material. It consists of $Ca(OH)_2$ in a crystal structure and is considerably weaker than the C-S-H. Finally, the aluminate

products form up to one fifth of the final material. They are the first to form and create the initial structure in the cement paste.

2.2.2 Pozzolanic Reaction

A pozzolanic reaction occurs when a siliceous material reacts with calcium hydroxide and water to form solid cement paste. In cement, the calcium hydroxide is available from the hydration of Portland cement. This reaction occurs at a slower rate than Portland cement hydration, thus strength gain will be more gradual when there are pozzolans present. The benefits of using pozzolanic materials include a finer pore structure and conversion of the calcium hydroxide in the paste to a C-S-H product (Mehta & Monteiro, 2006).

2.2.3 Alkali Silica Reaction

Alkali-silicate reaction (ASR) involves a reactive aggregate and the pore solution of concrete. It was first discussed by Thomas Stanton in the 1930's after a substantial quantity of structures had experienced deleterious expansion in southern California (Stanton, 1940). This expansion causes the concrete to crack. It has been found that the high pH of cement promotes the dissolution of silica contained in aggregates. The alkalis contained in the pore solution will then bond with the silica ions in the reactive particle, creating an ASR gel around the particle (Idir, Cyr, & Tagnit-Hamou, 2011). If the reacted layer cracks, more ions are able to easily reach aggregate that has not yet reacted and the ASR is able to continue (Mehta & Monteiro, 2006). If it does not crack, the layer of reaction product will decrease the diffusion rate of the ions, causing the reaction to slow. Expansive pressure can be created when the ions diffuse into the reacted product as well as when water is adsorbed (Chatterji, 2005). Enough pressure can develop to crack the aggregate and the surrounding paste. This reaction can readily occur in concrete containing glass particles as they mostly consist of silica.

ASR contains the same basic elements as C-S-H, however the ratios differ. The ASR gel has higher amounts of silica and alkalis. The composition of gel found in field samples was studied by Thaulow, Hjorth Jakobsen and Clark, their results are presented in Figure 2.1 (1996). In their specimens, the sodium content was between 10 and 25%. The ratio of calcium to silica was highly variable, with the silica content being mostly above 50% of the sample. Kawamura and Fuwa created concrete samples in a lab setting with reactive aggregate to study the composition of the resulting gel (2003). The ratio of CaO to SiO_2 for samples without any treatment ranged from 0.05 to 0.3. The alkali to silica ratio was then approximately 0.1 to 0.4. The amount of alkalis in these

samples is more variable than those found by Thaulow et al. Both of these studies found that the gel is composed of high amounts of silica.

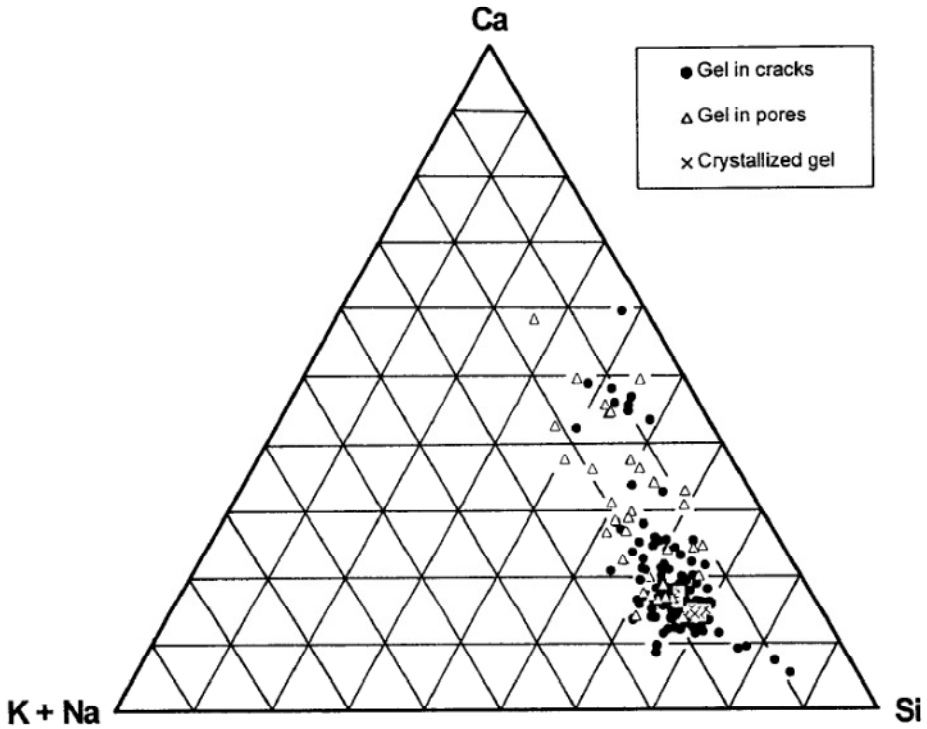

Figure 2.1: Composition of ASR in Field Samples (Thaulow, Hjorth Jakobsen, & Clark, 1996)

Mitigation of ASR can be achieved through several methods. Firstly, the use of reactive aggregate can be limited. Second, the alkali content of the cement to be used can be reduced. It has been recommended that the total amount of alkalis in the cement be limited to 3 kg/m^3 (Mehta & Monteiro, 2006). Adding pozzolanic material to the cement mix can reduce the quantity of alkalis and it also reacts with the silica to form non-expansive products. Finally, for alkali silica reaction to occur, water needs to be available to transport the ions in the solution. Keeping the concrete in a dry environment will prevent ASR from occurring.

2.3 Supplementary Cementing Material

Supplementary cementing materials (SCMs) are added to concrete as a replacement to cement. They can either be cementitious or pozzolanic. Commonly used materials include silica fume, ground granulated blast furnace slag and fly ash. SCMs add to the durability of cement as their additions lead to a finer pore structure. They also decrease the environmental impact by reducing the quantity of new natural resources required to produce Portland cement and adding waste by-products from other industries. Recycled glass has been studied for its use as a supplementary cementitious material (Federico & Chidiac, 2009). Unlike other SCMs, it requires significant energy to be imputed before it is suitable as it requires grinding to a specified fineness.

2.4 Recycled Glass

Glass is an amorphous solid that consists of inorganic elements (Paul, 1982). It is made by cooling a liquid faster than it is able to crystallize, forming an amorphous solid. Commonly, glass is made of silica and various impurities. The addition of chemical impurities into amorphous silica will decrease its resistance to chemical attack (De Jong, Beerkens, van Nijnatten, & Le Bourhis, 2011). The most common type of glass used is soda-lime glass; it contains soda, usually in the form of sodium carbonate, as a network modifier in the amorphous silica structure (Bray, 2001). Other important modifiers include aluminum oxide, boron trioxide, and lead oxide (De Jong, Beerkens, van Nijnatten, & Le Bourhis, 2011).

Waste glass has been studied as a cement and as a fine aggregate replacement by various researchers. Partially due to its fluctuating composition, mixed results have been reported concerning its reactivity. Researchers who have added glass as a replacement for fine aggregate have commonly experienced the deleterious effects of ASR. The specimens that have experienced ASR have expanded past ASTM test limits (Park & Lee, 2004), (Park, Lee, & Kim, 2004),(Dhir, Dyer, & Tang, 2009),(Idir, Cyr, & Tagnit-Hamou, 2010). These mixes would be unsuitable to use in an exposed environment. It was found that as the size of the glass particle increases, there is more expansion up until a pessimum point, and then the amount of expansion decreases (Rajabipour, Maraghechi, & Fisher, 2010). It has been successfully shown that when mixes contain reactive aggregate, such as glass, the addition of a pozzolan will decrease the amount of expansion (Dhir, Dyer, & Tang, 2009),(Idir, Cyr, & Tagnit-Hamou, 2010). Therefore, the use of this reactive glass is still possible if measures are taken to reduce the harmful reactions.

Researchers have also found glass to undergo a pozzolanic reaction when it has been ground to a fine enough powder (Shi, Wu, Riefler, & Wang, 2005); (Federico, Chidiac, & Raki, 2011); (Chidiac & Mihaljevic, 2011). Specimens that have undergone pozzolanic reaction have either experienced no additional expansion in comparison to control bars or a reduced amount of expansion (Ismail & Al-Hashmi, 2009). These mixes will have a higher strength than control mixes with an equivalent amount of inert filler material, indicating that a pozzolanic reaction has occurred (Idir, Cyr, & Tagnit-Hamou, 2011). Over time, the strength of the material increases at a rate similar or greater than that of fly ash (Shao, Lefort, Moras, & Rodriguez, 2000), (Schwarz & Neithalath, 2008). There has been some contradicting research regarding the conditions necessary for a pozzolanic reaction rather than ASR. From SEM images, some researchers have found that a pozzolanic reaction will occur on the surface of glass aggregate and then inside the cracks of the glass aggregate will have ASR (Maraghechi, Shafaatian, Fischer, & Rajabipour, 2012). Since there is uncertainty into the conditions required for ASR and pozzolanic reactions, the chemistry of these reactions will be examined.

2.5 Dissolution of silica

Alexander, Heston and Iler studied the dissolution of silica in water to determine its solubility at various pH levels (1954). They studied different types of amorphous silica and found the solubilities, presented in Figure 2.2, to be equal regardless of its initial form. For all solutions below pH=10.6, the silica in the solution is present in the form of monosilic acid.

Sjöberg explained the increasing quantity of soluble silica by examining the different species formed at various pH levels (1996). Below a pH of 8, the silica in solution is monosilicic acid. Above this level, the ions formed are increasingly more complex. The notation used to describe the bonding of silicon is Q^n; where n is the number of Si-Si bonds. For example, Q^0 indicates a monomer and Q^1 indicates a silicon atom at the end of a chain. From a pH of approximately 9.8 to 11, the silicon is mostly in the form of Q^4 ions. From pH 11 to 13.5, Q^3 is the predominant species. Cement will typically have a pH in this range, so this is the form of silicon that is expected to be present in the pore solution. Since the silicon has been converted from monosilicic acid to a more complex form, the monosilicic acid in the solution remains unsaturated, allowing the continued dissolution of the solid silica.

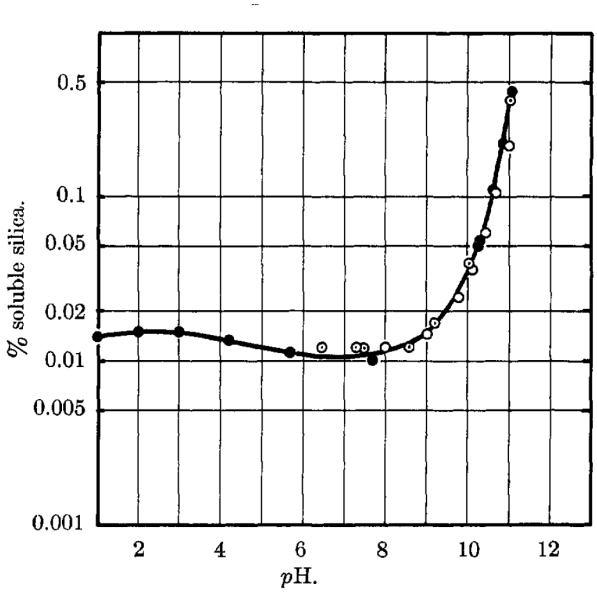

Figure 2.2: Solubility of Silica at Various pH Levels (Alexander, Heston, & Iler, 1954)

At pH values above 10.7, all amorphous silica is soluble (Iler, 1979, p. 47). The ionic Equation 2-1 is valid at all pH levels at 25°C; however, the silicate ion changes to other ionic species. The equilibrium equations for other silica species are in Equation 2-2 to Equation 2-5 (Iler, 1979, p. 136). Since the silica is converted into multiple species, there is continued dissolution of the amorphous silica. This condition is expected in concrete where the pH is typically 12.5 to 13.5 (Mehta & Monteiro, 2006).

$$[H_3SiO_4^-] = 1.85 \times 10^4 [Si(OH)_4][OH^-] \quad \textbf{Equation 2-1}$$

$$Si(OH)_4 + OH^- \leftrightarrows Si(OH)_3^- + H_2O \quad \textbf{Equation 2-2}$$

$$Si(OH)_4 + 2OH^- \leftrightarrows SiO_2(OH)_2^{2-} + 2H_2O \quad \textbf{Equation 2-3}$$

$$4Si(OH)_4 + 2OH^- \leftrightarrows Si_4O_4(OH)_6^{2-} + 6H_2O \quad \textbf{Equation 2-4}$$

$$4Si(OH)_4 + 4OH^- \leftrightarrows Si_4O_4(OH)_4^{4-} + 8H_2O \qquad \textbf{Equation 2-5}$$

The mechanism of dissolution proposed by Iler involves an anion catalyst to start the reaction (1979, pp. 62-63). In alkaline solutions, the catalyst is a hydroxide ion that is adsorbed onto the silica surface. The adsorbed hydroxyl ion increases the coordination number of the silicon ion; this weakens the strength of the bonds to the oxygen atoms. The silicon atom is then able to enter the solution as soluble silica. When the pH rises above 11, hydroxyl ions in the solution will also react with the silica, forming silicate ions. This keeps the solution unsaturated with respect to soluble silica.

Alkali ions can also act as catalysts for the dissolution (Dove & Rimstidt, 1994). The effects of sodium and potassium ions are very similar while lithium and magnesium are less effective catalysts. Additionally, the presence of salts in solutions will increase the dissolution rate of silica (Iler, 1979),(Wirth & Gieskes, 1978). Wirth and Gieskes found that both sodium chloride and magnesium chloride increased the dissolution rate of silica (1978). They concluded that it was the chlorine ion that had the catalytic effect on the reaction.

2.6 Reaction Models

The dissolution rate of silica in solution has been fit by many researchers to Equation 2-6 (O'Connor & Greenberg, 1958). In this equation, C is the concentration of monosilicic acid, S is the surface area and k_2 and C_e are rate constants.

$$\frac{dC}{dt} = k_2 S(C_e - C) \qquad \textbf{Equation 2-6}$$

At a high pH, the rate of dissolution is much greater than the rate of polymerization of silica. Therefore, Equation 2-6 is simplified to the Hixson-Crowell cubic root law given by Equation 2-7. This equation was initially developed by Hixson and Crowell to model the dissolution of particles in an agitated solution (1931). In this equation, the rate, k, is a function of the surface area. Assumptions include mostly spherical particles, dissolution in the direction normal to the surface and constant agitation.

$$[\mathrm{Si}]_{(s)}^{\frac{1}{3}} = [Si]_{initial}^{\frac{1}{3}} - kt \qquad \textbf{Equation 2-7}$$

This model only accounts for the dissolution and polymerization of silica and does not model any reactions occurring on the surface of the silica with other ions in the solution. This is accounted for in the model by Ichikawa and Miura (2007).

Ichikawa and Miura conducted an experimental study to determine what conditions will create expansive pressure which will crack glass aggregates (2007). Five millimetre diameter glass beads were dropped in aqueous solutions containing various concentrations of sodium hydroxide and calcium hydroxide. The method that resulted in cracked beads was a two day immersion in a sodium hydroxide solution, followed by three days in calcium hydroxide, then finally one day in sodium hydroxide. The researcher postulated that the sodium hydroxide solution first created a soft alkali silicate on the surface of the glass. When submerged in the calcium hydroxide, the outside layer is converted to a harder calcium alkali silicate. The sodium hydroxide then is able to penetrate through this layer while the silica diffusion out of the particle has been slowed. Expansive pressure is created which cracks the particle.

Ichikawa then developed a model to predict the expansive pressure using his experimental results (Ichikawa, 2009). The first portion of the model is the probability, p_r, that the particle will develop a reaction rim with a certain thickness, h_r, can withstand the accumulation of enough pressure that would be able to crack the particle. The thicknesses are assumed to follow a normal distribution.

$$p_r = 1 - \frac{1}{\sqrt{2\pi\sigma_r^2}} \int_{h_r}^{\infty} \exp\left[-\frac{1}{2}\left(\frac{(h-h_a)}{\sigma_r}\right)^2\right] dh$$

$$p_r \approx \begin{cases} 0 & for\ h_r \le h_a - 1.5\sigma_r \\ 0.5 + \dfrac{h_r - h_a}{3\sigma_r} & for\ h_a - 1.5\sigma_r \le h_r \le h_a + 1.5\sigma_r \\ 1 & for\ h_r \ge h_a + 1.5\sigma_r \end{cases} \qquad \textbf{Equation 2-8}$$

In Equation 2-8, h_a is the average thickness of the reaction rim and σ_r is the standard deviation of the rim thickness.

The model then estimates whether there is enough pressure to crack the particle. The probability, p_c, that the particle will crack is estimated with the following normal distribution.

$$p_c = 1 - \frac{1}{\sqrt{2\pi\sigma_c^2}} \int_{\frac{U_A}{\alpha U_S}}^{\infty} \exp\left[-\frac{1}{2}\left(\frac{(P - P_a)}{\sigma_c}\right)^2\right] dP$$

$$\approx \begin{cases} 0 & for\ U_A \leq (P_a - 1.5\sigma_c)\alpha U_S \\ 0.5 + \dfrac{U_A - \alpha U_S P_a}{3\sigma_c \alpha U_S} & for\ (P_a - 1.5\sigma_a)\sigma U_S \leq U_A \leq (P_a + 1.5\sigma_c)\alpha U_S \\ 1 & for\ U_A \geq (P_a + 1.5\sigma_c)\alpha U_S \end{cases} \quad \textbf{Equation 2-9}$$

Where U_S is the volume of the reacting aggregate, U_A is the volume that is converted to alkali-silicate, this volume is compressed to the volume, U. P is the expansive pressure, P_a, the average expansive pressure and σ_c is the standard deviation of the pressure. The term α is found using Equation 2-10, where κ_S is the compressibility of the aggregate, and ϵ is the reaction expansion ratio.

$$\alpha = \frac{\kappa_S}{\epsilon - 1} \quad \textbf{Equation 2-10}$$

Ichikawa's model then predicts the reaction rim thickness according to the concentrations of ions in the pore solutions.

2.7 Silica and sodium hydroxide solutions

Niibori, Kunita, Tochiyama and Chida studied the dissolution kinetics of silica in alkaline solutions with an initial pH of 13 (2000). Researchers mixed 100 milligrams of amorphous silica or 200 milligrams of silica scale in 500 millilitres of 0.1M sodium hydroxide. Figure 2.3 shows the dissolution rates at various temperatures. The researchers then fit a shrinking spherical model to the experimental results. The rate of dissolution at a certain time, or alternatively, the rate of change of concentration in the solution, is proportional to the surface area of the spherical particles. It was found that this model fit well with the dissolution rates at high temperatures, whereas it deviated at low temperatures.

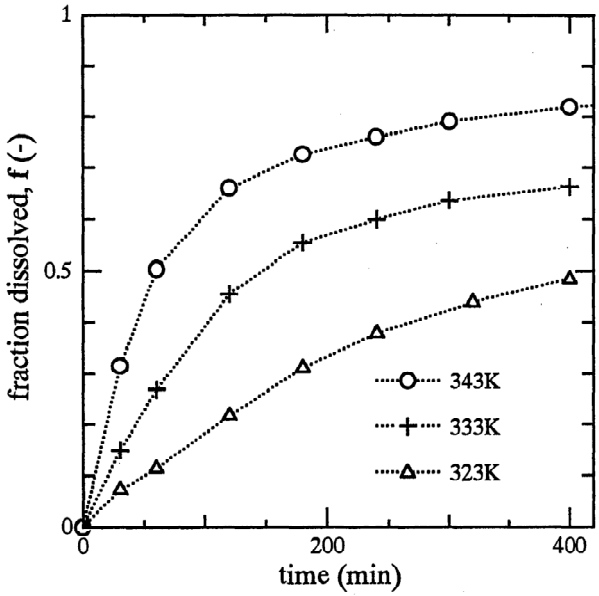

Figure 2.3: Dissolution of amorphous silica in sodium hydroxide (Niibori, Kunita, Tochiyama, & Chida, 2000)

Dron and Brivot studied solutions containing silica in the form of opal and sodium hydroxide (Dron & Brivot, 1993). The initial portion of their study concerned the dissolution rate of the opal in a sodium hydroxide solution, shown in Figure 2.4. Dron and Brivot mixed 25ml of solution with 10g of opal. The equilibrium concentration reached was equal to the initial concentration of sodium hydroxide, indicating that the limiting reagent in this study was the sodium hydroxide. The authors were not certain if the initial portion of the curve before one hour was a result of the solution heating to the desired temperature or another phenomenon.

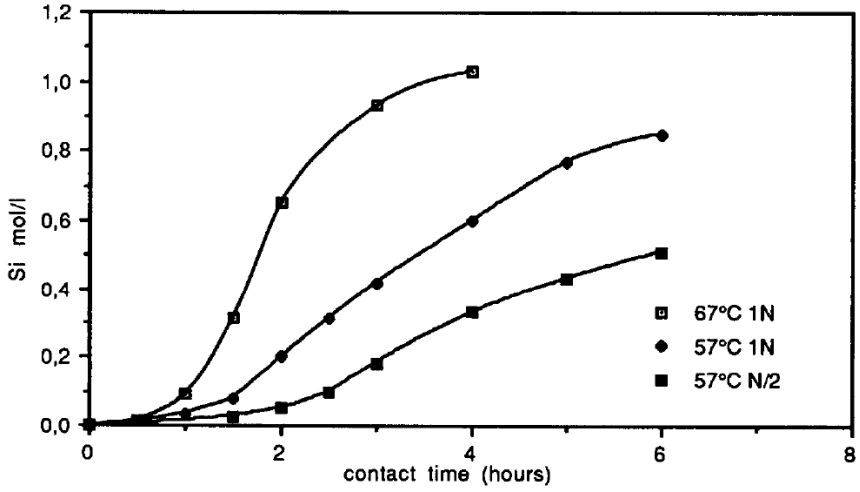

Figure 2.4: Dissolution of Opal in a Sodium Hydroxide Solution (Dron & Brivot, 1993)

Greenberg studied the factors impacting the dissolution of silica in sodium hydroxide solutions (1957). Holding all variables constant, adding more silica to a solution of sodium hydroxide will increase the rate of reaction. This agrees with other findings that an increase in surface area results in a faster reaction. Greenberg also found an increase in pH will cause the silica to react faster. Finally, they investigated the impacts of stirring and temperature. As expected, a temperature increase and stirring will cause a faster reaction.

2.8 Silica and Lime Solutions

The reaction between silica and calcium hydroxide involves the dissolution of silica and then a reaction between the silicon ions and calcium hydroxide to form calcium silicate hydrate products (Greenberg, 1961). One of the earliest studies on this system was conducted by Shaw and MacIntire (1930). They found the speed of the reaction increased with smaller particles, due to increasing the surface area. Additionally, when calcium chloride was added to the solutions, more calcium reacted with the silica in the solution. This is evidence of chlorine ions having a catalytic effect on the dissolution of silica as stated by Wirth and Gieskes (1978). Greenberg also investigated the rates of reaction between silica and calcium hydroxide solutions (1961). It was determined that the rate determining step in the reaction was the dissolution of silica. As a result of this conclusion, it was found that the rate of reaction was proportional to the quantity of

silica added to the solution. In the range that was studied, the quantity of calcium hydroxide did not impact the reaction rate.

Barret, Ménétrier and Cottin studied solutions containing silica and lime (1977). One gram of silica was combined with one litre of calcium hydroxide solutions of varying concentrations. The solutions were measured at various points to understand the progression of the reaction. The solutions were filtered and the solids were measured by atomic adsorption spectrophotometry. Barret et al. also used varying initial concentrations of lime. The lime in the solutions reached their equilibrium points at approximately 5 days. The solutions with less initial lime reached equilibrium faster. The silica in the solution reached its equilibrium point slightly after the lime. Barret et al. observed that in this specific scenario, the silica enters the solution faster than the lime precipitates, indicating the dissolution of silica is occurring at a faster rate than the precipitation of silica-lime products.

El-Shimy, Abo-El-Enein, El-Didamony and Osman investigated systems containing lime and silica fume at C/S ratios of 0.8 to 2.0 (2000). Due to the large surface area of silica fume, the silica reacted rapidly with the calcium in the solution. After a short period, a reacted rim formed around the grains of silica fume. These reaction rims are similar to those that have been modeled by Ichikawa (2009).

2.9 Calcium, Sodium and Silica Solutions

Systems with calcium hydroxide, sodium hydroxide and silica have been studied with the purpose of creating synthetic C-S-H and studying alkali silica reaction. The solutions had varying calcium to silica ratios depending whether the goal was to study the formation of C-S-H or ASR.

Solutions containing both calcium hydroxide and sodium hydroxide reacting with silica will have both the effects of the two component systems competing and forming new products. The silica will be dissolving readily due to the high pH of system and the catalytic effects of the sodium and the silica ions will be available to react with the calcium and sodium ions in the solution. Due to the interaction of the sodium hydroxide and the calcium hydroxide in the solution, the solubility of calcium hydroxide is repressed. The solubility of calcium hydroxide is determined from the solubility product in Equation 2-11, where $\gamma_{\pm}$ is the mean activity coefficient. Including the activity coefficient increases the accuracy of solutions with high ionic strengths.

$$K_{sp} = [Ca^{2+}][OH^-]^2\gamma_{\pm}$$ (Wright, 2007) **Equation 2-11**

The mean activity coefficient may be found by using Equation 2-12. The equation is derived from Debye-Hückel theory. In this equation, A and B are constants which depend on the solvent and the temperature, I is the ionic strength of the solution, z is charge on the ions in the solution and bI is a linear term to account for an increase of solubility when the solution has a higher ionic strength.

$$\log\gamma_{\pm} = -A|z_+z_-|\frac{\sqrt{I}}{1 + B\mathring{a}\sqrt{I}} + bI$$ (Wright, 2007) **Equation 2-12**

The concentration of hydroxide in Equation 2-11 is equal to the total concentration in the solution rather than the hydroxide originating from the calcium hydroxide. Since there is hydroxide originating from both sodium hydroxide and calcium hydroxide, Equation 2-11 can be transformed to Equation 2-13.

$$K_{sp} = [Ca^{2+}]([OH^-]_{Na} + [OH^-]_{Ca})^2\gamma_{\pm}$$ **Equation 2-13**

In this equation, the subscripts indicate whether the hydroxide ion originated from the sodium hydroxide or the calcium hydroxide. Since the presence of sodium hydroxide suppresses the solubility of the calcium hydroxide, it can be assumed that the calcium hydroxide is saturated. The ions in the solution are in equilibrium with the solid calcium hydroxide according to Equation 2-14**.**

$$Ca(OH)_{2(s)} \leftrightarrows Ca^{2+}_{(aq)} + 2OH^-_{(aq)}$$ **Equation 2-14**

From Equation 2-14, it can be seen that the amount of calcium ions in the solution is half that of the hydroxyl ions from the calcium hydroxide, shown in Equation 2-15.

$$2[Ca^{2+}] = [OH^-]_{Ca}$$ **Equation 2-15**

Substituting Equation 2-15 into Equation 2-13 gives the following:

$$K_{sp} = \frac{1}{2}[OH^-]_{Ca}\{[OH^-]_{Na} + [OH^-]_{Ca}\}^2\gamma_{\pm} \qquad \textbf{Equation 2-16}$$

Expanding the formula gives the following cubic function.

$$K_{sp} = \left\{\frac{1}{2}[OH^-]_{Ca}^3 + [OH^-]_{Na}[OH^-]_{Ca}^2 + \frac{1}{2}[OH^-]_{Na}^2[OH^-]_{Ca}\right\}\gamma_{\pm} \qquad \textbf{Equation 2-17}$$

There is one real root of Equation 2-17 and it is given by Equation 2-18.

$$[\mathrm{OH^-}]_{\mathrm{Ca}} = \frac{\left([\mathrm{OH^-}]_{\mathrm{Na}} - 3\times\left(\frac{\mathrm{K_{sp}}}{\gamma_{\pm}} + \frac{[\mathrm{OH^-}]_{\mathrm{Na}}^3}{27} + \left(\frac{\mathrm{K_{sp}}^2}{\gamma_{\pm}} + \frac{2\times\mathrm{K_{sp}}\times[\mathrm{OH^-}]_{\mathrm{Na}}^3}{27\gamma_{\pm}}\right)^{\frac{1}{2}}\right)^{\frac{1}{3}}\right)^2}{9\times\left(\frac{\mathrm{K_{sp}}}{\gamma_{\pm}} + \frac{[\mathrm{OH^-}]_{\mathrm{Na}}^3}{27} + \left(\frac{\mathrm{K_{sp}}^2}{\gamma_{\pm}} + \frac{2\times\mathrm{K_{sp}}\times[\mathrm{OH^-}]_{\mathrm{Na}}^3}{27\gamma_{\pm}}\right)^{\frac{1}{2}}\right)^{\frac{1}{3}}} \qquad \textbf{Equation 2-18}$$

Therefore, the concentration of calcium ions in the solution in terms of the concentration of sodium ions and the solubility product of calcium hydroxide is given in Equation 2-19.

$$[\mathrm{Ca^{2+}}] = \frac{\left([\mathrm{Na^+}] - 3\times\left(\frac{\mathrm{K_{sp}}}{\gamma_{\pm}} + \frac{[\mathrm{Na^+}]^3}{27} + \left(\frac{\mathrm{K_{sp}}^2}{\gamma_{\pm}} + \frac{2\times\mathrm{K_{sp}}\times[\mathrm{Na^+}]^3}{27\gamma_{\pm}}\right)^{\frac{1}{2}}\right)^{\frac{1}{3}}\right)^2}{18\times\left(\frac{\mathrm{K_{sp}}}{\gamma_{\pm}} + \frac{[\mathrm{Na^+}]^3}{27} + \left(\frac{\mathrm{K_{sp}}^2}{\gamma_{\pm}} + \frac{2\times\mathrm{K_{sp}}\times[\mathrm{Na^+}]^3}{27\gamma_{\pm}}\right)^{\frac{1}{2}}\right)^{\frac{1}{3}}} \qquad \textbf{Equation 2-19}$$

Given Ksp=9.04x10^{-6} and $\gamma_{\pm}$=0.647, the expected concentration of calcium hydroxide in the solution is shown in Figure 2.5 (Greenberg & Copeland, 1960).

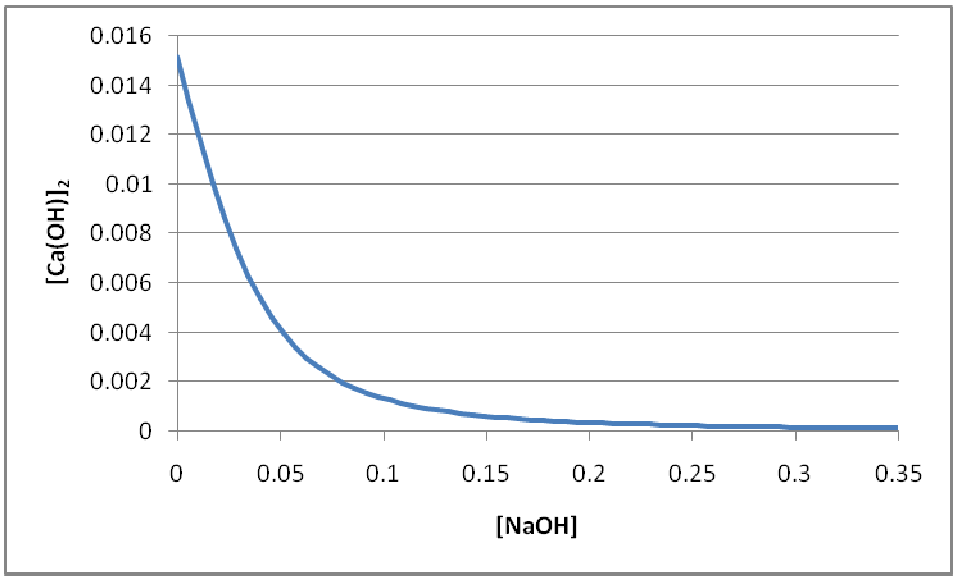

Figure 2.5: Calcium hydroxide concentration given sodium hydroxide concentration, 25°C

Diamond studied pore solutions of cements and compared the actual ion concentrations with those calculated with Debye-Hückel theory equations (1975). He determined during the first two to three months that the calcium concentration in the cement was extremely similar to the theoretical calculations. This demonstrates that these equations are valid for estimating concrete ion concentrations. However, after this time span, the calcium disappeared from the pore solution when theoretically it should have still been present. Diamond hypothesized that a reacted layer had formed over the calcium hydroxide in the cement, preventing further dissolution.

Way and Shayan investigated alkali calcium silicates to further understand the structure of the products from alkali silica reaction (1992). They mixed solutions of sodium hydroxide and silica with lime. The initial ratios of calcium to silica ranged from 0.116 to 1.81. Once mixed, the solutions were agitated for 2 hours and then shaken once each day. After four weeks, the solutions were analyzed by the gravimetric method and by x-ray diffraction. Solutions were also created with calcium hydroxide instead of lime and there were no significant changes to the results. Solutions that initially contained a C/S ratio up to 1.17 produced precipitate with higher ratios, indicating that more of the calcium was dissolved into the solution. Above this ratio, the precipitate had approximately the same C/S ratio as the initial ratio. This study did not include any time dependent findings.

Kalousek studied the products formed when a sodium silicate solution was mixed with sodium hydroxide, calcium hydroxide and distilled water (1944). The samples were shaken for the first few hours after they were mixed and then once per day afterwards. They were tested at random intervals from two weeks up to eighteen weeks. Kalousek observed that there were no visible changes in the solutions up to the time they were tested. Several methods of testing the solutions were utilized to find the concentrations of the various components. The concentration of calcium hydroxide was found using a gravimetric method. The sodium oxide concentration was found by titrating the solution with hydrochloric acid and calculations were conducted to account for the calcium hydroxide that was neutralized as well. Finally, the solutions were dehydrated by using hydrochloric acid and then the resulting solids were burned and reacted with hydrofluoric acid. The weight loss from the process was considered silica. The concentrations found in the solutions are presented in Figure 2.6. The variation from the fitted line is due to testing the solutions at various ages. The line has been fitted best to solutions that were four weeks old. The composition of the precipitates is shown in Figure 2.7. It can be observed that for solutions that contained above approximately 25g/L of sodium oxide, the ratio of sodium to silica is constant. The same conclusion was drawn concerning the ratio of calcium to silica; however, there does not appear to be sufficient data points to draw a definite conclusion regarding the trend. Kalousek varied the quantity of silica in the solution while holding the concentration of sodium oxide constant. The observed changes in the solutions were not greater than the errors produced by preparation of the samples, thus no conclusions can be drawn from the data.

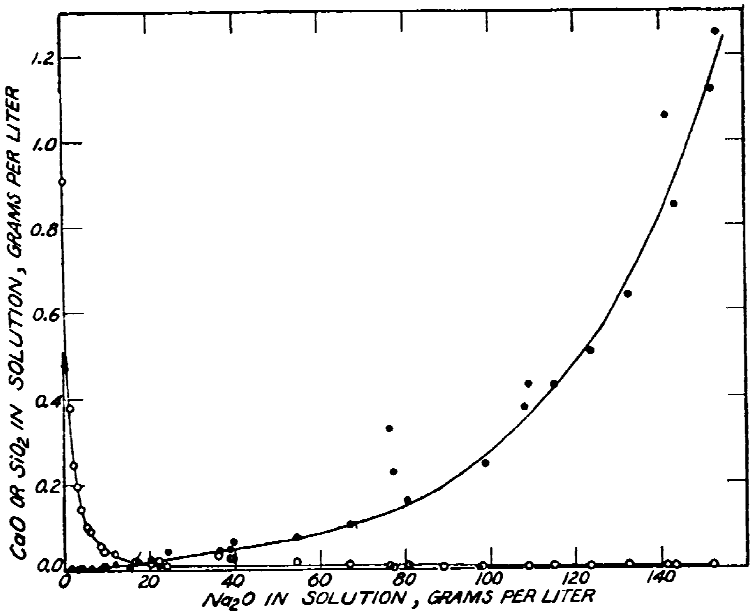

Figure 2.6: Concentration of Chemicals at Various Na_2O Concentrations. ∘ = SiO2, • = CaO (Kalousek, 1944)

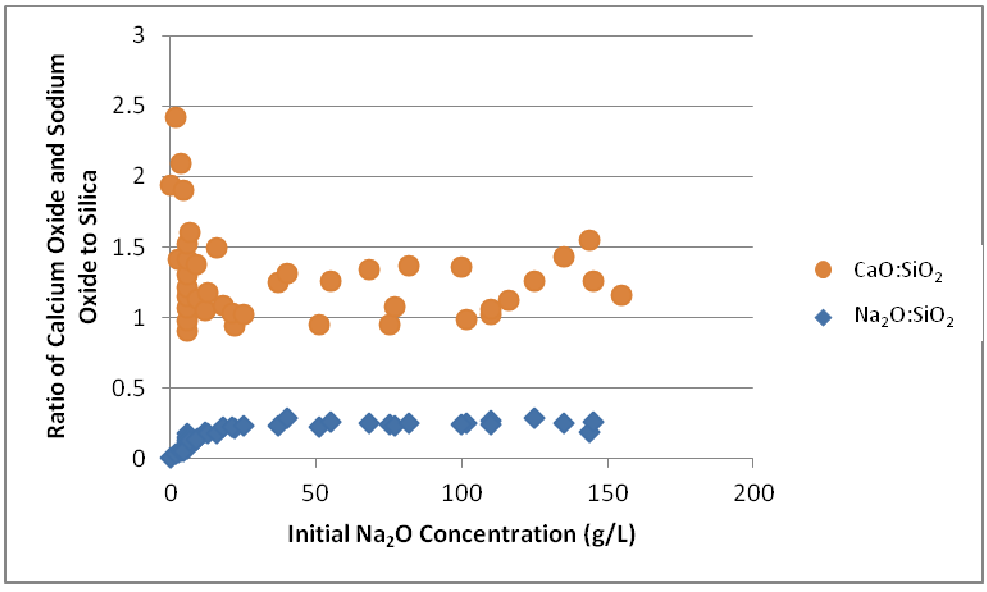

Figure 2.7: Composition of Precipitate at Various Initial Na_2O Concentrations with Oversaturated Calcium Oxide and Silica. (Kalousek, 1944)

Macphee, Luke, Glasser and Lachowski studied solutions containing calcium oxide, soda gels, sodium hydroxide and silicic acid (1989). The initial compositions contained

C/S ratios from 1 to 1.9 and sodium hydroxide concentrations from 0.25M to 0.8M. The solutions were mixed in an atmosphere without carbon dioxide. They were shaken for one week following mixing and then at intervals thereafter. The solutions were analyzed by using flame emission spectroscopy, the automated colorimetric method, and pH measurements. Some of the results from solutions are presented in Figure 2.8 and Figure 2.9. The solid lines indicate the best fit lines when analyzing a system with silicic acid, calcium oxide and sodium hydroxide while the dashed best fit line is for systems created with C_3S. Over time, both the quantity of calcium ions and silicon ions in the solution decreased, indicating solids forming. The molar ratios in the synthetic C-S-H formed are presented in Figure 2.10 and Figure 2.11. The best fit lines are for each initial ratio of C/S. The fitted lines range from initial C/S ratio of 1 to 1.9. The solutions with lower C/S ratios have precipitate compositions very similar to the initial ones. As the initial C/S ratio increases, the precipitate composition increasingly becomes lower than the initial ratio. By comparing Figure 2.10 and Figure 2.11, it can be observed that the precipitate composition over time is highly dependent on the initial concentration of sodium hydroxide. The precipitates formed in [NaOH]=0.25M change significantly over the course of the testing period while those in [NaOH]=0.8M experience very little changes.

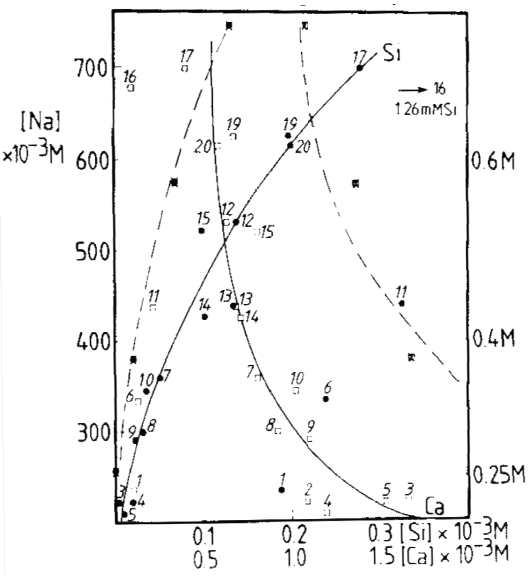

Figure 2.8: Ion Concentrations in Solutions at 2 Weeks(Macphee, Luke, Glasser, & Lachowski, 1989)

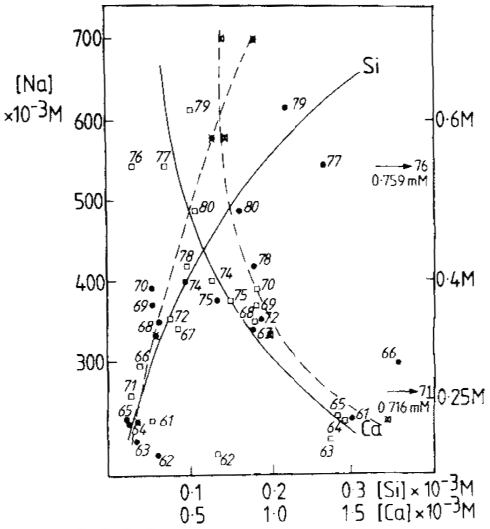

Figure 2.9: Ion Concentrations in Solutions at 6 Months(Macphee, Luke, Glasser, & Lachowski, 1989)

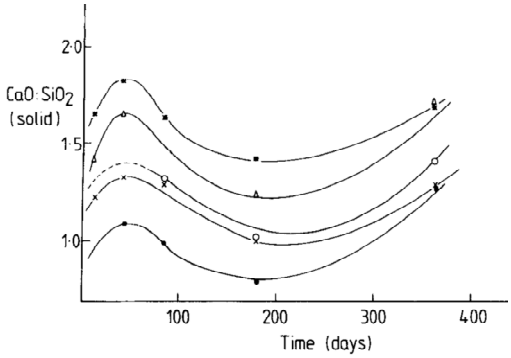

Figure 2.10: Precipitate Composition, initial [NaOH]=0.25M(Macphee, Luke, Glasser, & Lachowski, 1989)

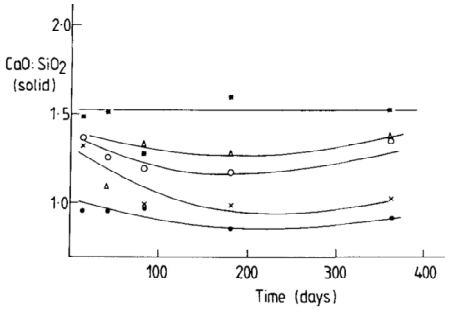

Figure 2.11: Precipitate Composition, initial [NaOH]=0.8M(Macphee, Luke, Glasser, & Lachowski, 1989)

Leemann, Saout, Winnefeld, Rentsch and Lothenbach studied the conditions required to develop an alkali silica reaction by creating a synthetic pore solution, silica fume and portlandite (2011). 1M sodium hydroxide or potassium hydroxide was mixed with the microsilica and the portlandite at a solid to liquid ratio at 1:2. The ratio of calcium hydroxide to silica ranged from 0:1 to 0.58:1. The samples were mixed for 6 days and then were placed in a desiccator at a high relative humidity to promote the formation of ASR products. It was found that the addition of portlandite slowed the dissolution of silica, but allowed more to dissolve over time. The concentration of silica and calcium remained low in the solution while C-S-H was being formed. Once all of the calcium was consumed, the solution's silica concentration increased. This was accompanied by a gradual loss of alkali from the solution.

2.10 Alkali Glass Systems

Kouassi, Andji, Bonnet and Rossignol studied the dissolution of glass in highly alkaline solutions with the goal of understanding the behaviour of glass in concrete (2010). Two grams of crushed recycled glass was added to thirty millilitres of 0.5M to 5M alkaline solutions and placed into an oven to accelerate the reaction. Samples were removed at various times and an ICP-AES analysis was conducted to determine the contents of the solutions. TGA analysis was carried out as well as SEM. Finally, IR analysis was performed. The recycled glass mostly consisted of silica, sodium oxide and calcium oxide.

As expected, it was found that the smaller particles dissolved the fastest. Additionally, when the concentration of the alkali solution was increased, the dissolution rate of the glass increased slightly. This effect can be seen in Figure 2.12. Kouassi et al.

identified the three distinct stages of the dissolution of glass, the first is while the solution remains unsaturated, next, there is dissolution and precipitation because the solution has become saturated and finally the last stage is when a reaction layer has developed on the surface of the glass.

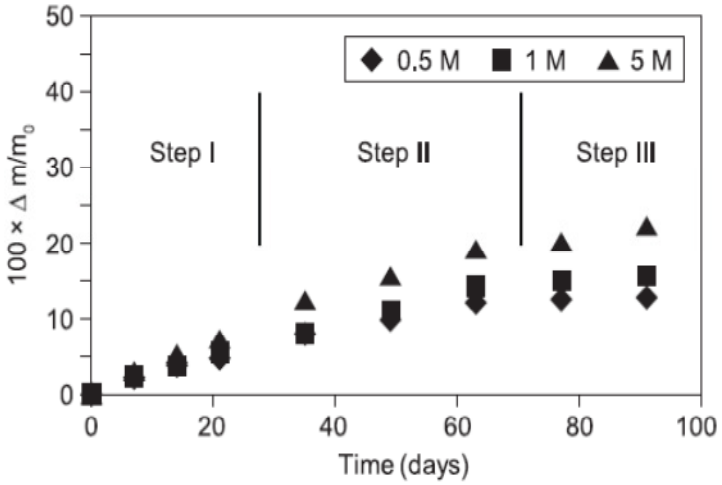

Figure 2.12: The dissolution of a glass in various concentrations of alkali solution (Kouassi, Andji, Bonnet, & Rossignol, 2010)

2.11 Thermo Gravimetric Analysis

Kim, Foley and Reda Taha created synthetic calcium silicate hydrate samples from solutions of sodium metasilicate, commonly known as waterglass, and calcium oxide (2013). The samples were dried to eleven percent relative humidity and then tested with thermo gravimetric analysis (TGA) to determine the percentage of calcium hydroxide, calcium carbonate and calcium silicate hydrate in the specimens. The samples were heated to 1000 degrees Celsius by 10 degrees per minute. The initial weight was taken at 145 degrees to exclude any absorbed water. The weight loss between 145 and 350 degrees Celsius was assumed to be loss of water from C-S-H. Between 350 and 500 degrees Celsius, the weight loss was due to the dehydration of the calcium hydroxide. Finally, the weight loss between 600 and 825 degrees Celsius was assumed to be due to the loss of carbon dioxide from calcium carbonate.

Zhang and Ye studied the dehydration of cement paste up to 1000 degrees Celsius (Zhang & Ye, 2012). They varied the heating rates from 1 to 30 degrees Celsius per minute. It was found that the dehydration of calcium hydroxide occurred between 400

and 550 degrees Celsius. Above 600 degrees, the rate of weight loss increases which corresponds to Kim et al.'s loss of carbon dioxide in the calcium carbonate (Kim, Foley, & Reda Taha, 2013). However, Zhang and Ye neglected analysis of this phase even though the loss of carbon dioxide from calcium carbonate consisted of approximately two percent of their sample. From their study of varying the heating rates, it is shown that a higher heating rate causes compounds to decompose at higher temperatures than if the heating rate was slow. The rate of mass loss per degree Celsius was lower when the samples were heated faster.

Jain and Neithalath studied the changes to porosity due to calcium leaching in cement and used TGA analysis to identify the quantities of calcium hydroxide and C-S-H in their system (2009). They identified the weight drop associated with calcium hydroxide dehydration to be between 400 and 450 degrees Celsius. The amount of calcium hydroxide in the mix was then calculated using Equation 2-20.

$$CH\% = WL_{CH}(\%) \times \frac{MW_{CH}}{MW_H} \quad \text{(Jain \& Neithalath, 2009)} \quad \textbf{Equation 2-20}$$

Where WL_{CH} is the weight loss of dehydrating calcium hydroxide, MW_{CH} is the molecular weight of calcium hydroxide and MW_H is the molecular weight of water. This equation was derived from the dehydration equilibrium of calcium hydroxide.

$$Ca(OH)_{2\,(S)} \xrightarrow{Heat} CaO_{(S)} + H_2O_{(g)} \quad \textbf{Equation 2-21}$$

2.12 Summary

A review of C-S-H and ASR formation has been presented in this chapter. C-S-H is a main component of hardened cement paste and is a strong and durable solid. ASR is a product of silica, alkalis and some calcium hydroxide. It is a gel that forms in the hardened cement paste that is able to expand when exposed to liquid and crack the concrete. This leads to safety and durability issues and should be prevented when concrete will be exposed to wet environments.

When using ground glass in concrete, the particles will undergo either a pozzolanic reaction or an alkali-silica reaction. Previous work has focused on how the size of particle will impact the expansiveness of the resulting product. It has been found that a pessimum size will create the largest expansion, sizes above and below will create a less

expansive product. Since there is a large amount of variability in the chemistry in these tests, there has not been a definite agreement as to what size of glass is required to produce a concrete product that will not expand. Thus the chemistry of the reactions between silica, sodium hydroxide and calcium hydroxide were examined.

Systems containing sodium hydroxide and silica will result in the silica dissolving at a rate proportional to the surface area of the silica particles. The sodium in the solution acts as a catalyst to the reaction and will result in faster dissolution compared to solutions without alkalis. The dissolution fits with the Hixson-Crowell cubic root law at elevated temperatures and deviates slightly at room temperature. At an elevated pH, like that found in concrete, the solubility of silica is greatly increased and it will continue to dissolve until all the solids have been converted to aqueous silicate ions.

Calcium hydroxide and silica will create calcium silicate products. The silica will dissolve into solution and react with the aqueous calcium. The rate of this reaction is determined by the dissolution of the silica. Eventually, reaction rims of calcium silicate can form on the surface of the silica. This will slow the reaction until equilibrium has been reached.

The system with calcium hydroxide, sodium hydroxide and silica is able to form products similar to C-S-H and to ASR. Due to the common hydroxide ion, the calcium hydroxide is kept saturated in these solutions. Silica will dissolve and can react with the sodium and calcium ions in the solution. Once it has reacted with some of the calcium, further dissolution of calcium occurs. Depending on the initial concentrations, and ASR product or a C-S-H product can be formed. The rates of reaction depend on the energy imputed into the system. These have been varied by changing the temperature of the solutions and the amount of agitation reaction vessels experience.

The method of Thermo Gravimetric Analysis was examined when researchers have used products with calcium hydroxide and calcium carbonate. The heating rate impacts the temperature at which compounds will decompose. In general, calcium hydroxide will decompose between 350 and 550 degrees Celsius and calcium carbonate will decompose above 650 degrees Celsius. From this, researchers are able to calculate the quantity of these substances that is present in their specimens.

Further research into the chemical reactions involved between glass and cement is needed to characterize the rate of silica dissolution and precipitation of solids and

product formed. This will aid in determining which mixes will create an expansive product due to ASR and which ones will have a pozzolanic reaction.

3 Experimental Program

The experimental program developed for this study includes the selection and characterization of the materials, the mixing and handling procedure adapted, and testing methods. Chemical reactions were monitored with time through changes in the pH values, and by testing the composition of the liquid and solid products using ICP-AES (inductively coupled plasma atomic emission spectroscopy) and Thermal Gravimetric Analysis (TGA), respectively. All of the experiments were conducted at room temperature.

3.1 Materials

The samples were created from stock solutions and powders. The sodium hydroxide stock solution was a 1N solution from EDM Millipore Corporation (EDM Millipore, 2013). Amorphous fumed silicon (IV) oxide from Alfa Aesar was used for the silica; its purity was 99.5% and passed a 400 mesh (Alfa Aesar, 2013). Finally, two different bottles of calcium hydroxide were used. The first was used for some of the calcium and silica reactions and was calcium hydroxide powder from EDM. Since this container was older, it had experienced partial carbonation and it contained 85% calcium hydroxide by mass. Initial concentrations presented in this work reflect the real quantity of calcium hydroxide contained in the samples. The second container of calcium hydroxide was also from EDM and had not experienced carbonation (EDM Millipore, 2013). The water used to mix the samples had undergone reverse osmosis (R.O.) filtration. The water used to create the calibration standards for the ICP-AES testing was filtered by a Milli-Q Integral filter. The reaction bottles were 30mL Thermo Scientific Nalgene Wide-Mouth Economy Bottles made with high-density polyethylene (HDPE).

3.2 Experimental Procedure

3.2.1 Mixture Composition

The concentrations of the samples were designed to represent the pore solution of cement. The corresponding pH range of the sodium hydroxide was 13.4 to 13.7 in order to represent the alkali concentration found in concrete.

The initial concentrations for the samples were divided into three groups, $Ca(OH)_2$ +SiO_2, NaOH + SiO_2 and NaOH + $Ca(OH)_2$ + SiO_2 as shown in Table 3.1. Abbreviation used in labeling is "CLSL" when "C" corresponds to Ca, "S" to Si, and "L" low concentrations. Terms "M" and "H" are used to represent medium and high concentrations respectively.

Table 3.1: Concentrations of NaOH, $Ca(OH)_2$, and SiO_2 used for the experimental program (M)

Group #	Sample #	$[Ca(OH)_2]$	[NaOH]	$[SiO_2]$	pH
1	CLSL	0.013	0	0.0016	12.41
	CLSM	0.013	0	0.02	12.41
	CLSH	0.015	0	0.10	12.48
	CMSL	0.023	0	0.0016	12.66
	CMSM	0.023	0	0.02	12.66
	CMSH1	0.023	0	0.10	12.66
	CMSH2	0.021	0	0.134	12.62
	CMSH3	0.023	0	0.153	12.66
	CHSL	0.045	0	0.0016	12.66
	CHSM	0.045	0	0.02	12.66
	CHSH	0.045	0	0.10	12.66
2	NLSL	0	0.30	0.115	13.48
	NLSM	0	0.30	0.134	13.48
	NLSH	0	0.30	0.153	13.48
	NMSL	0	0.42	0.134	13.62
	NMSM	0	0.42	0.153	13.62
	NMSH	0	0.42	0.165	13.62
	NHSL	0	0.53	0.153	13.72
	NHSM	0	0.53	0.165	13.72
	NHSH	0	0.53	0.180	13.72
3	CNLSL	0.023	0.30	0.115	13.48
	CNLSM	0.023	0.30	0.134	13.48
	CNLSH	0.023	0.30	0.153	13.48
	CNMSL	0.023	0.42	0.134	13.62
	CNMSM	0.023	0.42	0.153	13.62
	CNMSH	0.023	0.42	0.165	13.62
	CNHSL	0.023	0.53	0.153	13.72
	CNHSM	0.023	0.53	0.165	13.72
	CNHSH	0.023	0.53	0.180	13.72

3.2.2 Mixing Procedure

Eight samples of each composition were created for testing at 12 hours, 1 day, 4 days, 7 days, 14 days, 30 days, 92 days and one for pH measurements. The samples were prepared by first weighing the required quantity of silica and then, if needed the calcium hydroxide into the 30mL reaction bottles, shown in Figure 3.1. In a glove bag that contained a nitrogen atmosphere as seen in Figure 3.2, the R.O. water was added via an automatic pipette. Subsequently, the appropriate quantity of sodium hydroxide was added to the solution with the automatic pipette, Figure 3.3. The reaction bottles

were tightly closed then removed from the glove bag and vigorously shaken by hand to dissolve the calcium hydroxide. The bottles containing the mixed solutions were placed onto rollers, Figure 3.4, which kept the solutions rotating at a rate of approximately 0.92 rpm until they were tested. The purpose of the rollers was to prevent the solids from settling and to ensure all of the solids were reacting. The samples were kept at constant room temperature.

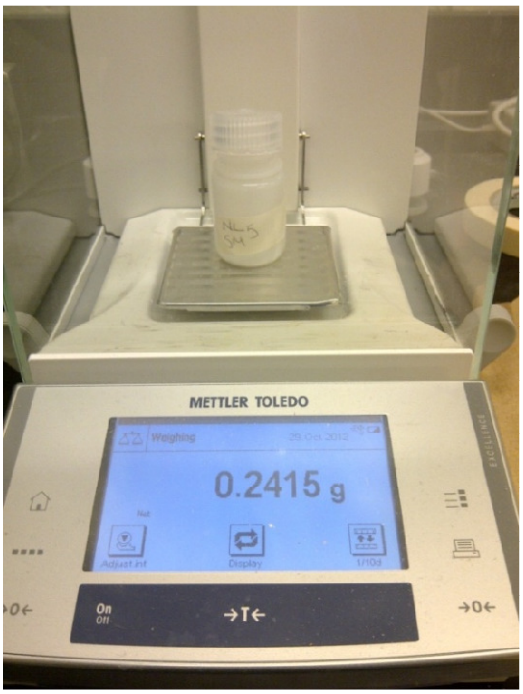

Figure 3.1: Electronic scale with ±0.0001g accuracy used to weigh the powder

Figure 3.2: Glove bag with N_2 to mitigate contamination

Figure 3.3: Additions of liquids, R.O. water and NaOH to reaction bottle inside the glove bag

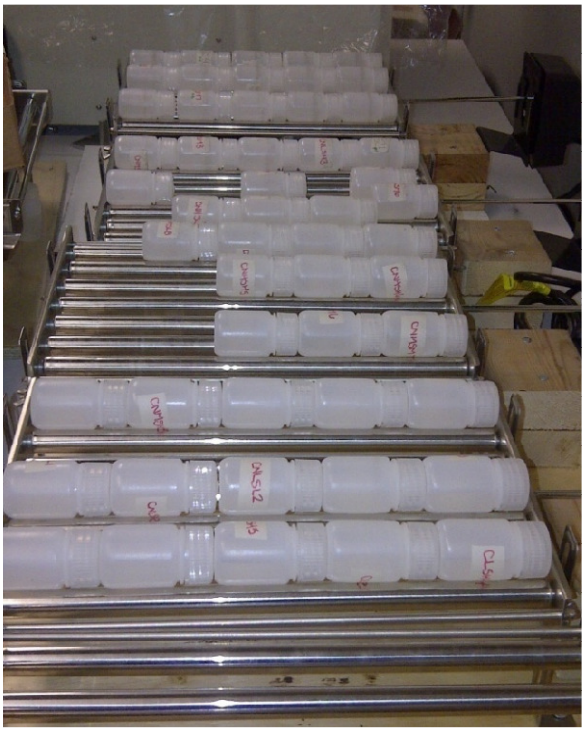

Figure 3.4: Rollers used for continuous mixing of samples

At the specified time, the solutions were filtered by gravimetric filtration under a nitrogen atmosphere, Figure 3.5. The separated solids were left to dry in the glove bag under a nitrogen atmosphere. While the solutions were filtering, a different container containing the same solution was used to test for the solution's pH. The filtered solutions and solids were then stored in sealed reaction bottles until they were tested.

Figure 3.5: Sample being filtered

3.3 Testing

3.3.1 pH Values

The progression of the pH in the various solutions was measured using, one of the eight samples for each mixture. When using normal pH electrodes, sodium in the solution can be confused with the hydrogen ions; leading to large errors in the pH readings. Therefore, an electrode tailor made for measuring pH in high sodium environments was selected. The Oakton pH electrode is shown in Figure 3.6 (Cole-Parmer Canada Inc., 2012). Amber glass was used to minimize the sodium error. The voltage was measured by the Thermo Scientific Orion Star A211 pH Benchtop Meter. Its accuracy is to ±0.002 pH or to ±0.2 mV (Cole-Parmer Canada Inc., 2012).

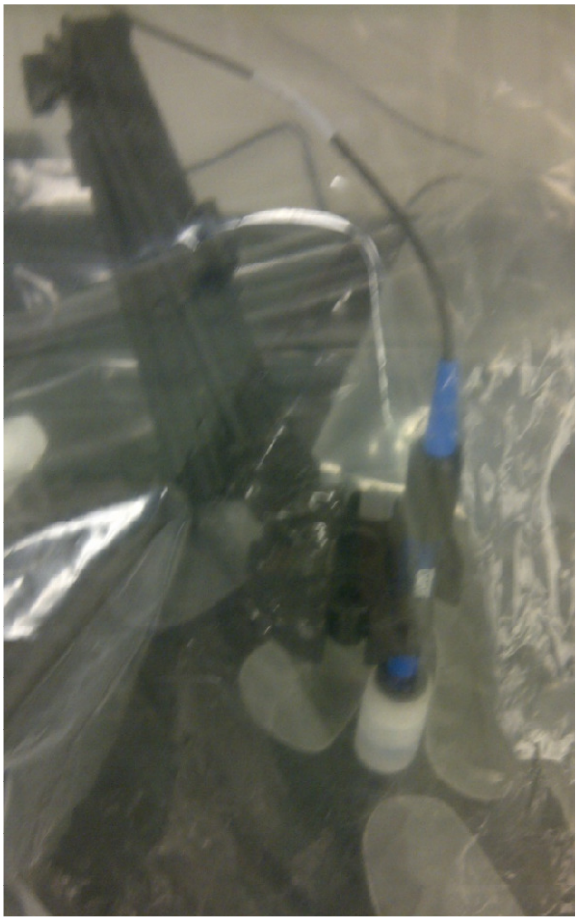

Figure 3.6: pH electrode inside the glove bag

The pH meter was calibrated before every measurement as seen in Figure 3.7. The meter contained a calibration method in which the electrode is placed into different buffer solutions. The meter then identifies the solution and correlates the pH of the buffer to the voltage it reads. Between each reading, the probe was rinsed with tap water. The buffer solutions used were pH 4, 7 and 10. The meter then displays both the pH of its readings and the potential difference between the solution and the reference cell.

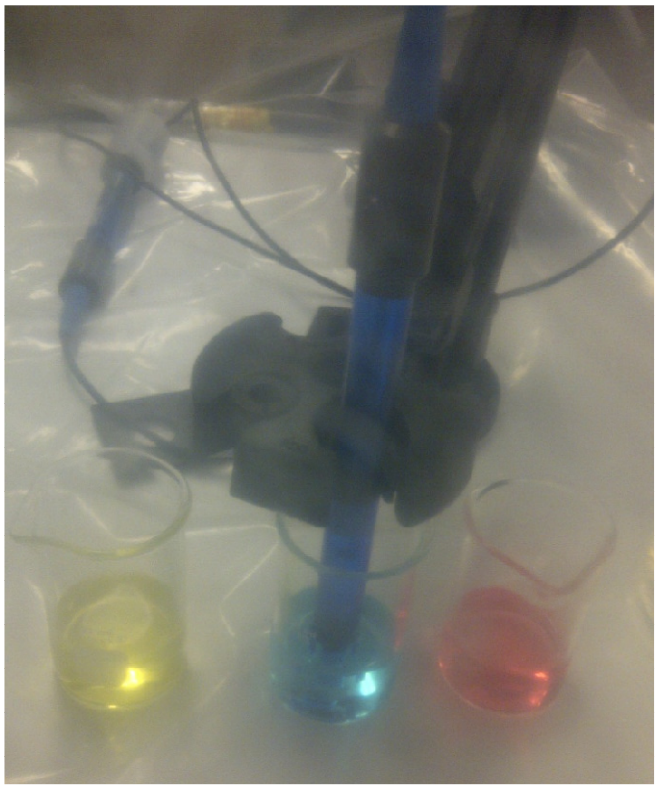

Figure 3.7: Calibrating pH electrode

Once calibrated, the pH probe was rinsed with tap water again and then placed into the reacting solution. When the reading of the pH probe was stabilized, the meter displayed the solution's pH. Following a measurement, the probe was placed in a pH 4 buffer solution for fifteen minutes. This was found to reduce the errors encountered following successive alkaline pH measurements.

3.3.2 ICP-AES Testing

ICP-AES (inductively coupled plasma atomic emission spectroscopy) testing was carried out to quantify the concentration of silicon, calcium and sodium ions in the solutions. The ICP-AES machine, seen in Figure 3.8, first turns a portion of the sample into a mist with the nebulizer and injects it into a chamber where there is a plasma torch. The plasma excites the ions in the solution. When the ions return to their normal state, they emit radiation which is measured. Technical details on the test equipment can be found in the Varian Vista ICP brochure (Varian, 2013).

Figure 3.8: ICP AES machine located in BSB at McMaster University

Three calibration solutions were created for each of the elements to be tested. Each set of solutions contained a low, medium and high concentration of the element to be analyzed. To aid the dissolution of the silica calibration solutions, hydrochloric acid was added to the mix. The solutions to be tested were diluted in order for the concentrations to be within the limits of the calibrations solutions. The dilution was performed under a nitrogen atmosphere in a glove bag to ensure that the solutions did not experience carbonation. The solutions were diluted to 5x their original concentrations. A second dilution was necessary for the samples containing sodium as it is a strong catalyst for silicon dissolution and they were out of range of the silicon calibration solutions. These samples were diluted to 10x or 25x when necessary.

Once the ICP-AES machine was setup and ready to operate, the method was entered into the ICP expert II software. First, the element to be analyzed was entered into the program. Three wavelengths were then selected to be read during the testing. The wavelengths selected were the top three recommended by the software. For each of the wavelengths, the interactions with other elements were checked to ensure the interacting elements were not present in the solutions. The software calculated the calibration curve from the calibration solutions.

The test method consisted of running a blank sample, three calibration solutions and then the test solutions. The machine was recalibrated after every ten samples. At the end of the procedure, the software calculated the average concentration from the three wavelengths measured. This average was taken as the concentration of ions present in the solution.

While the ICP-AES machine was capable of identifying the concentration of all three elements simultaneously, this could not be done since the calibration solutions would require all three elements in one solution. This would have caused reactions and precipitation similar to the sample solutions. Therefore, the solutions were tested for each element individually.

3.3.3 TGA Testing

Thermal Gravimetric Analysis (TGA) was completed on the dried precipitate samples. The testing was completed using a TGA/SDT Q600 machine made by TA Instruments (TA Instruments, 2013). The equipment heats an alumina cup filled with a sample shown in Figure 3.9 at a constant rate. The weight and the heat flow into the sample are measured. Both the sample cup and the reference cup are placed onto the balance arms and the machine is tared. The sample cup is then removed and approximately 20mg of solids was added to the cup. Less was added if the reactions did not produce enough precipitate. The cup was then placed back on the balance and the furnace was left for 20 minutes so that the air would be purged and replaced with nitrogen. All of the samples were then heated at a rate of 20 degrees per minute up to at least 1000°C. Both the weight and heat flow were recorded for the duration of the experiment.

Figure 3.9: Sample cups on TGA beams

The weight change was analyzed using the software "Advantage" developed by TA instruments (TA Instruments, 2013). The weight loss was taken as the loss from the onset of the curve to the end, as shown by the arrows in Figure 3.10. There was some moisture in all the samples since they were not initially heated to remove the free water. The initial water content was calculated from the mass loss that occurred around 100°C. The percent losses from compounds were then changed to the percent loss from a dried sample using Equation 3-1.

$$\text{Dried \% lost} = \text{initial \% lost} \times \frac{100\%}{100\% - \text{\% free water}} \qquad \textbf{Equation 3-1}$$

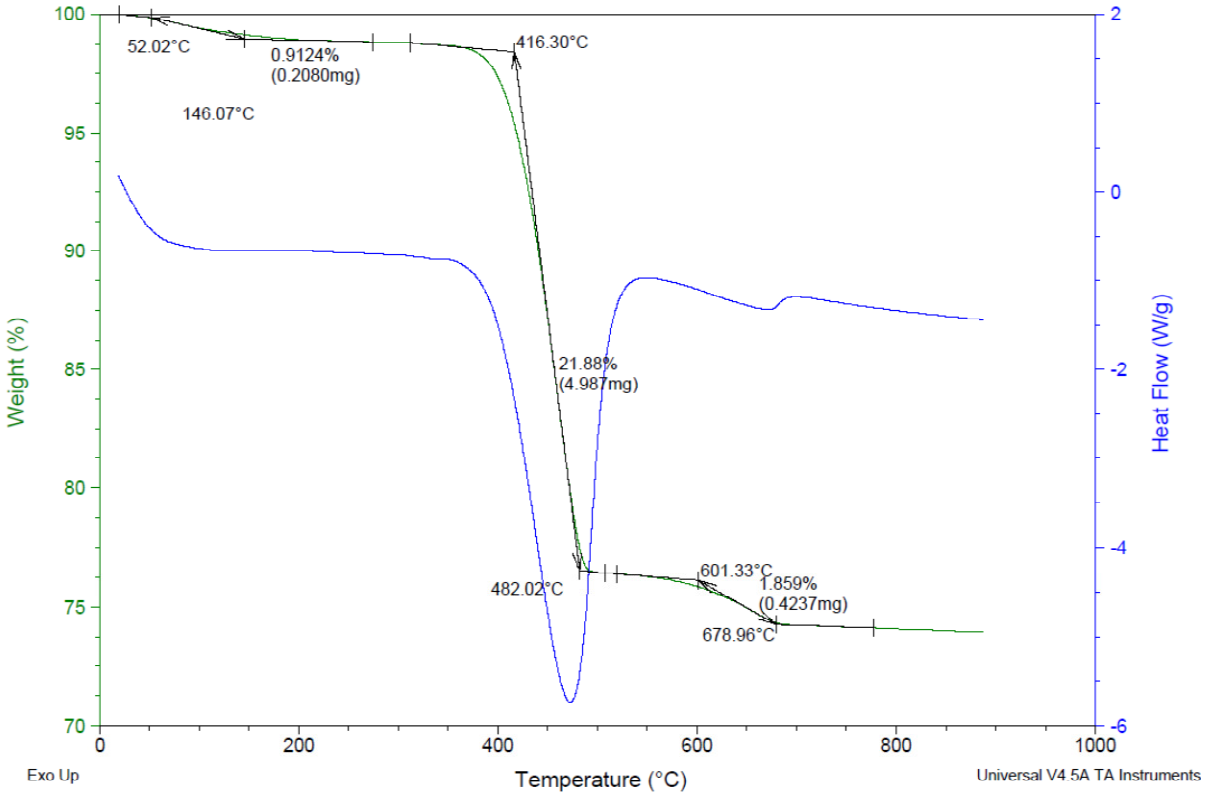

Figure 3.10: TGA Weight Loss Calculations for $Ca(OH)_2$

Mass balances were used to find the mass of calcium hydroxide in the precipitate. Some of the samples had experienced carbonation while drying as they were exposed to air. The carbonation reaction is given in Equation 3-2. This shows that 1 mol of calcium hydroxide is converted to 1 mol of calcium carbonate. The molar masses of these compounds are 74.1 g/mol and 100.09 g/mol, respectively. When the samples are heated, the weight percentage lost between 400 and 550°C corresponds to the decomposition of calcium hydroxide, shown in Equation 3-3. The mass lost above 600°C is then the decomposition of calcium carbonate into calcium oxide and carbon dioxide, shown in Equation 3-4. The weights lost due to decomposition are converted to percentage of calcium hydroxide by Equation 3-5 and Equation 3-6.

$$Ca(OH)_2 + CO_2 \rightarrow CaCO_3 + H_2O$$ **Equation 3-2**

$$Ca(OH)_{2\,(S)} \xrightarrow{heat} CaO_{(S)} + H_2O_{(g)}$$ **Equation 3-3**

$$CaCO_{3(S)} \xrightarrow{heat} CaO_{(S)} + CO_{2(g)} \qquad \textbf{Equation 3-4}$$

$$1\%\ H_2O \text{ lost } 400 - 550℃ \times \frac{74.1\ g/mol\ Ca(OH)_2}{18.01\ g/mol\ H_2O} = 4.11\%\ Ca(OH)_2 \qquad \textbf{Equation 3-5}$$

$$1\%\ CO_2 \text{ lost above } 600℃ \times \frac{100.09\ g/mol\ CaCO_3}{44.01\ g/mol\ CO_2} \times \frac{74.1\ g/mol\ Ca(OH)_2}{100.09\ g/mol\ CaCO_3} = 1.68\%\ Ca(OH)_2 \qquad \textbf{Equation 3-6}$$

4 Experimental Results

4.1 Introduction

Results of the experimental program are presented in this chapter. This includes the concentrations of ions in the solutions as found by the ICP-AES testing, the pH levels with time, and the composition of the precipitate with time. The results are presented in graphical form as a function of time.

4.2 Calcium and Silicon Concentrations over Time

The results for the samples containing solely calcium hydroxide and silica are presented in the following section. For low concentrations of calcium hydroxide with low, medium and high contents of silica, the results are presented in Figure 4.1, Figure 4.2, and Figure 4.3. The composition of the precipitate plotted as a ratio of calcium to silica is shown in Figure 4.4. For the combination of medium concentrations of calcium hydroxide with all the different contents of silica, the results are plotted in Figure 4.5, Figure 4.6, Figure 4.8, Figure 4.10, and Figure 4.12. The composition of the precipitate for the medium concentration of calcium hydroxide with silica is shown in Figure 4.7, Figure 4.9, Figure 4.11, and Figure 4.13 and is shown as the ratio of calcium to silica. For the high concentrations of calcium hydroxide with the low, medium and high contents of silica, the results are shown in Figure 4.14, Figure 4.16 and Figure 4.17. The ratio of calcium to silica in the precipitate is plotted in Figure 4.15 and Figure 4.18.

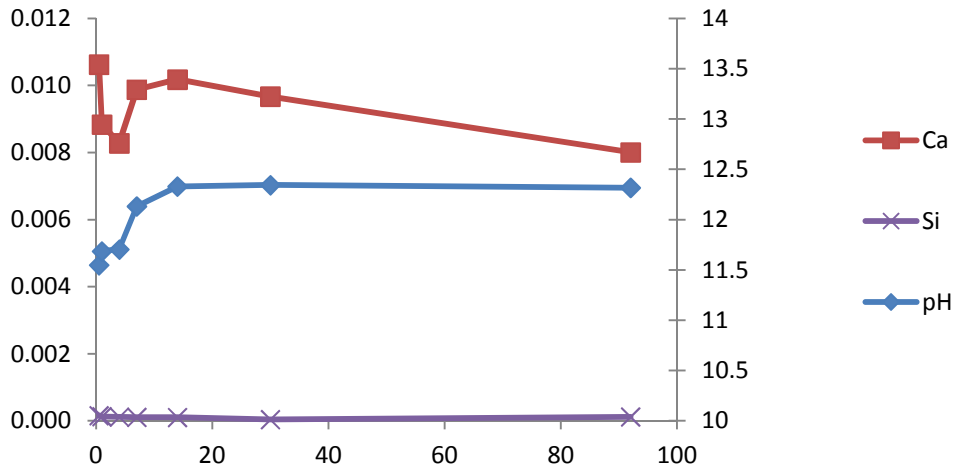

Figure 4.1: Concentration and pH vs. Time; $[Ca(OH)_2]_0$=0.013, $[SiO_2]_0$=0.0016

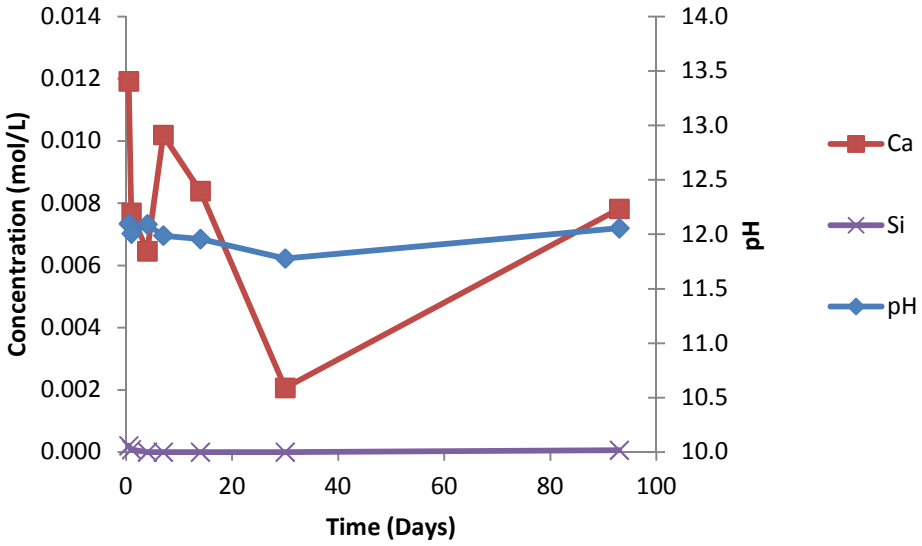

Figure 4.2: Concentration and pH vs. Time; $[Ca(OH)_2]_0$=0.013, $[SiO_2]_0$=0.020

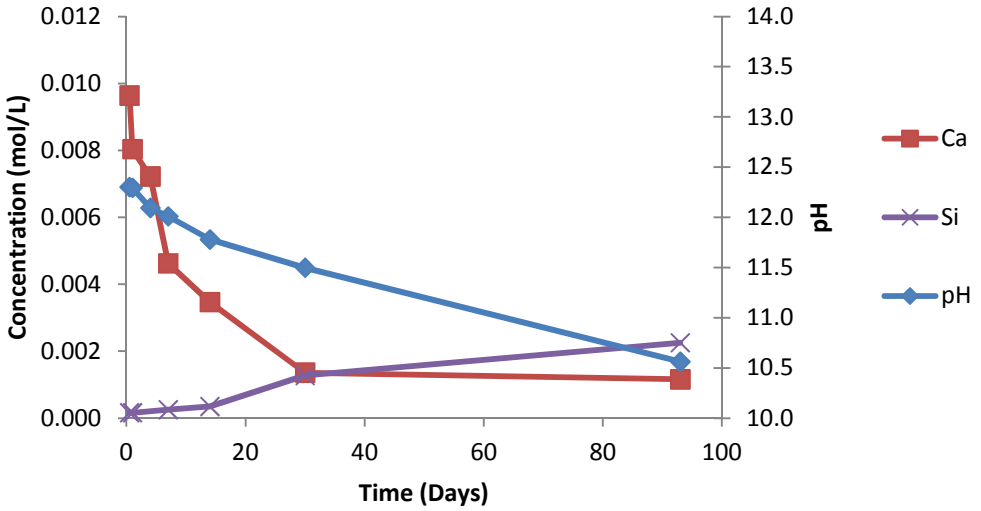

Figure 4.3: Concentration and pH vs. Time; $[Ca(OH)_2]_0$=0.015, $[SiO_2]_0$=0.100

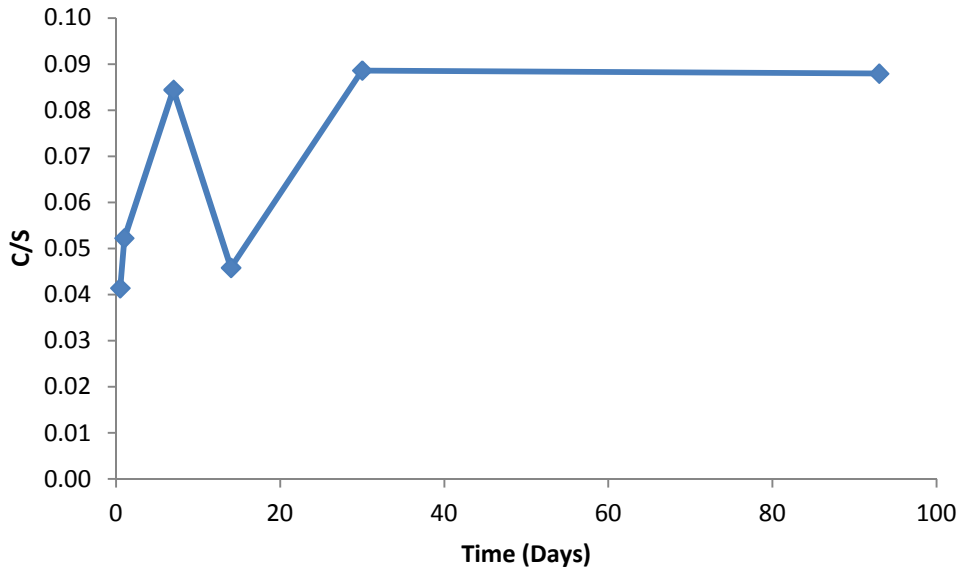

Figure 4.4: Precipitate Composition; $[Ca(OH)_2]_0$=0.015, $[SiO_2]_0$=0.100

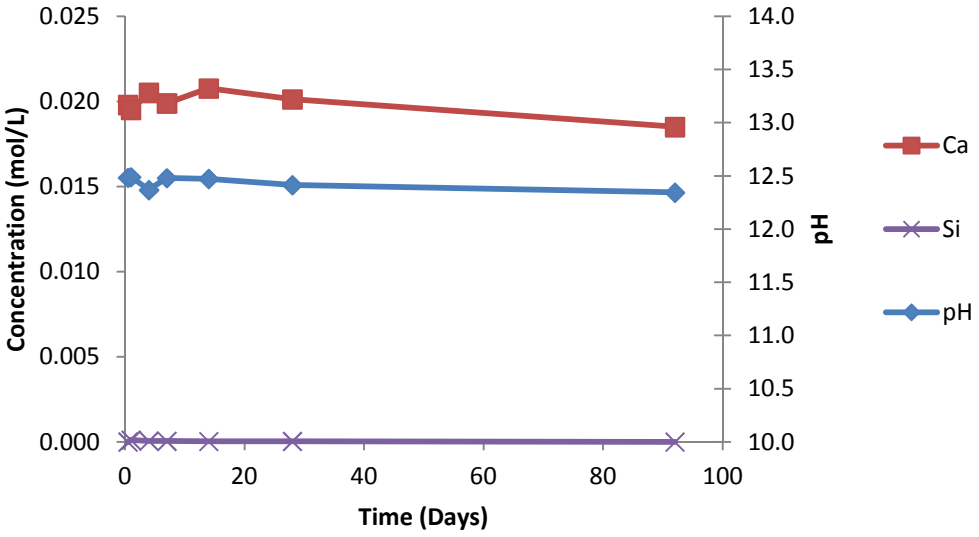

Figure 4.5: Concentration and pH vs. Time; $[Ca(OH)_2]_0$=0.023, $[SiO_2]_0$=0.0016

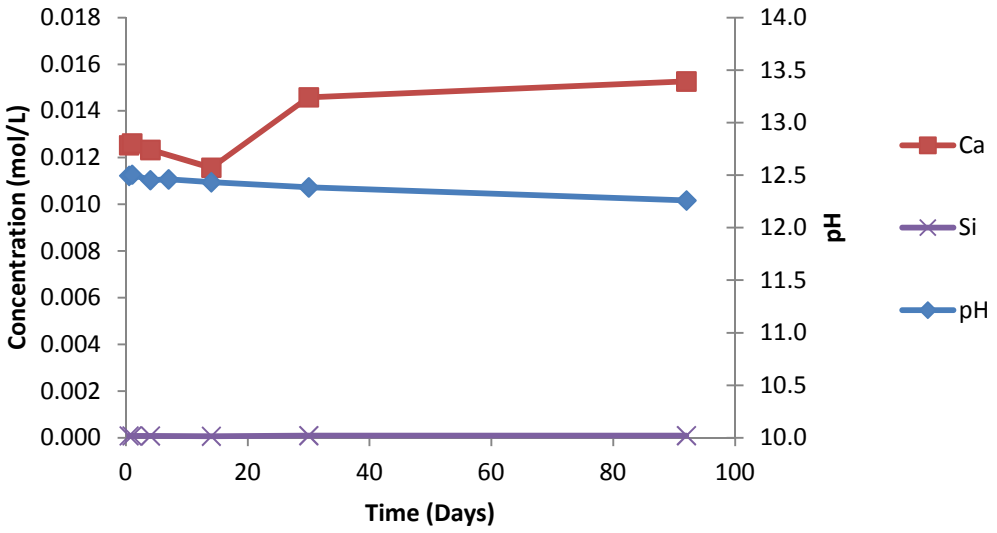

Figure 4.6: Concentration and pH vs. Time; $[Ca(OH)_2]_0$=0.023, $[SiO_2]_0$=0.020

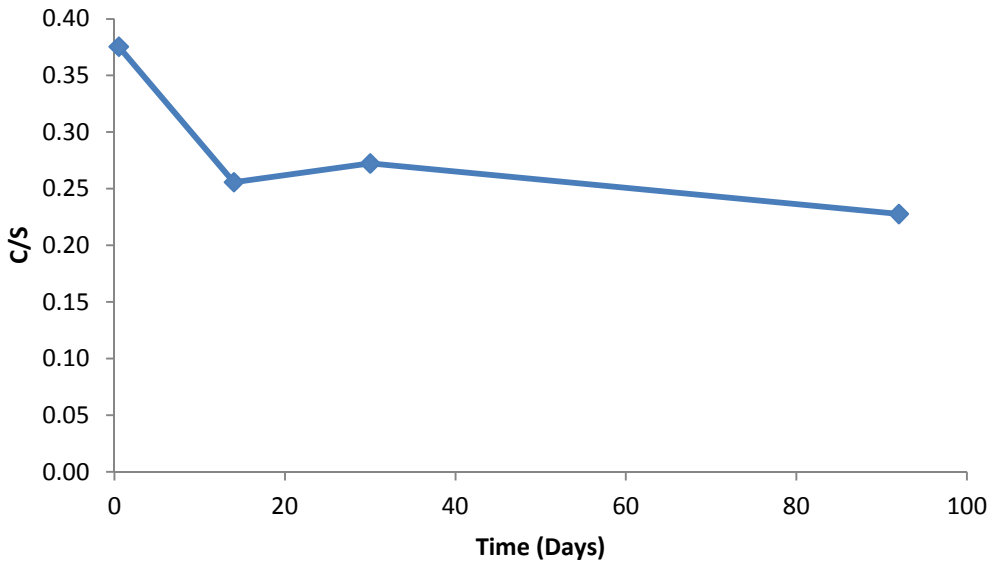

Figure 4.7: Precipitate Composition; $[Ca(OH)_2]_0$=0.023, $[SiO_2]_0$=0.020

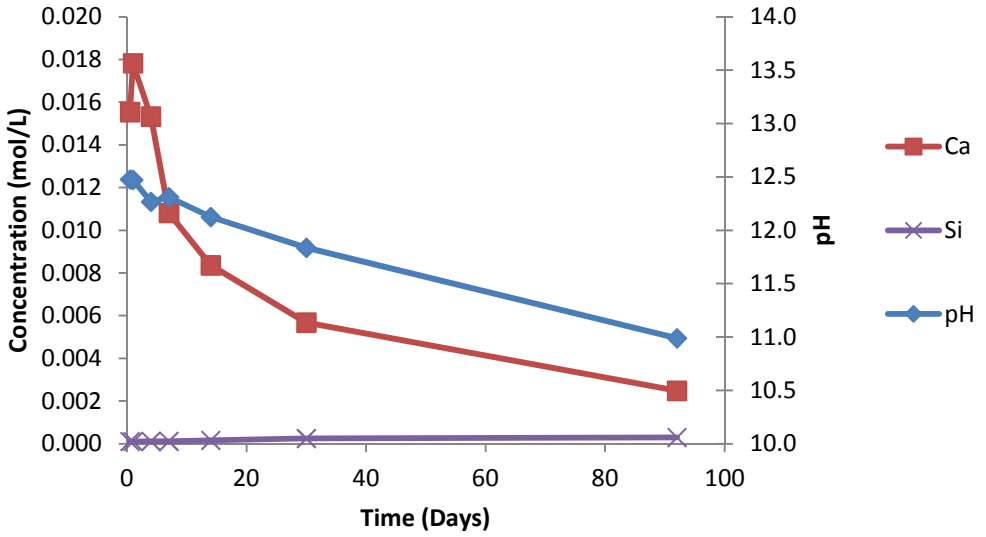

Figure 4.8: Concentration and pH vs. Time; $[Ca(OH)_2]_0$=0.023, $[SiO_2]_0$=0.100

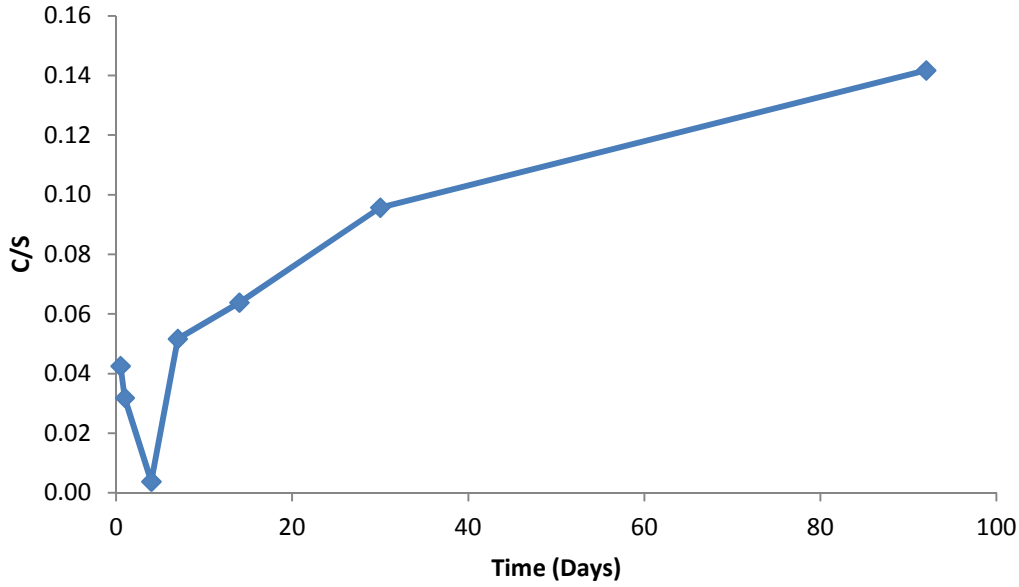

Figure 4.9: Precipitate Composition; $[Ca(OH)_2]_0$=0.023, $[SiO_2]_0$=0.100

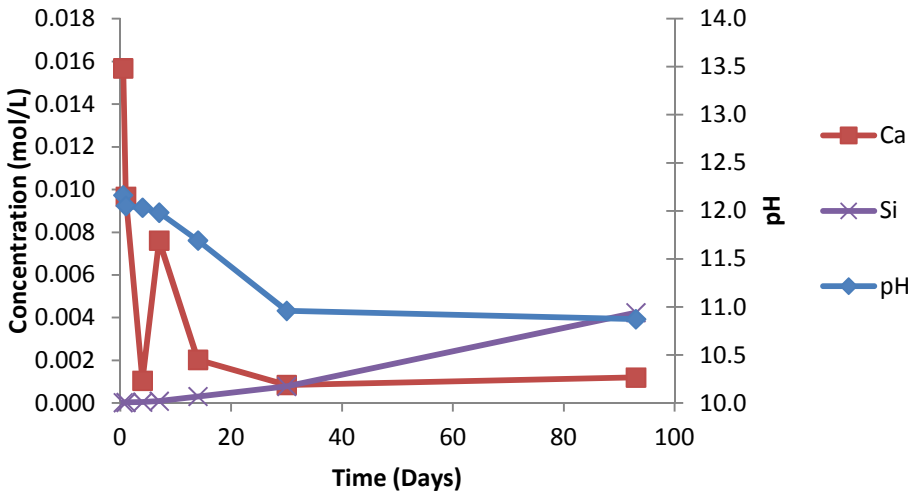

Figure 4.10: Concentration and pH vs. Time; $[Ca(OH)_2]_0$=0.021, $[SiO_2]_0$=0.134

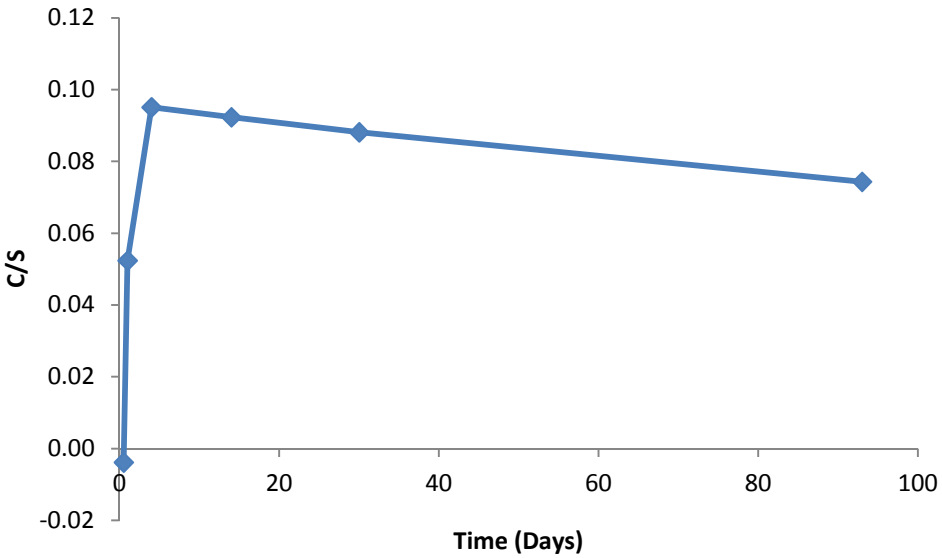

Figure 4.11: Precipitate Composition; $[Ca(OH)_2]_0$=0.021, $[SiO_2]_0$=0.134

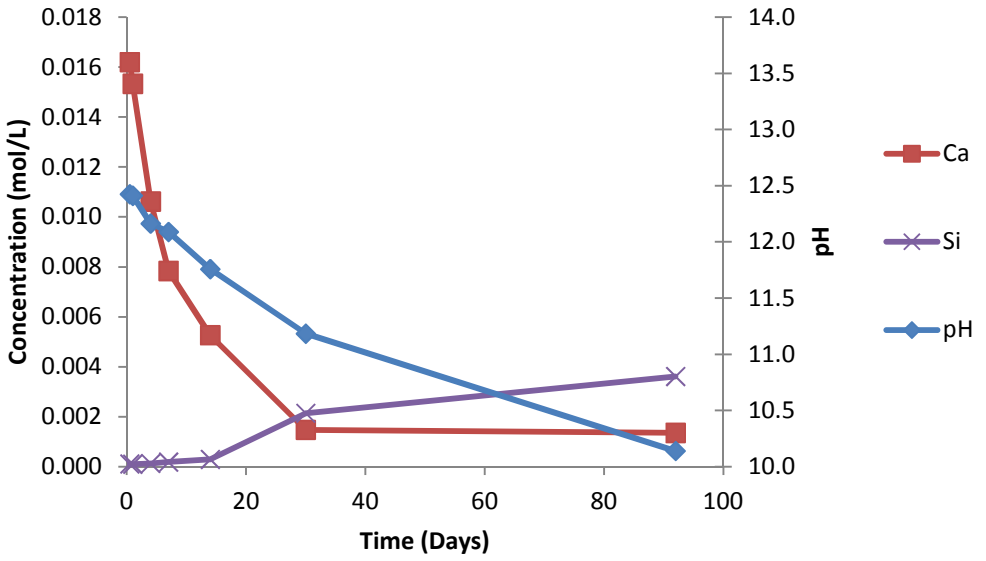

Figure 4.12: Concentration and pH vs. Time; $[Ca(OH)_2]_0$=0.023, $[SiO_2]_0$=0.153

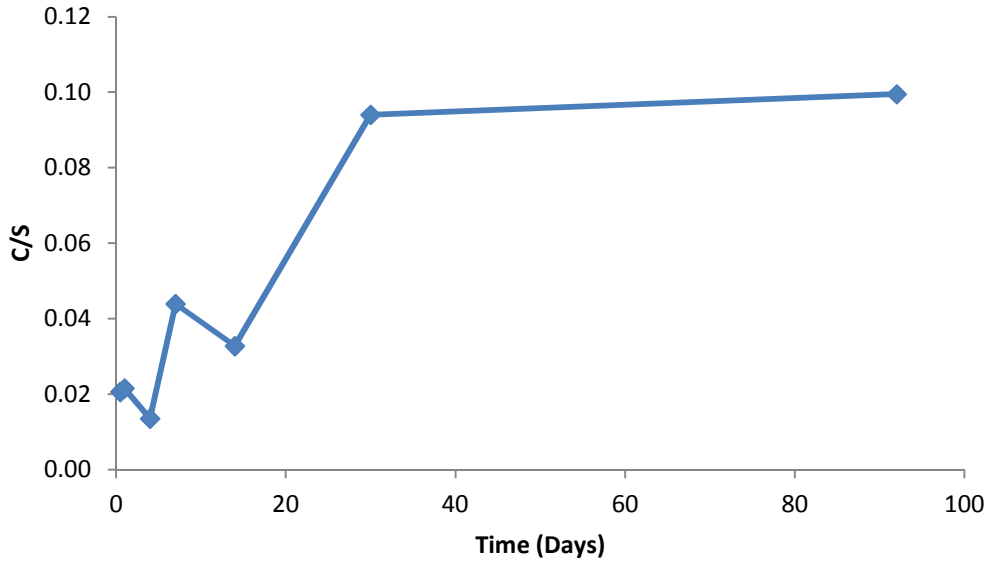

Figure 4.13: Precipitate Composition; $[Ca(OH)_2]_0$=0.023, $[SiO_2]_0$=0.153

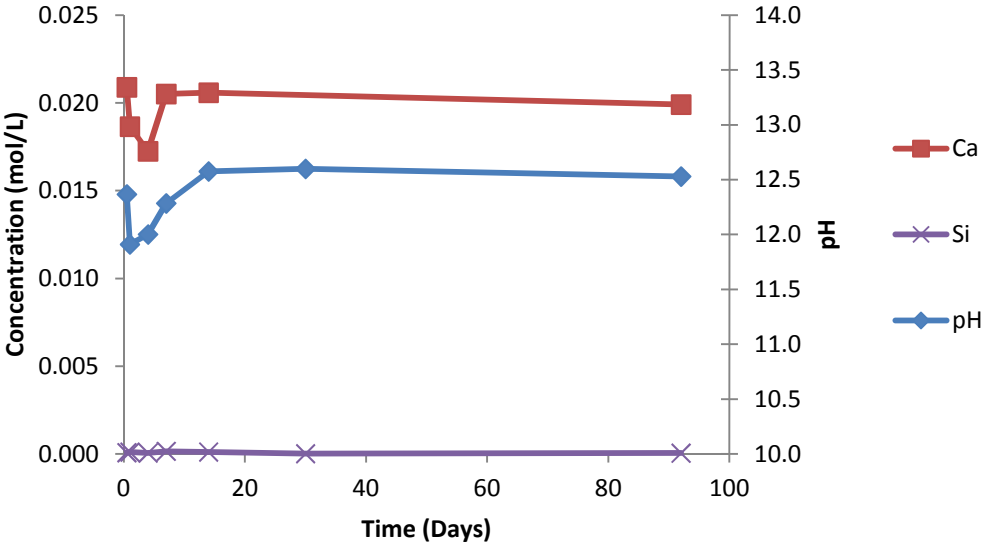

Figure 4.14: Concentration and pH vs. Time; $[Ca(OH)_2]_0$=0.045, $[SiO_2]_0$=0.0016

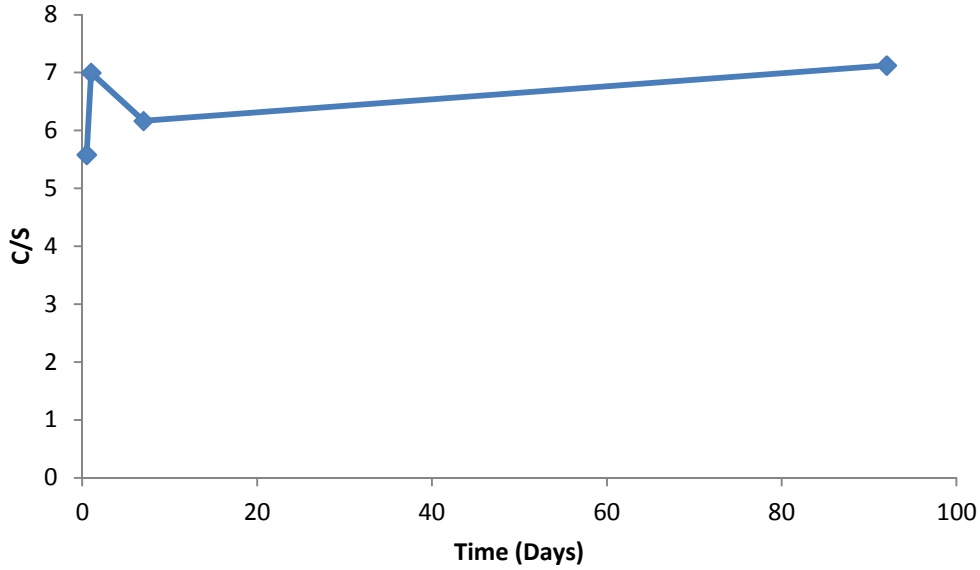

Figure 4.15: Precipitate Composition; $[Ca(OH)_2]_0$=0.045, $[SiO_2]_0$=0.0016

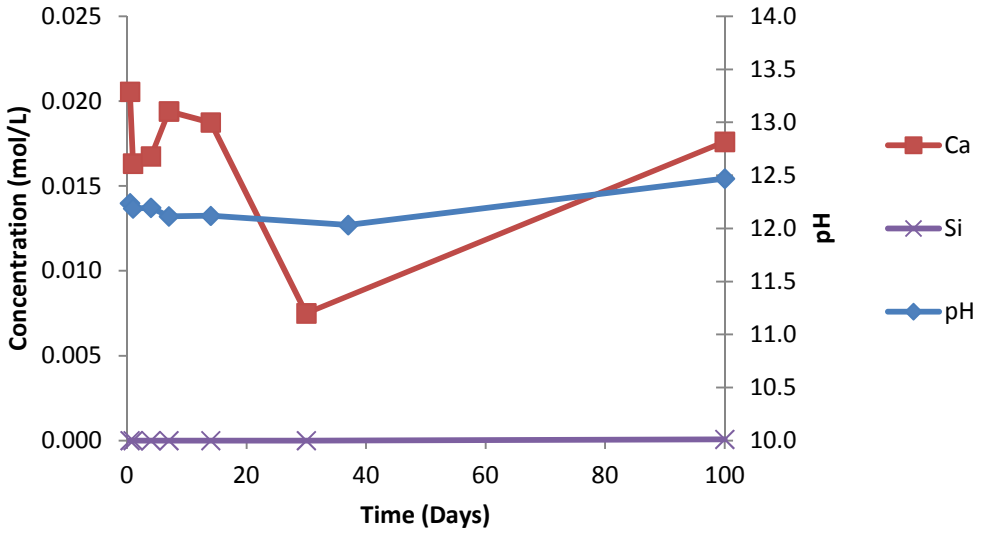

Figure 4.16: Concentration and pH vs. Time; $[Ca(OH)_2]_0$=0.045, $[SiO_2]_0$=0.020

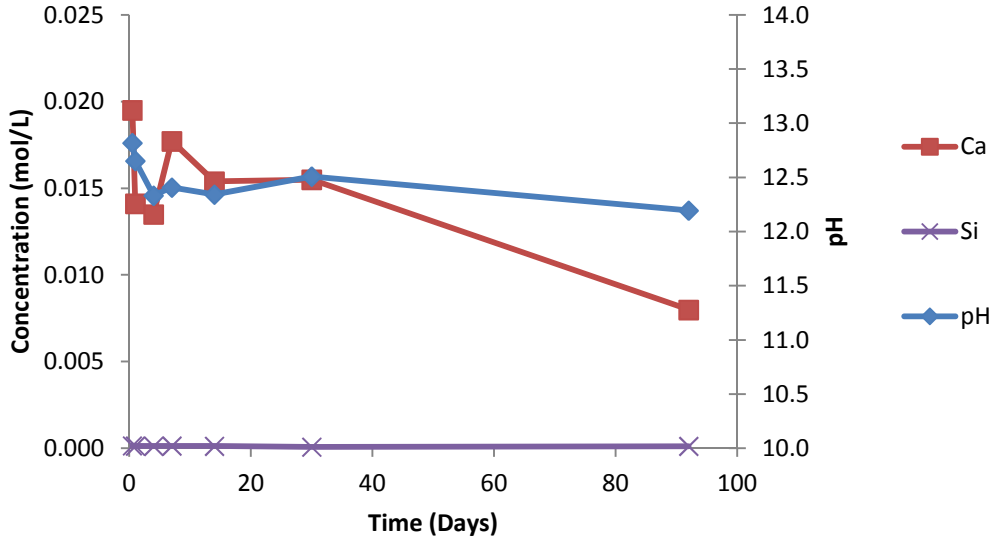

Figure 4.17: Concentration and pH vs. Time; $[Ca(OH)_2]_0$=0.045, $[SiO_2]_0$=0.100

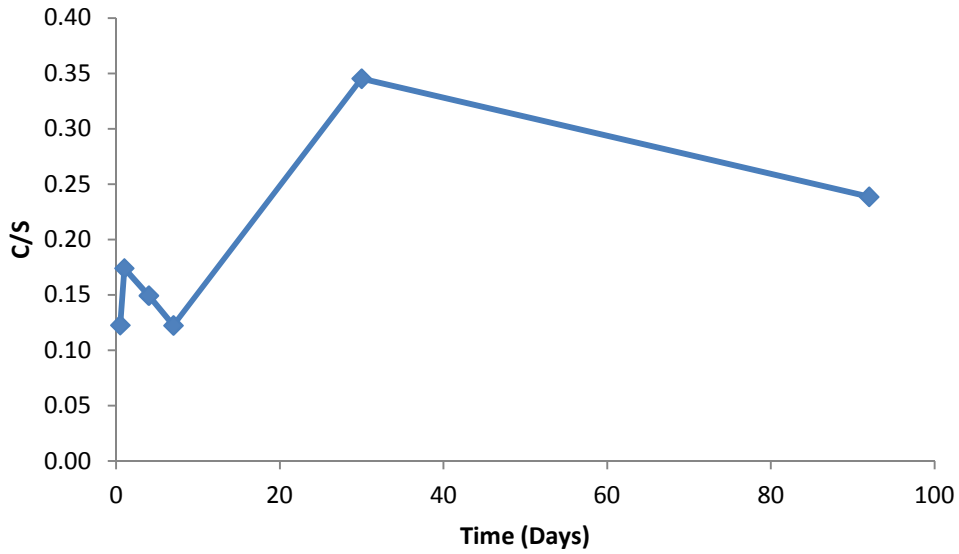

Figure 4.18: Precipitate Composition; $[Ca(OH)_2]_0$=0.045, $[SiO_2]_0$=0.100

4.3 Sodium and Silicon Solution Concentrations over Time

The results for the samples containing sodium hydroxide and silica are shown in this section. The results for the low content of sodium hydroxide and the low, medium and high concentrations of silica are presented in Figure 4.19, Figure 4.20 and Figure 4.21. The results for the medium concentration of sodium hydroxide with low, medium and high concentrations of silica are shown in Figure 4.22, Figure 4.23 and Figure 4.24. The results for the high concentration of sodium hydroxide with all of the silica contents are presented in Figure 4.25, Figure 4.26 and Figure 4.27.

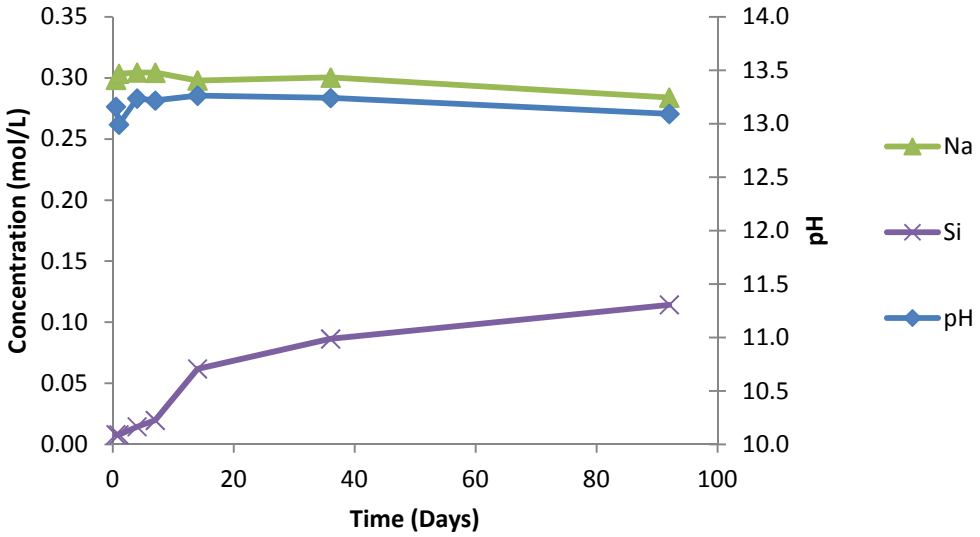

Figure 4.19: Concentration and pH vs. Time; $[NaOH]_0$=0.30, $[SiO_2]_0$=0.115

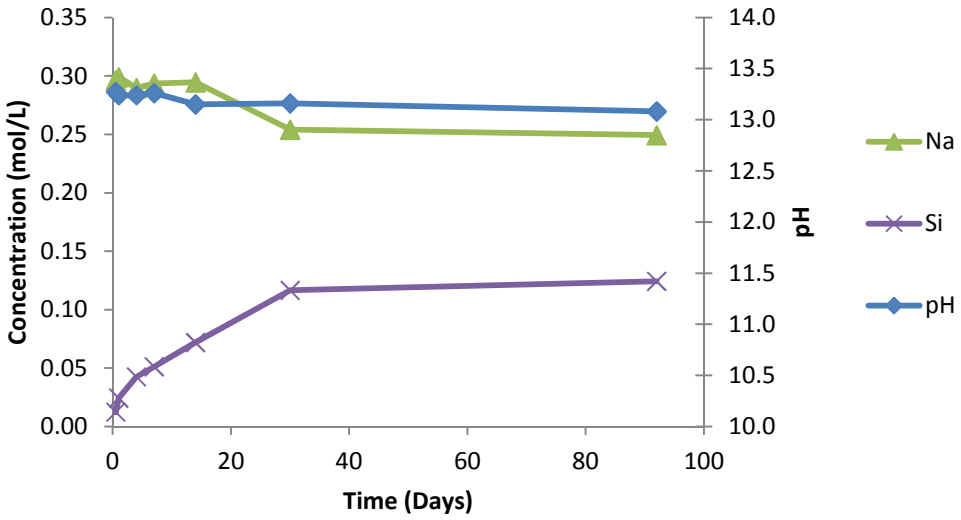

Figure 4.20: Concentration and pH vs. Time; $[NaOH]_0$=0.30, $[SiO_2]_0$=0.134

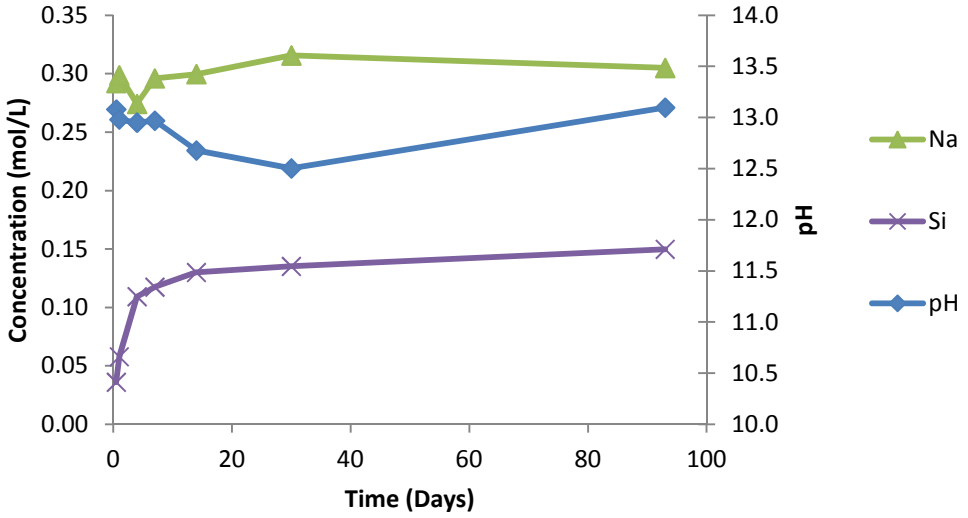

Figure 4.21: Concentration and pH vs. Time; $[NaOH]_0$=0.30, $[SiO_2]_0$=0.153

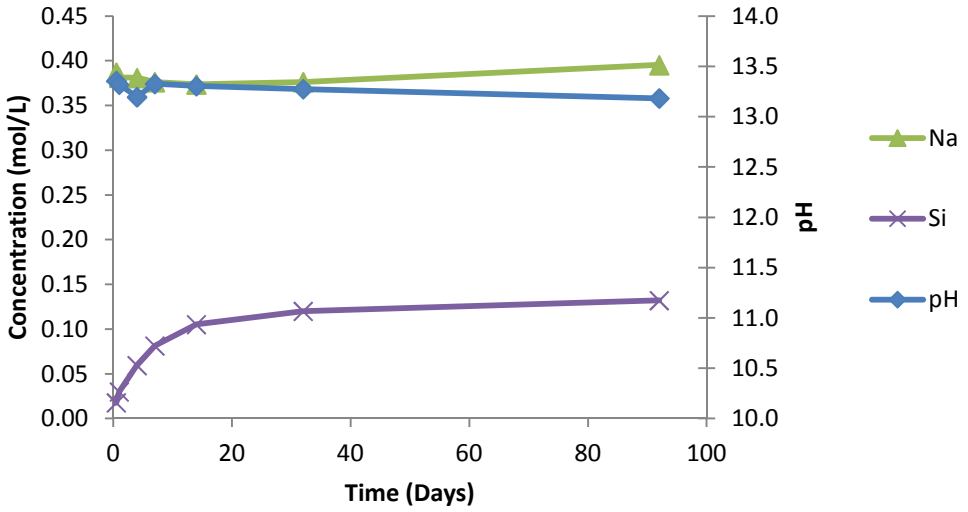

Figure 4.22: Concentration and pH vs. Time; $[NaOH]_0$=0.42, $[SiO_2]_0$=0.134

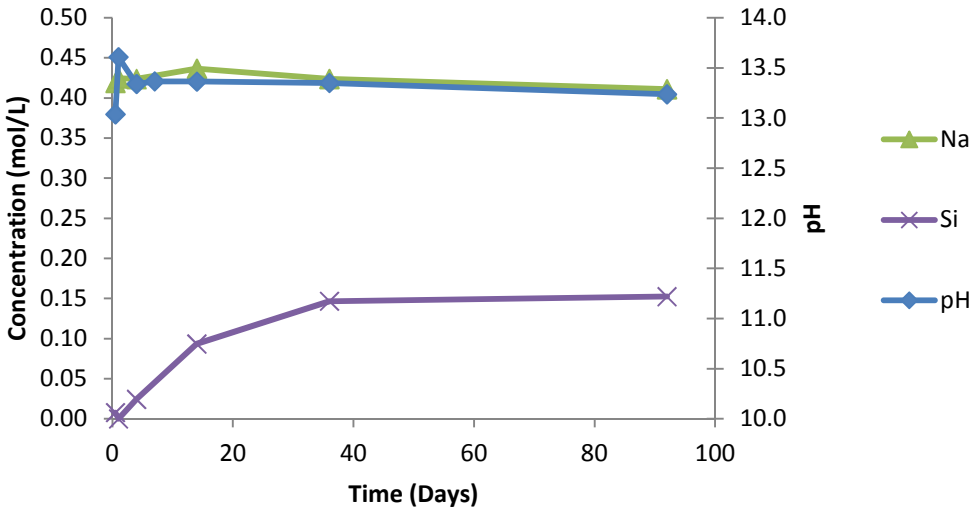

Figure 4.23: Concentration and pH vs. Time; $[NaOH]_0$=0.42, $[SiO_2]_0$=0.153

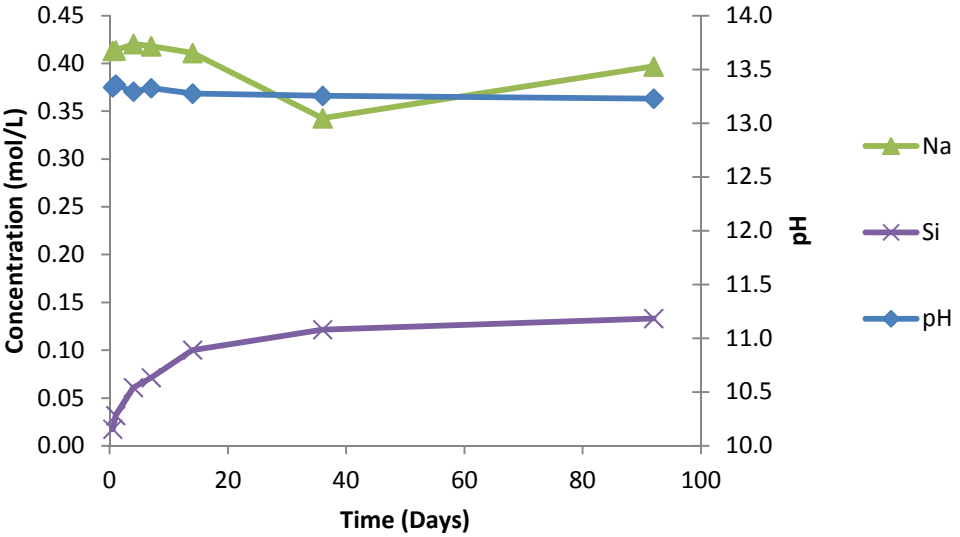

Figure 4.24: Concentration and pH vs. Time; $[NaOH]_0$=0.42, $[SiO_2]_0$=0.165

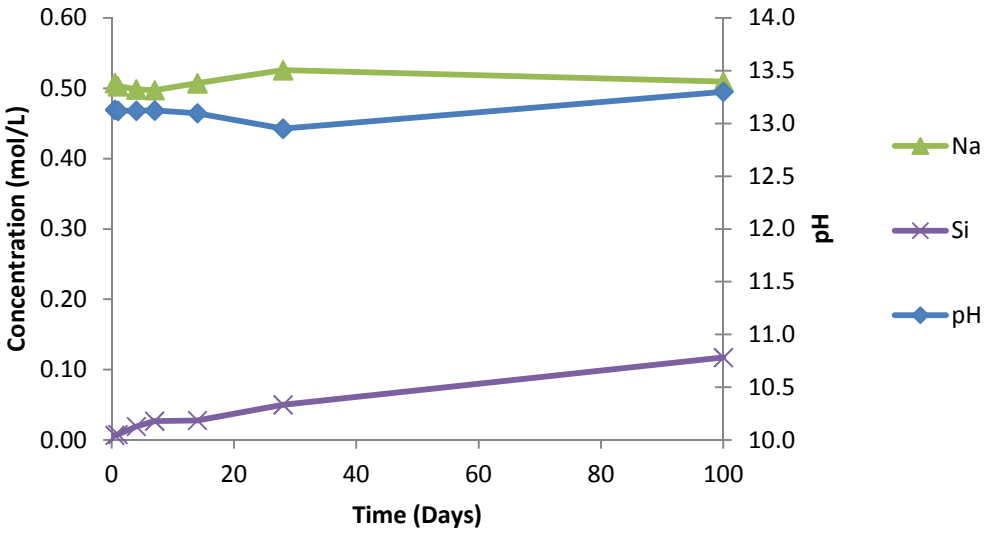

Figure 4.25: Concentration and pH vs. Time; $[NaOH]_0$=0.53, $[SiO_2]_0$=0.153

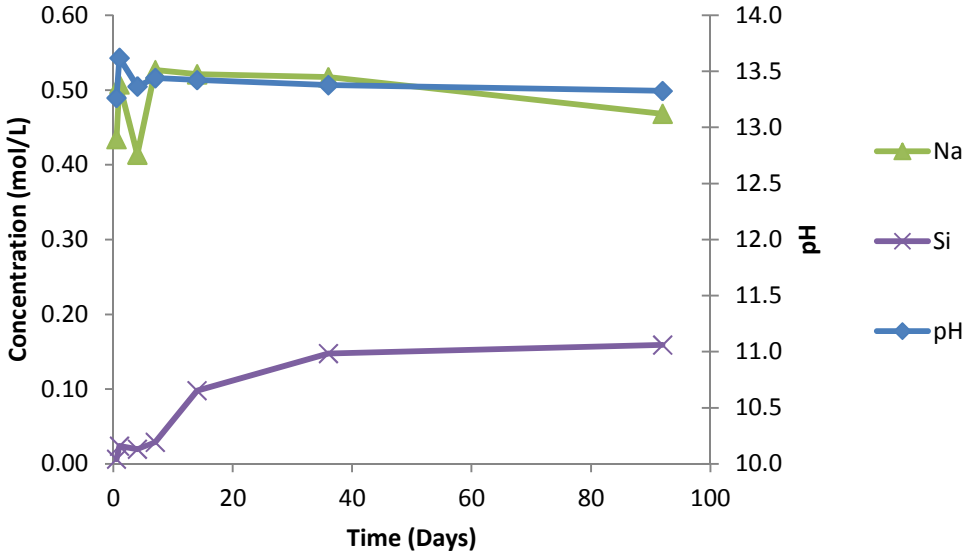

Figure 4.26: Concentration and pH vs. Time; $[NaOH]_0$=0.53, $[SiO_2]_0$=0.165

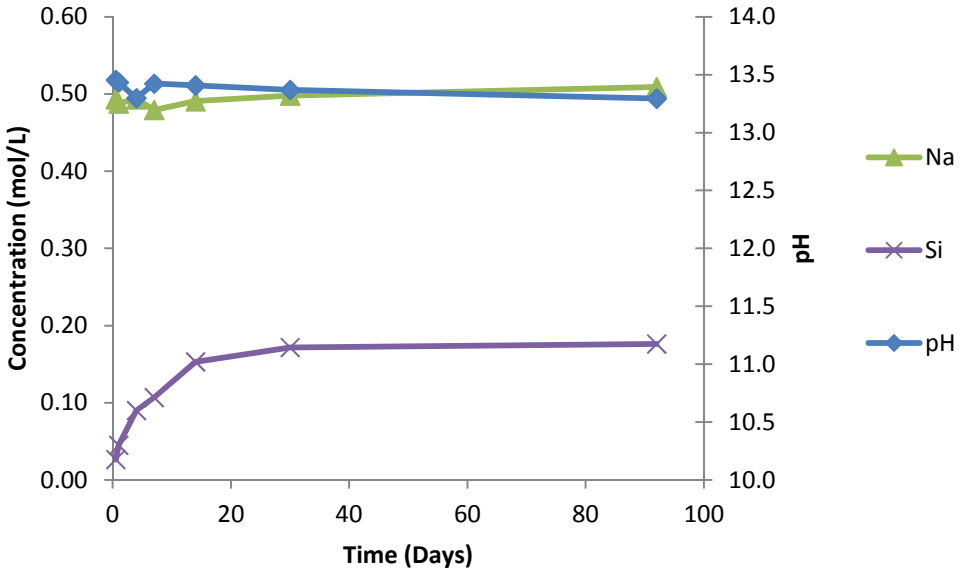

Figure 4.27: Concentration and pH vs. Time; $[NaOH]_0$=0.53, $[SiO_2]_0$=0.180

4.4 Sodium, Calcium and Silicon Concentrations over Time

This section contains the results for the samples containing sodium hydroxide, calcium hydroxide and silica. The results for the low concentration of sodium hydroxide with calcium hydroxide and low, medium and high concentrations of silica are shown in Figure 4.28, Figure 4.30 and Figure 4.32. The precipitate composition is plotted as the ratio of calcium to silica and sodium to silica and is shown in Figure 4.29, Figure 4.31 and Figure 4.33. The results for the medium concentration of sodium hydroxide with calcium hydroxide and low, medium and high contents of silica are plotted in Figure 4.34, Figure 4.36 and Figure 4.38. The precipitate composition is shown in Figure 4.35, Figure 4.37 and Figure 4.39. The results for the high concentration of sodium hydroxide with calcium hydroxide the low, medium and high contents of silica are shown in Figure 4.40, Figure 4.42 and Figure 4.44. The precipitate composition is displayed in Figure 4.41, Figure 4.43 and Figure 4.45.

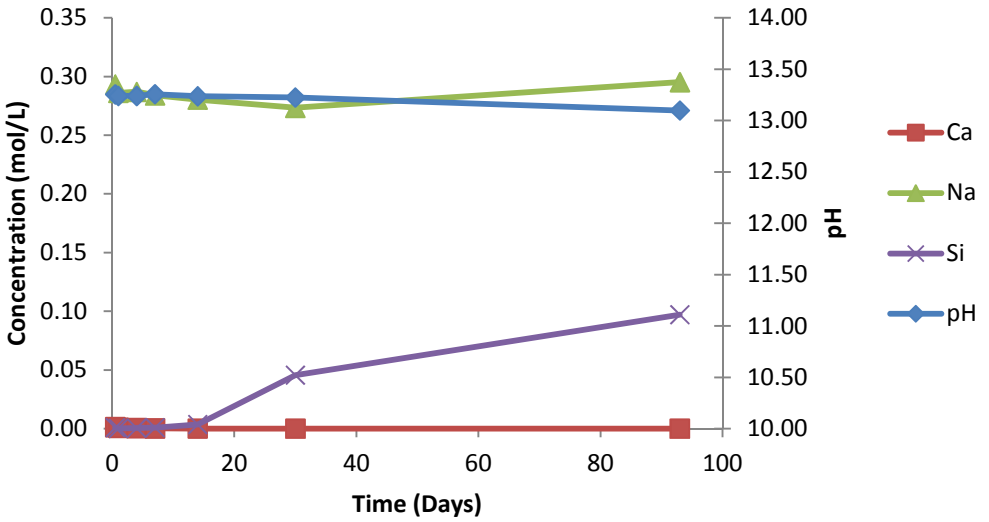

Figure 4.28: Concentration and pH vs. Time; $[Ca(OH)_2]_0$=0.023, $[NaOH]_0$=0.30, $[SiO_2]_0$=0.115

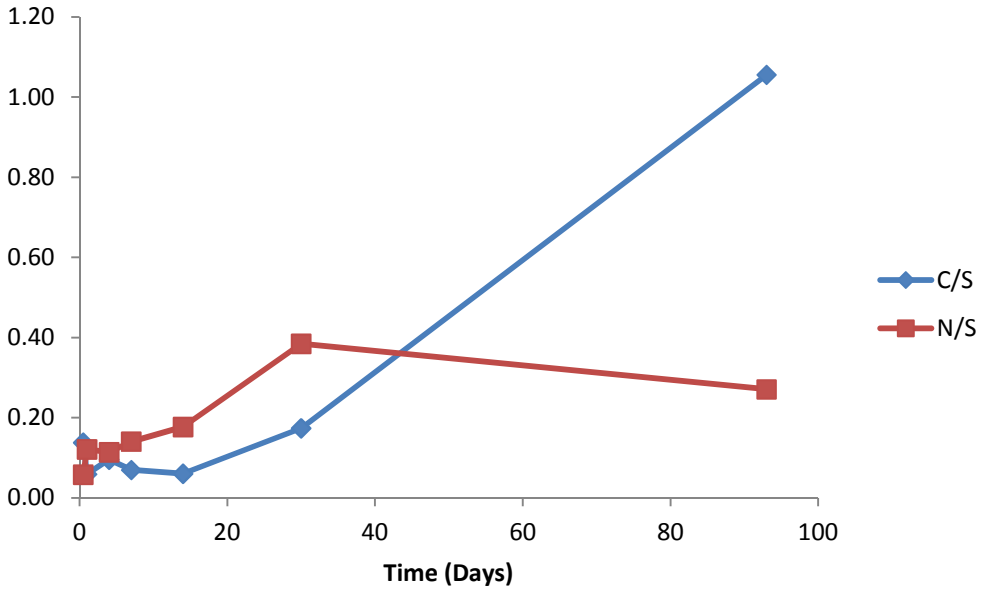

Figure 4.29: Precipitate Composition; $[Ca(OH)_2]_0$=0.023, $[NaOH]_0$=0.30, $[SiO_2]_0$=0.115

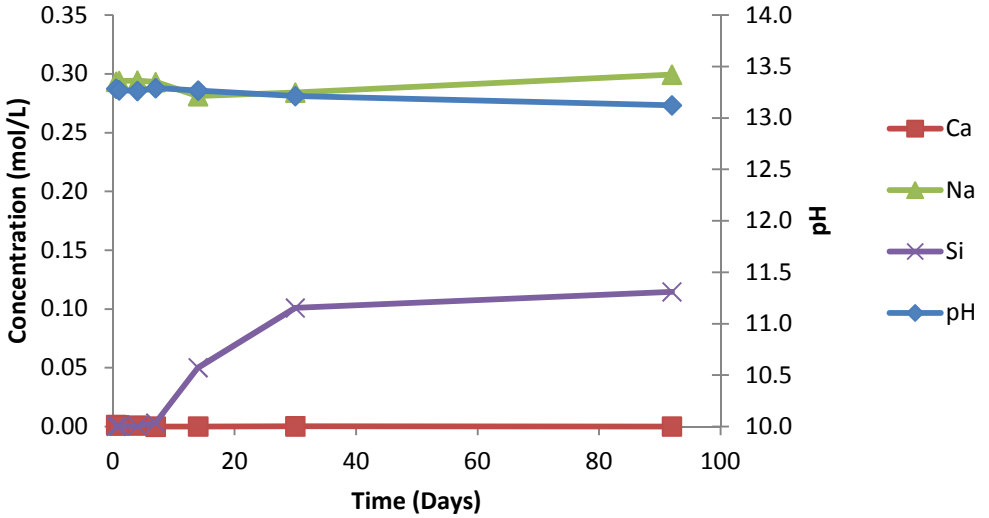

Figure 4.30: Concentration and pH vs. Time; $[Ca(OH)_2]_0$=0.023, $[NaOH]_0$=0.30, $[SiO_2]_0$=0.134

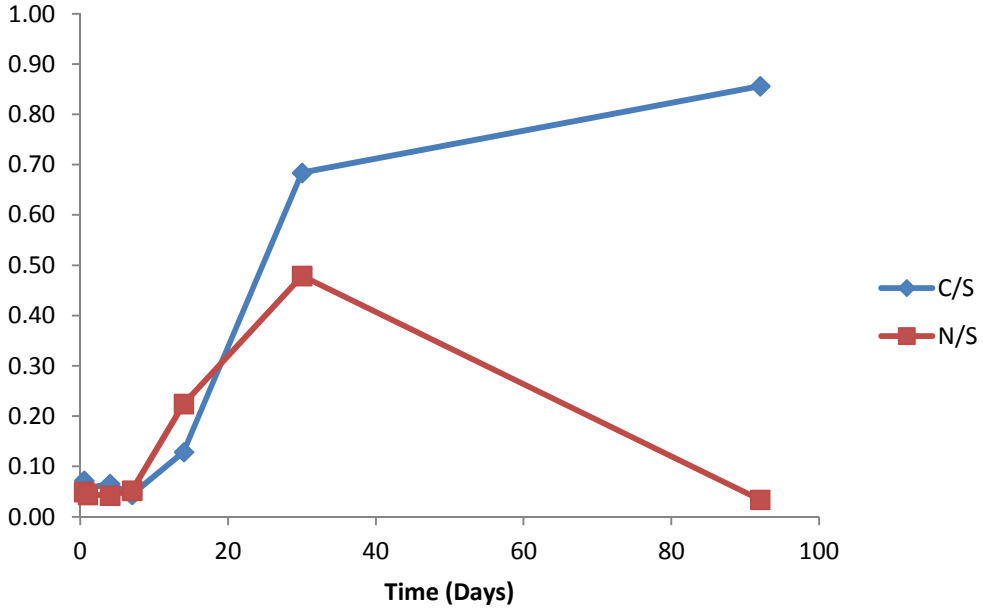

Figure 4.31: Precipitate Composition; $[Ca(OH)_2]_0$=0.023, $[NaOH]_0$=0.30, $[SiO_2]_0$=0.134

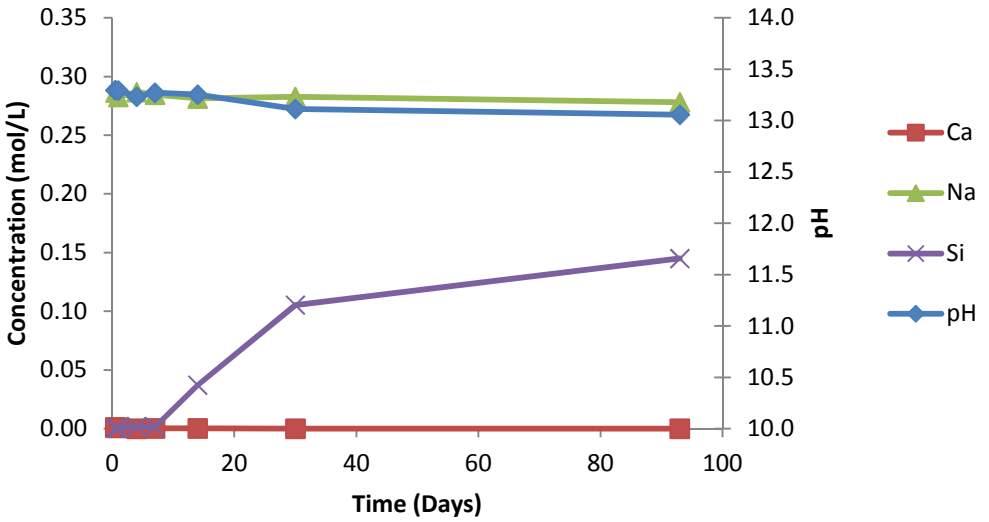

Figure 4.32: Concentration and pH vs. Time; $[Ca(OH)_2]_0$=0.023, $[NaOH]_0$=0.30, $[SiO_2]_0$=0.153

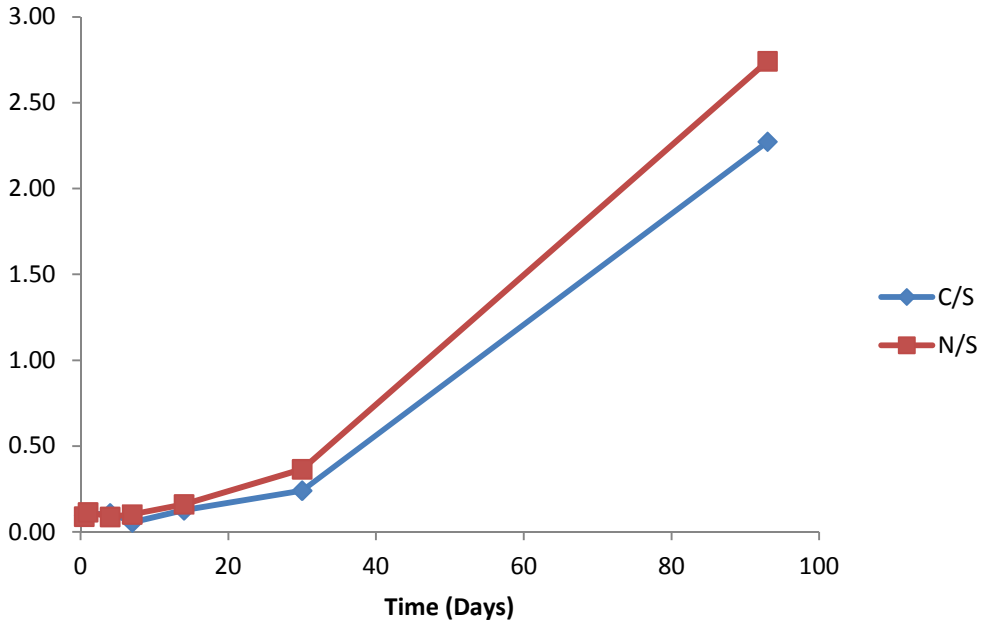

Figure 4.33: Precipitate Composition; $[Ca(OH)_2]_0$=0.023, $[NaOH]_0$=0.30, $[SiO_2]_0$=0.153

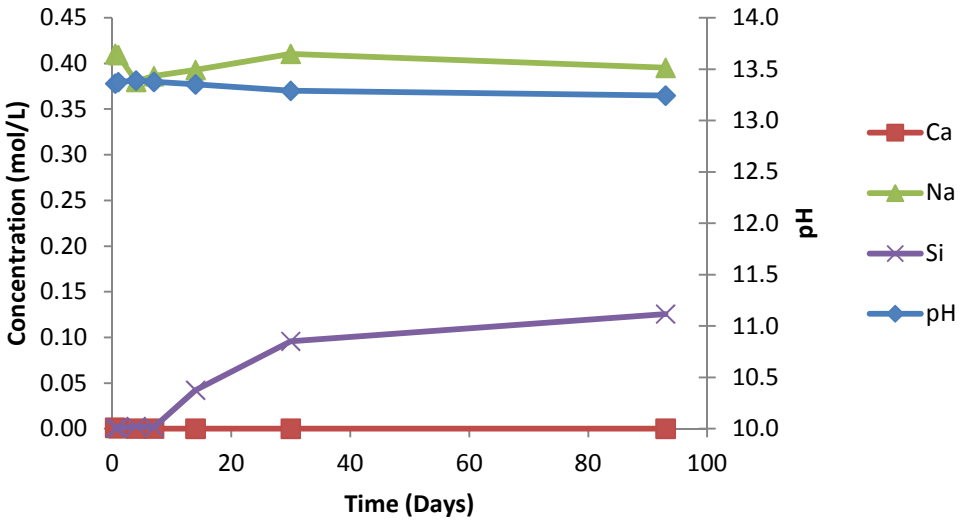

Figure 4.34: Concentration and pH vs. Time; $[Ca(OH)_2]_0$=0.023, $[NaOH]_0$=0.42, $[SiO_2]_0$=0.134

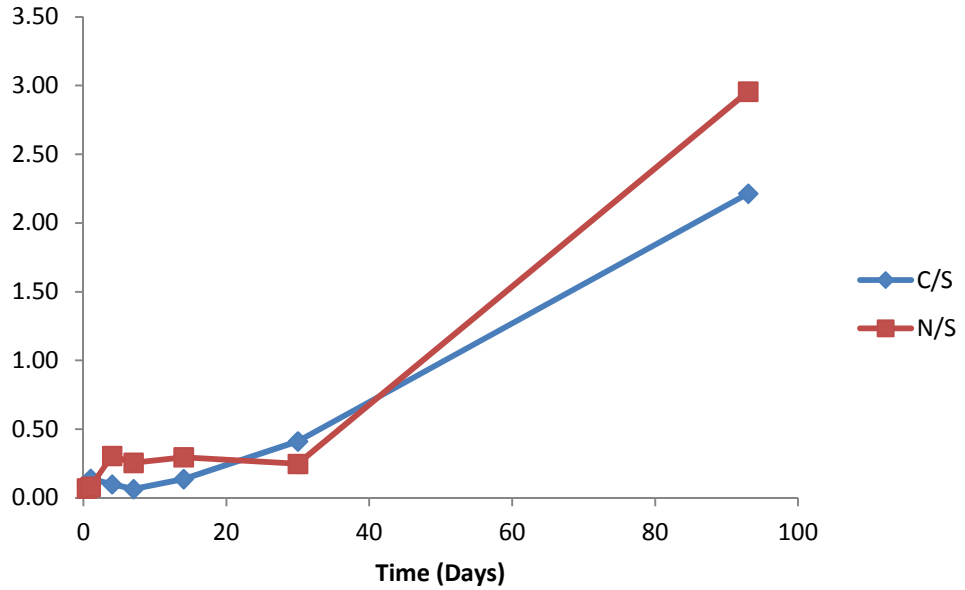

Figure 4.35: Precipitate Composition; $[Ca(OH)_2]_0$=0.023, $[NaOH]_0$=0.42, $[SiO_2]_0$=0.134

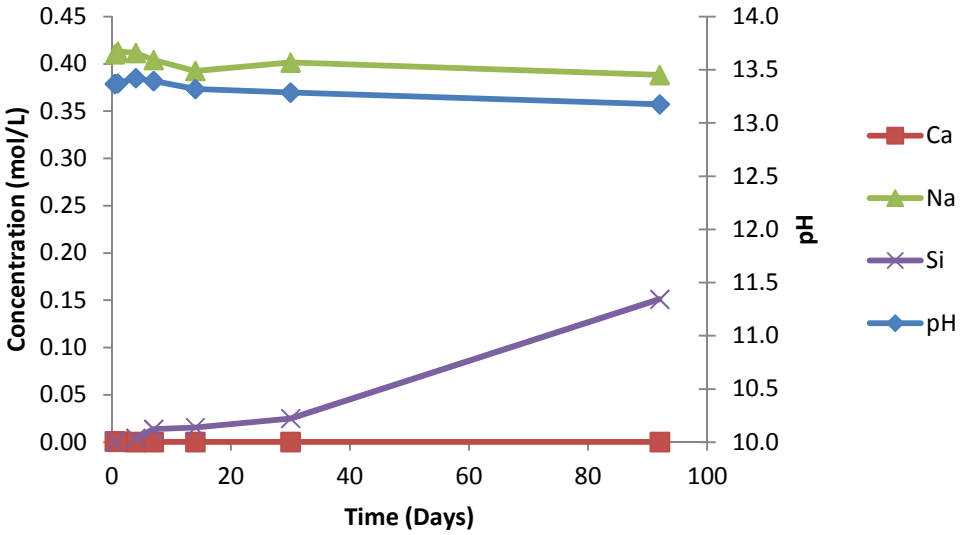

Figure 4.36: Concentration and pH vs. Time; $[Ca(OH)_2]_0$=0.023, $[NaOH]_0$=0.42, $[SiO_2]_0$=0.153

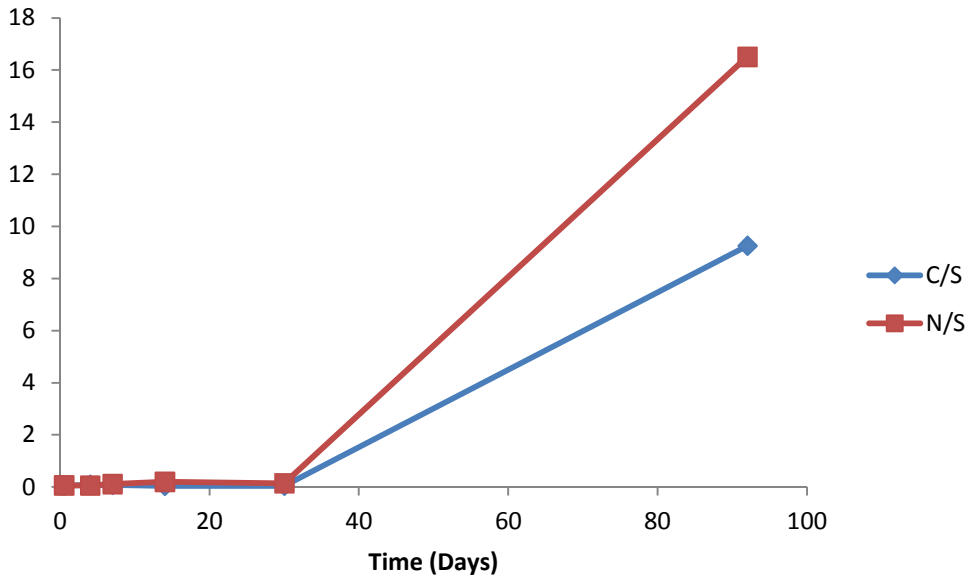

Figure 4.37: Precipitate Composition; $[Ca(OH)_2]_0$=0.023, $[NaOH]_0$=0.42, $[SiO_2]_0$=0.153

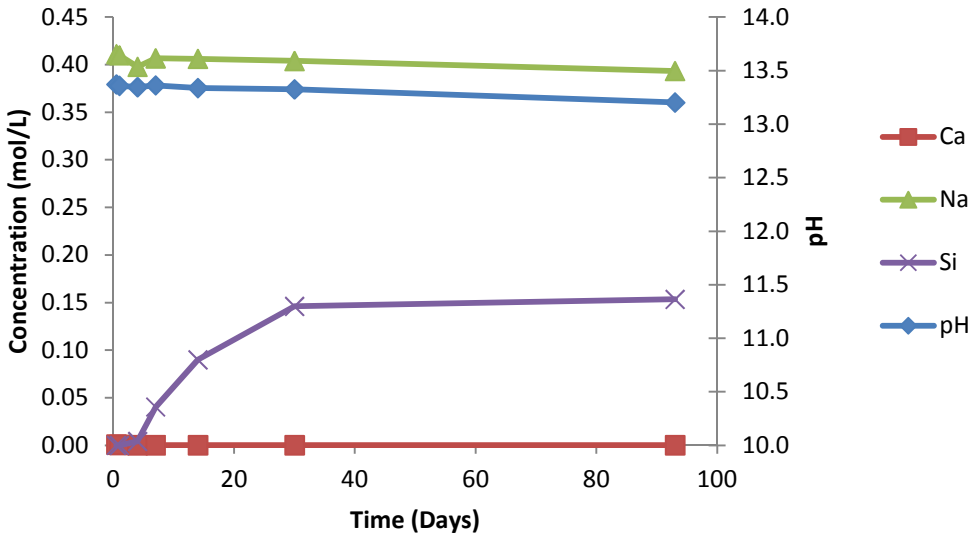

Figure 4.38: Concentration and pH vs. Time; $[Ca(OH)_2]_0$=0.023, $[NaOH]_0$=0.42, $[SiO_2]_0$=0.165

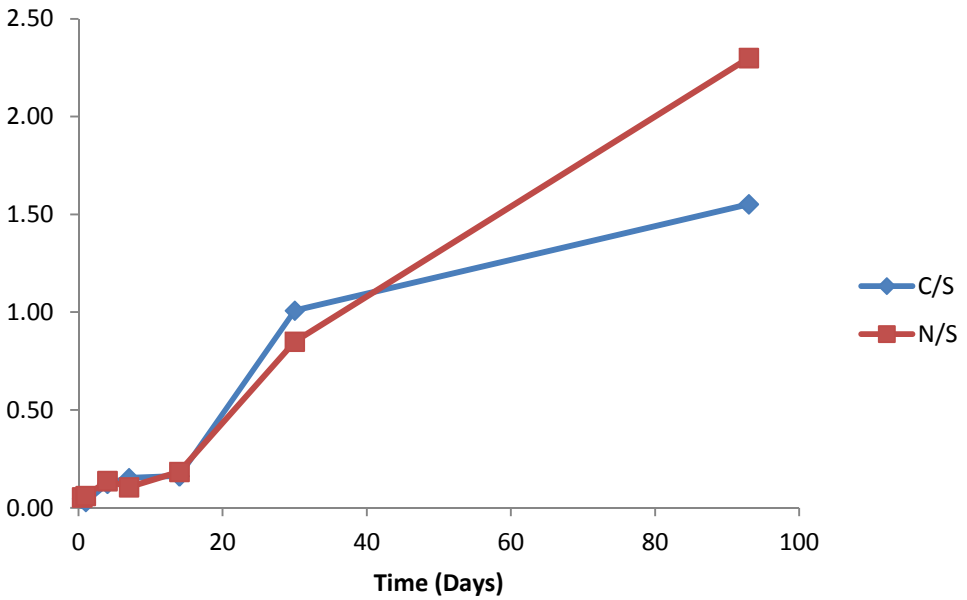

Figure 4.39: Precipitate Composition; $[Ca(OH)_2]_0$=0.023, $[NaOH]_0$=0.42, $[SiO_2]_0$=0.165

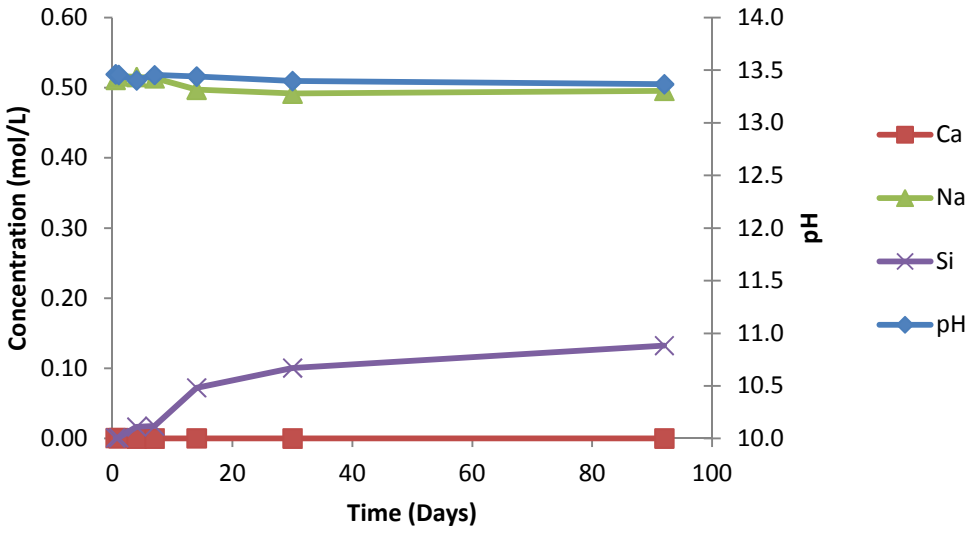

Figure 4.40: Concentration and pH vs. Time; $[Ca(OH)_2]_0$=0.023, $[NaOH]_0$=0.53, $[SiO_2]_0$=0.153

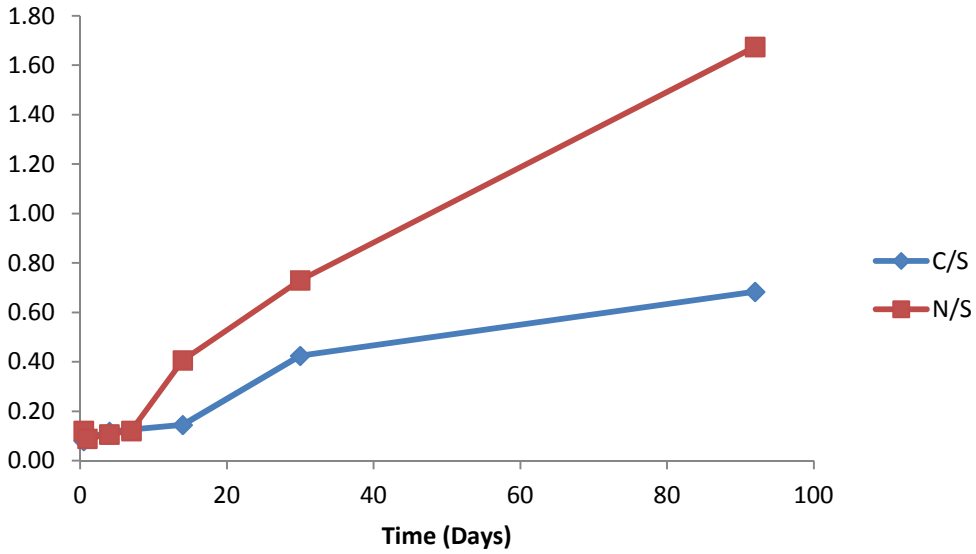

Figure 4.41: Precipitate Composition; $[Ca(OH)_2]_0$=0.023, $[NaOH]_0$=0.53, $[SiO_2]_0$=0.153

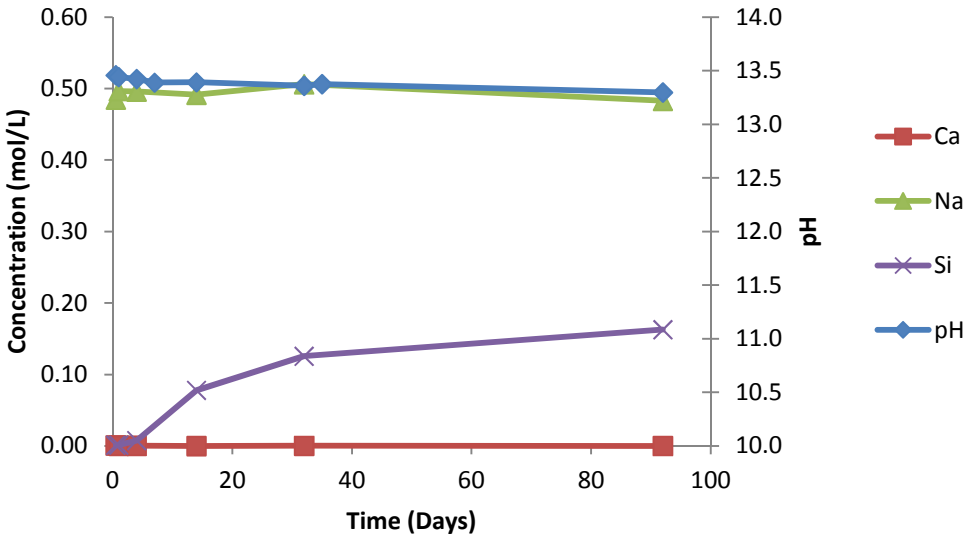

Figure 4.42: Concentration and pH vs. Time; $[Ca(OH)_2]_0$=0.023, $[NaOH]_0$=0.53, $[SiO_2]_0$=0.165

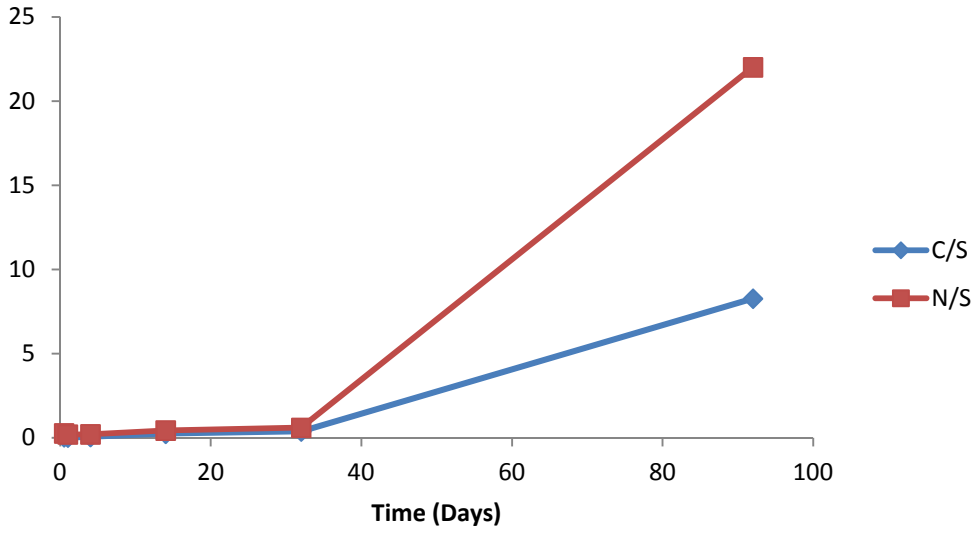

Figure 4.43: Precipitate Composition; $[Ca(OH)_2]_0$=0.023, $[NaOH]_0$=0.53, $[SiO_2]_0$=0.165

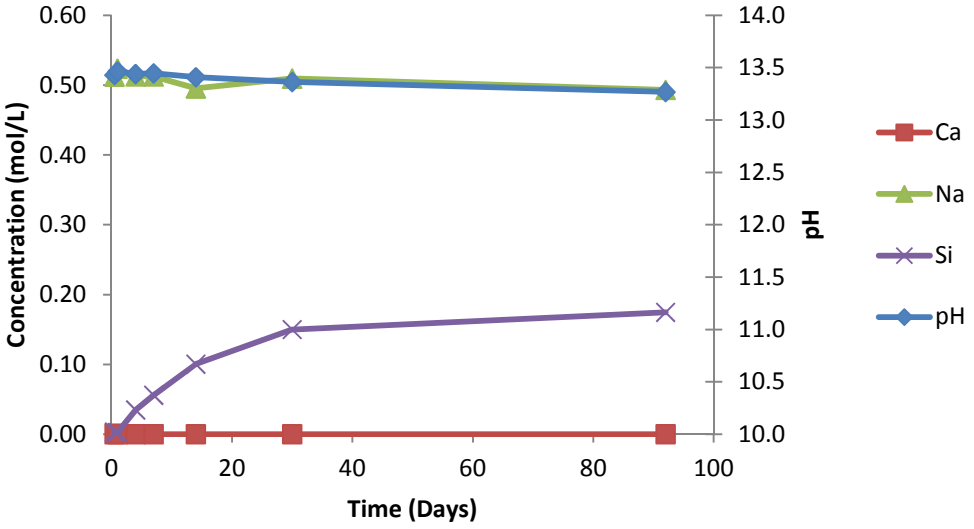

Figure 4.44: Concentration and pH vs. Time; $[Ca(OH)_2]_0$=0.023, $[NaOH]_0$=0.53, $[SiO_2]_0$=0.180

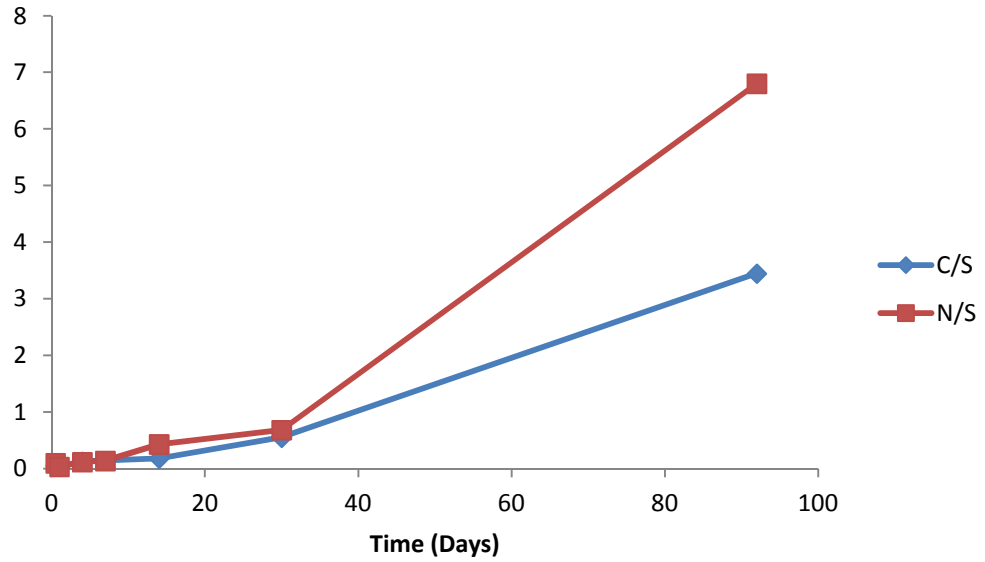

Figure 4.45: Precipitate Composition; $[Ca(OH)_2]_0$=0.023, $[NaOH]_0$=0.53, $[SiO_2]_0$=0.180

4.5 Precipitate Composition

Triaxial plots showing the composition of the reaction products are presented in this section. The figures are showing the values in atomic percent. The precipitate after 12 hours, 1 day, 4 days, 7 days, 7 days, 30 days and 92 days are shown in Figure 4.46 to Figure 4.52 respectively.

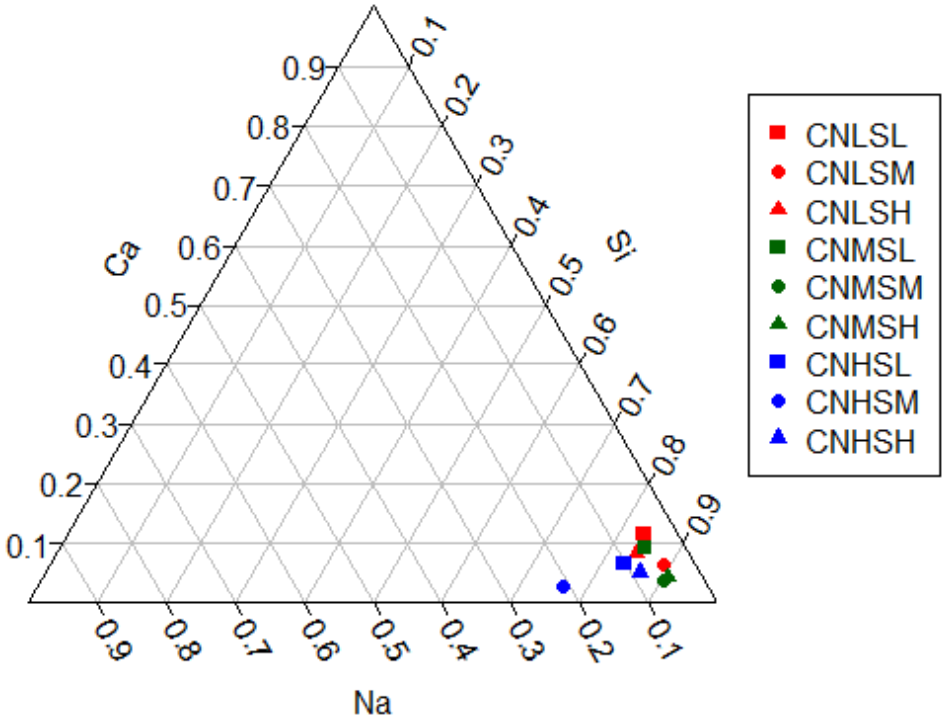

Figure 4.46: Precipitate Composition at 12 Hours

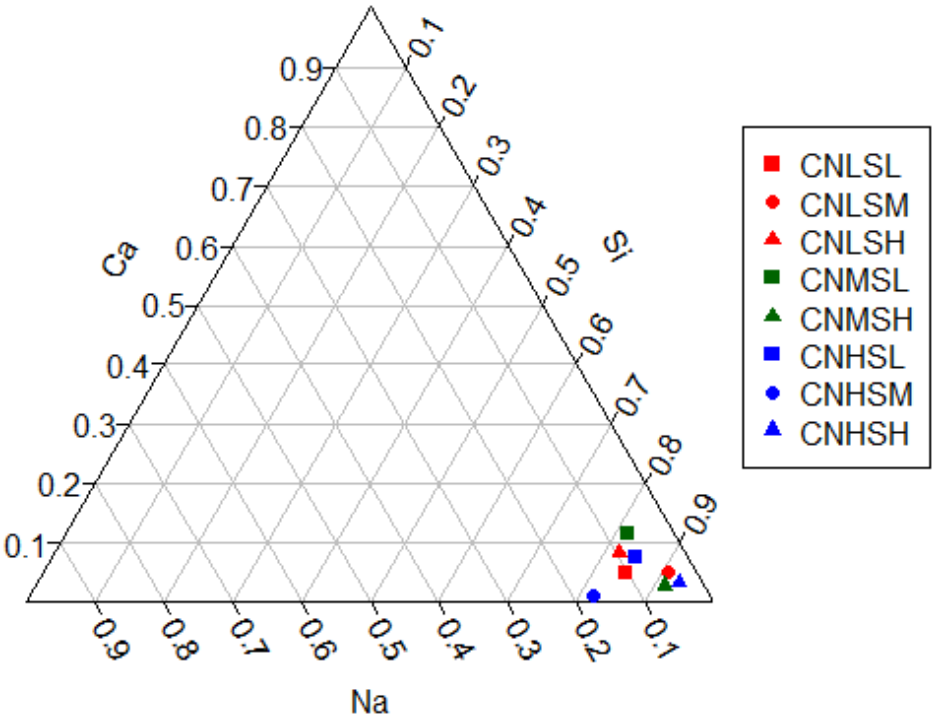

Figure 4.47: Precipitate Composition at 1 Day

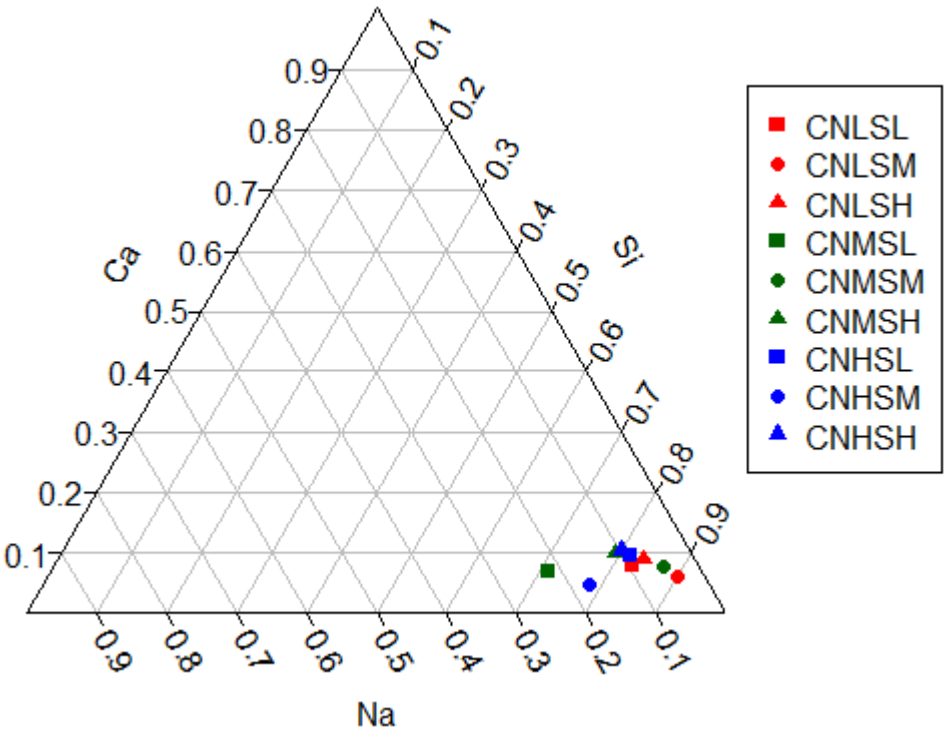

Figure 4.48: Precipitate Composition at 4 Days

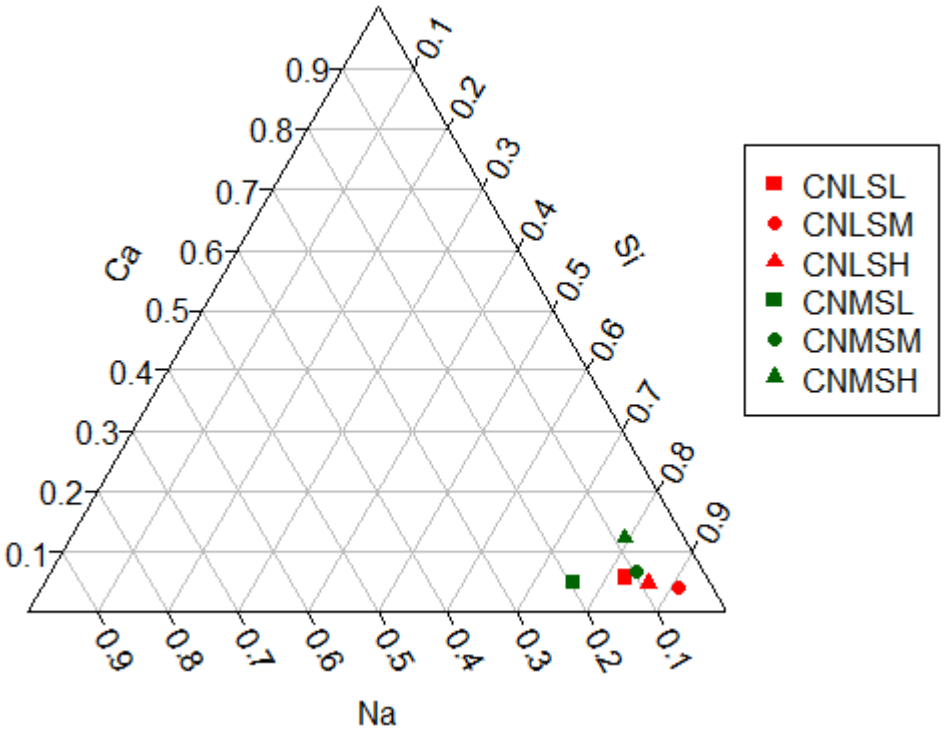

Figure 4.49: Precipitate Composition at 7 Days

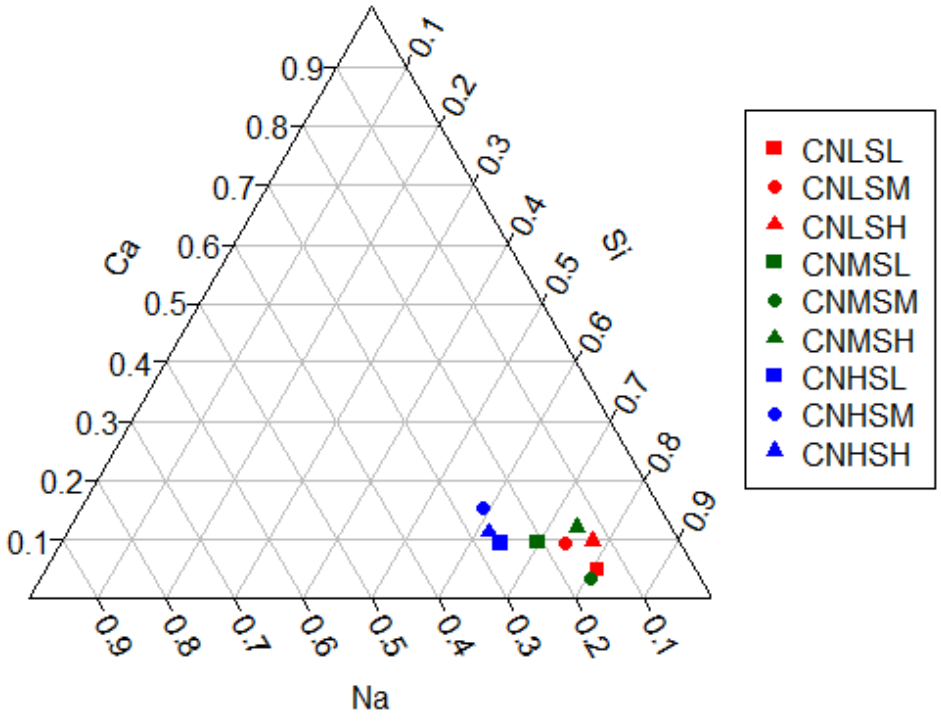

Figure 4.50: Precipitate Composition at 14 Days

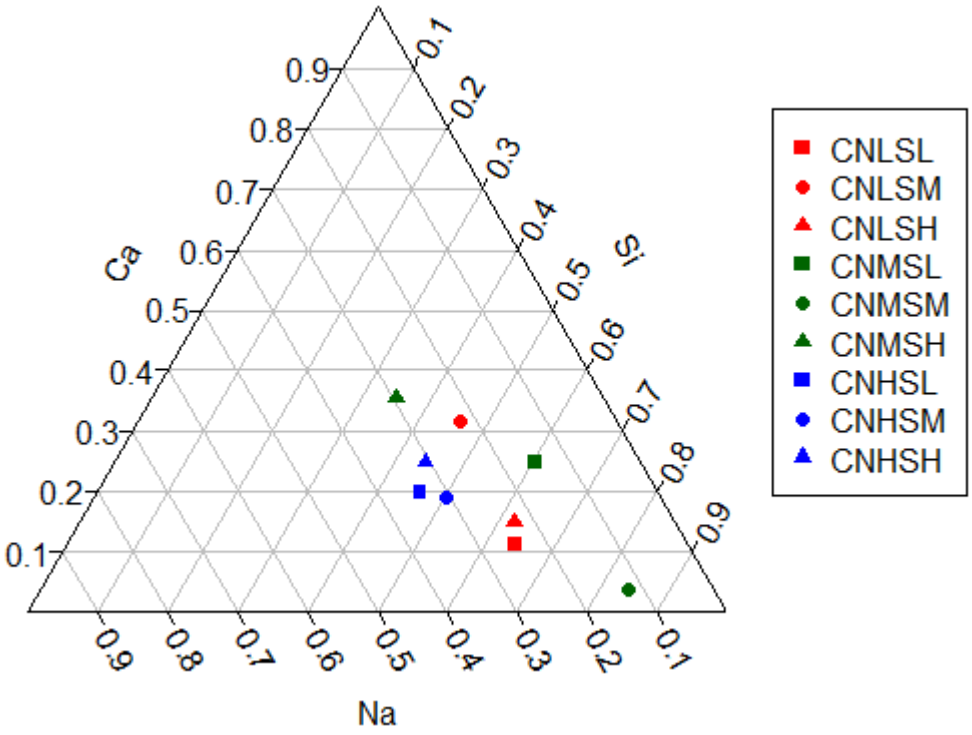

Figure 4.51: Precipitate Composition at 30 Days

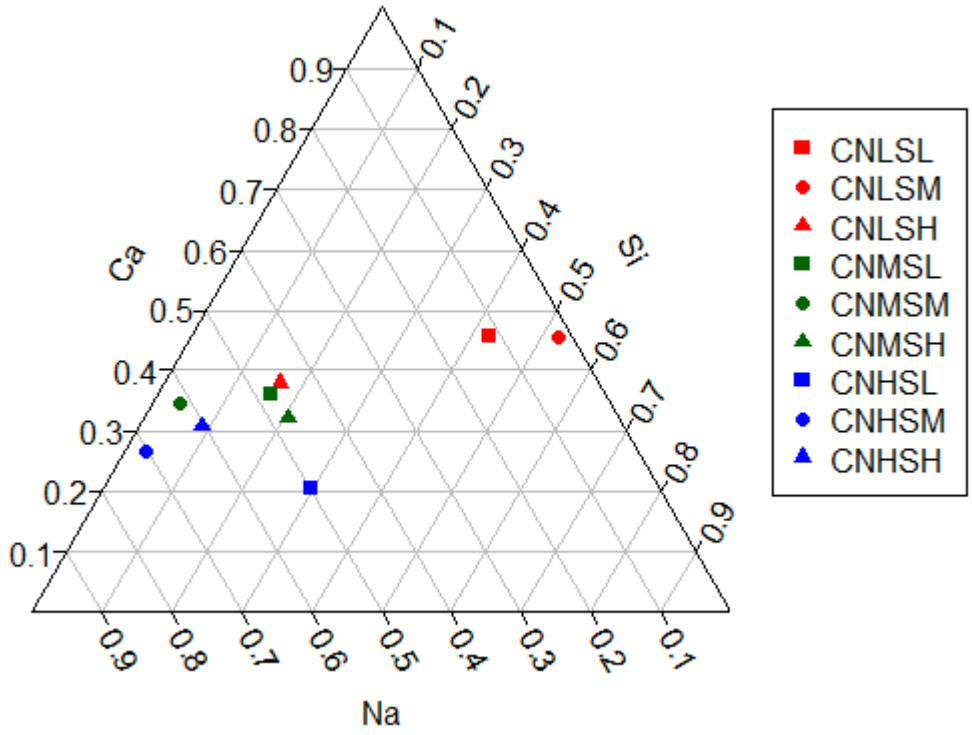

Figure 4.52: Precipitate Composition at 92 Days

5 Discussions and Analyses

5.1 Introduction

This chapter presents the analysis of the results presented in chapter 4. Section 5.2 presents the modeling of the silica dissolution and section 5.3 provides an analysis of the progression of the reaction products.

5.2 Silica Dissolution

The silica dissolution was modeled with the Hixson-Crowell cubic root law given in Equation 2-7. Linear regression was used to fit the data to the dissolution law. The intercept was forced to the initial concentration of silica. Additionally, the exponent in the expression was changed to better fit the data.

The Hixson-Crowell cubic root law was linearized in order to use linear regression to model the data. The linearized equation is shown as Equation 5-1, where the cubic root of the silicon concentration became y and intercept is the cubic root of the initial silicon concentration. The slope of the model is found by minimizing the sum of the squares of the difference between the real and fitted points, shown as Equation 5-2(Box, Hunter, & Hunter, 2005).

$$y = [Si]^n_{initial} - kt \qquad \textbf{Equation 5-1}$$

$$\mathrm{S} = \sum (y - [Si]^n_{initial} - kt)^2 \qquad \textbf{Equation 5-2}$$

No significant dissolution was observed in most of the solutions solely containing silica and calcium hydroxide. Only CMSH2 and CMSH3 had noticeable silica dissolution, as seen in Figure 4.10 and Figure 4.12. These solutions contained the lowest initial calcium to silica ratios and therefore, less calcium was available to react with the dissolved silicate ions that were able to remain in solution. Since the silica dissolution was observed mainly in the solutions containing sodium hydroxide, this section will focus on those samples.

5.2.1 Sodium Hydroxide and Silica

The dissolution rate of silica in the low medium and high concentrations of sodium hydroxide were fitted with Equation 5-1. The results are shown in Figure 5.1 to Figure 5.9.

Table 5.1: Coefficients for Dissolution Curves with Sodium Hydroxide and Silica

Sample	$[Si]_{initial}$	k	n
NLSL	0.115	-0.0044831	1/3
NLSM	0.134	1.09190	-1
NLSH	0.153	3.15810	-1
NMSL	0.134	0.216651	-1/2
NMSM	0.153	0.053165	-1/4
NMSH	0.165	10.8666	-2
NHSL	0.153	0.20466	-1
NHSM	0.165	0.11743	-1/2
NHSH	0.180	0.1678	-1/2

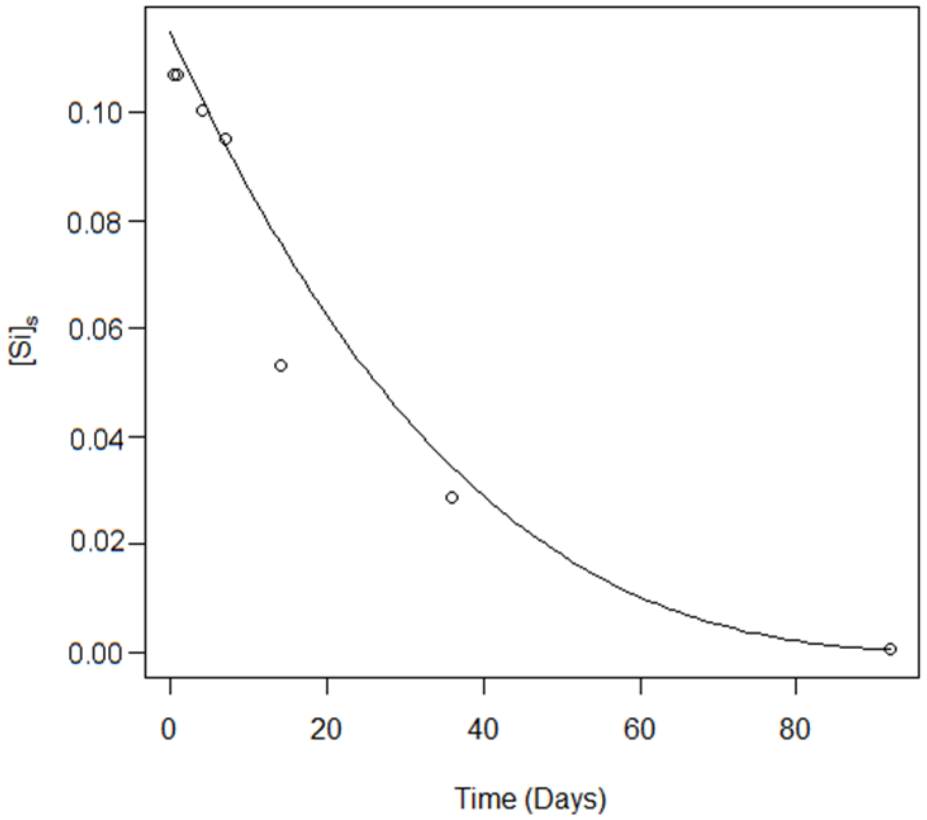

Figure 5.1: Silica Dissolution; $[NaOH]_0$=0.30, $[SiO_2]_0$=0.115

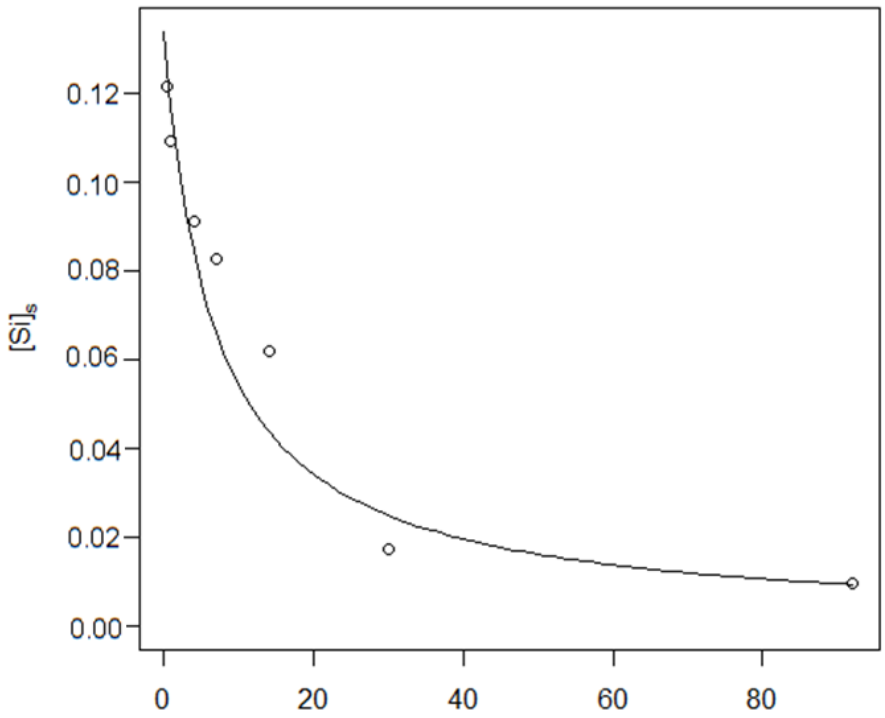

Figure 5.2: Silica Dissolution; $[NaOH]_0$=0.30, $[SiO_2]_0$=0.134

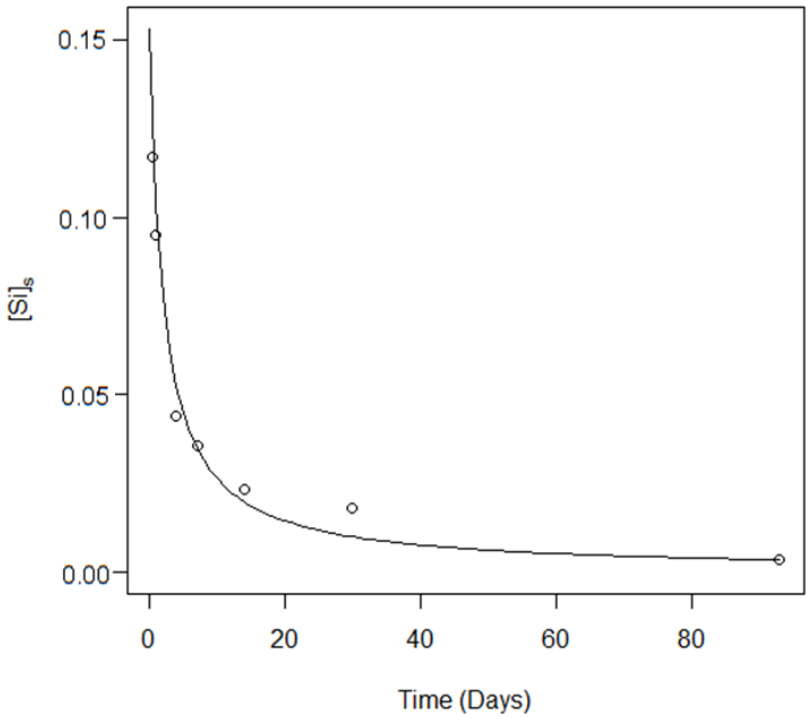

Figure 5.3: Silica Dissolution; $[NaOH]_0$=0.30, $[SiO_2]_0$=0.153

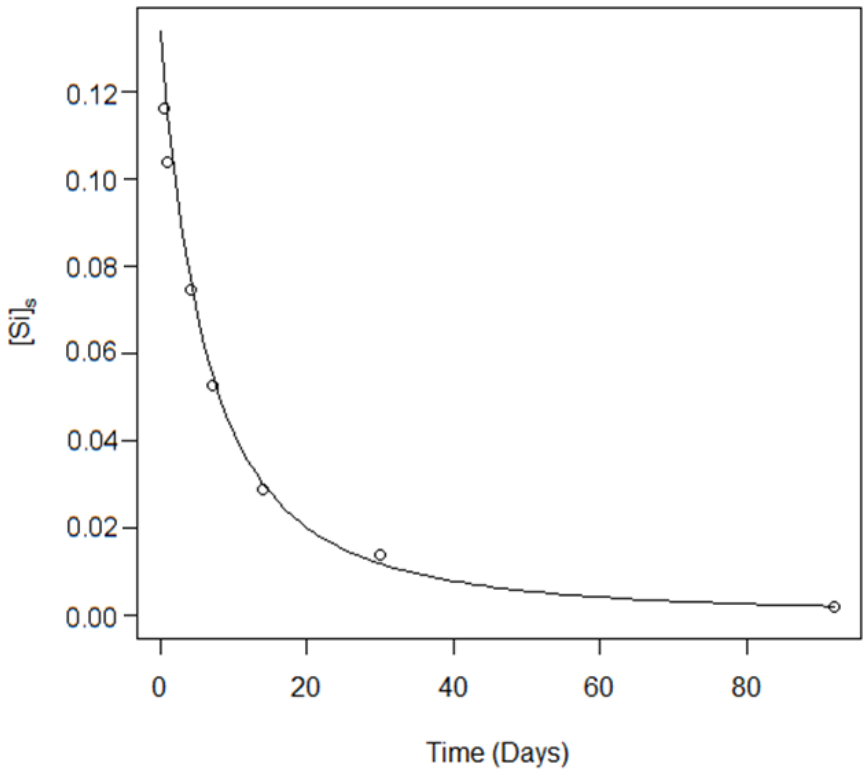

Figure 5.4: Silica Dissolution; $[NaOH]_0$=0.42, $[SiO_2]_0$=0.134

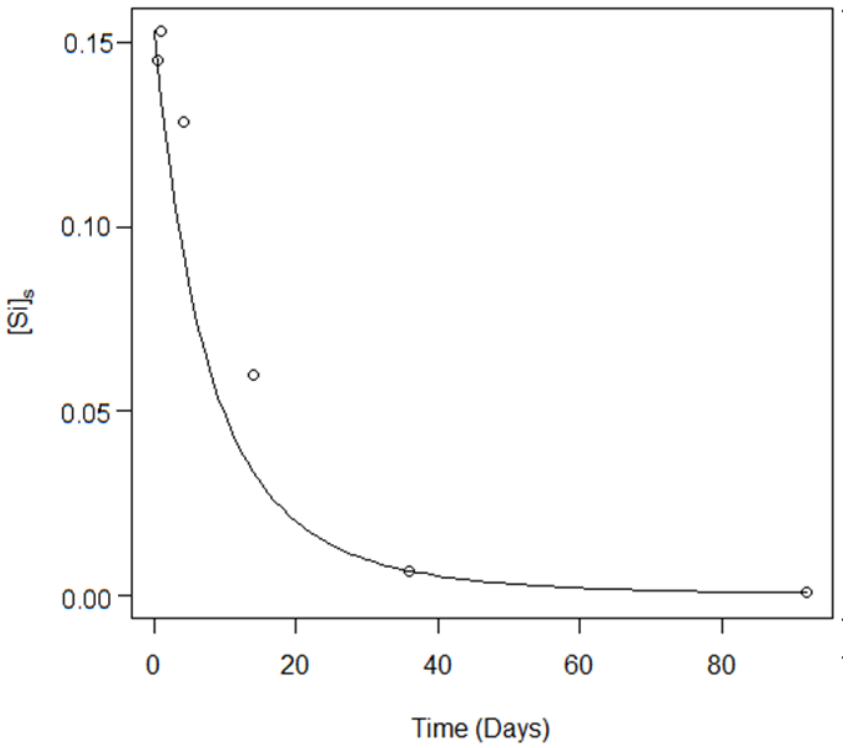

Figure 5.5: Silica Dissolution; $[NaOH]_0$=0.42, $[SiO_2]_0$=0.153

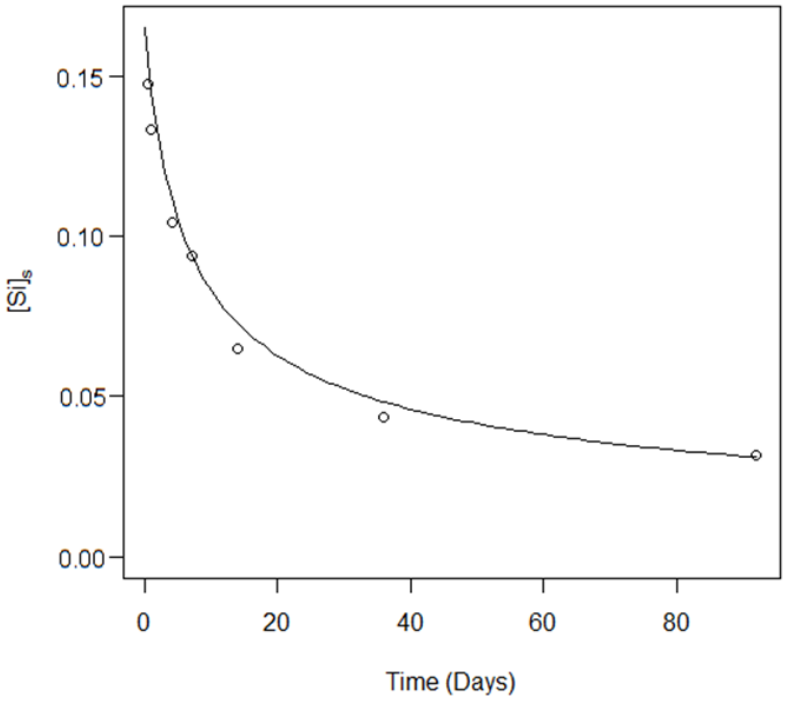

Figure 5.6: Silica Dissolution; $[NaOH]_0$=0.42, $[SiO_2]_0$=0.165

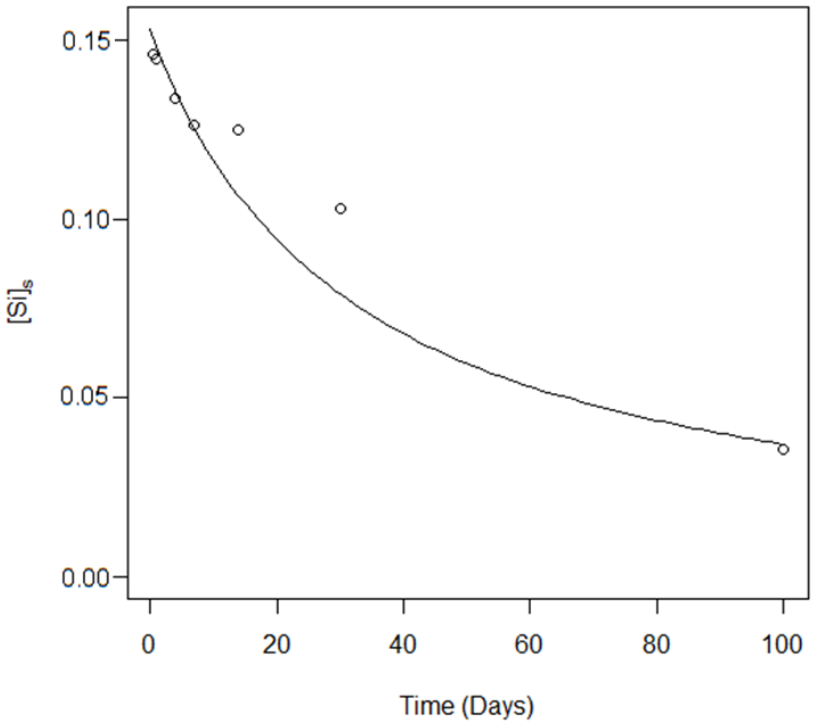

Figure 5.7: Silica Dissolution; $[NaOH]_0$=0.53, $[SiO_2]_0$=0.153

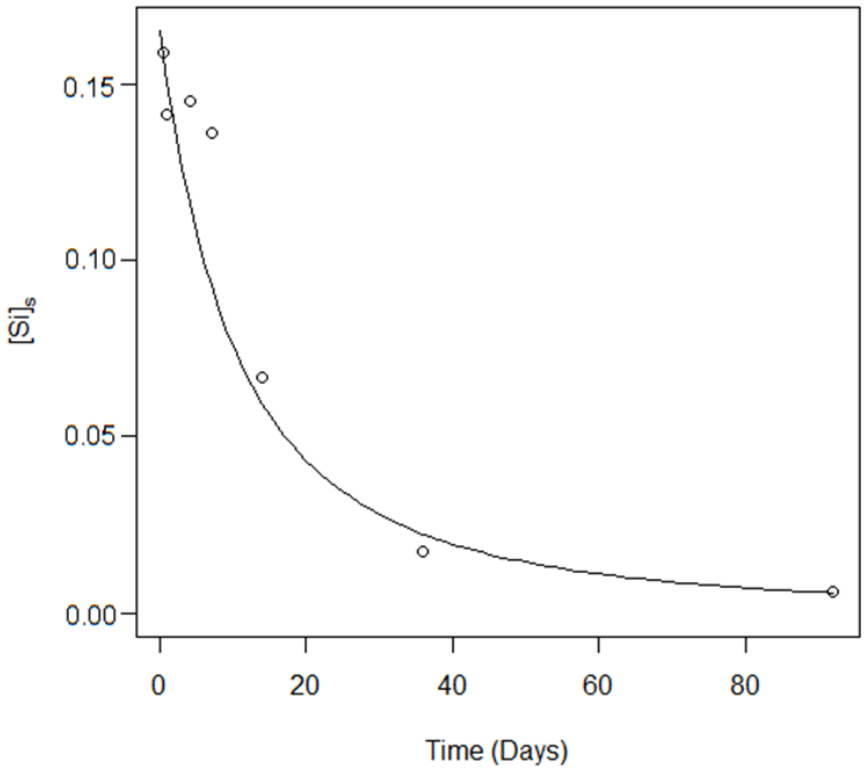

Figure 5.8: Silica Dissolution; $[NaOH]_0$=0.53, $[SiO_2]_0$=0.165

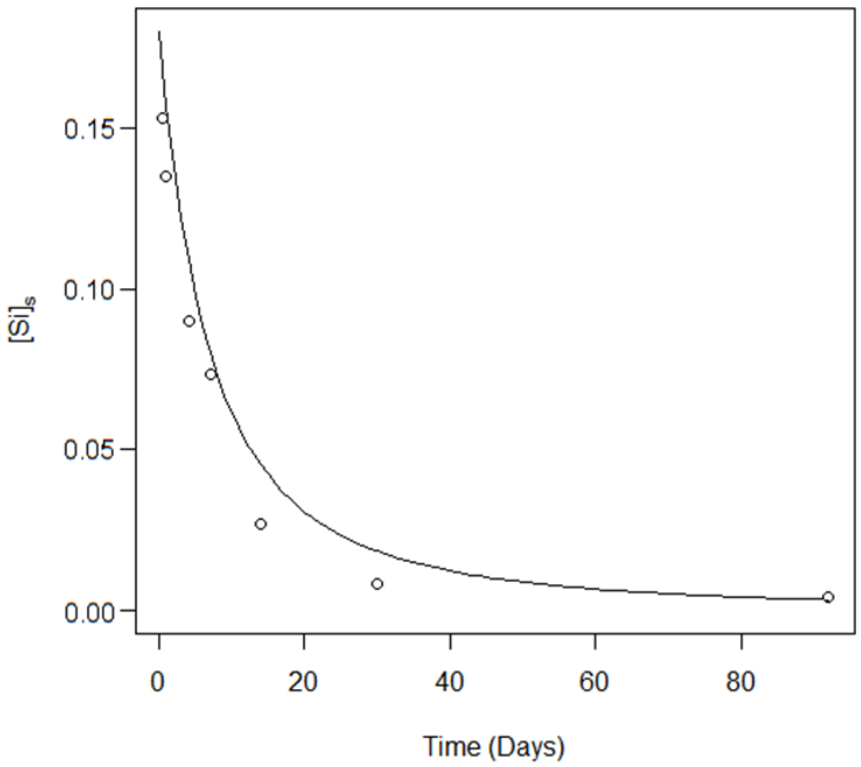

Figure 5.9: Silica Dissolution; $[NaOH]_0$=0.53, $[SiO_2]_0$=0.180

5.2.2 Calcium Hydroxide, Sodium Hydroxide and Silica

The dissolution rate of silica in the sodium hydroxide and calcium hydroxide solution was fitted to Equation 5-1. The results are shown in Figure 5.10 to Figure 5.18.

Table 5.2: Coefficients for Dissolution Curves with Calcium Hydroxide, Sodium Hydroxide and Silica

Sample	$[Si]_{initial}$	k	n
CNLSL	0.115	-0.0023743	1/3
CNLSM	0.134	0.49934	-1
CNLSH	0.153	-0.0037712	1/3
CNMSL	0.134	-0.0035547	1/3
CNMSM	0.153	-0.0040633	1/3
CNMSH	0.165	0.91641	-1
CNHSL	0.153	0.45262	-1
CNHSM	0.165	-0.0048228	1/3
CNHSH	0.180	0.0428363	-1/3

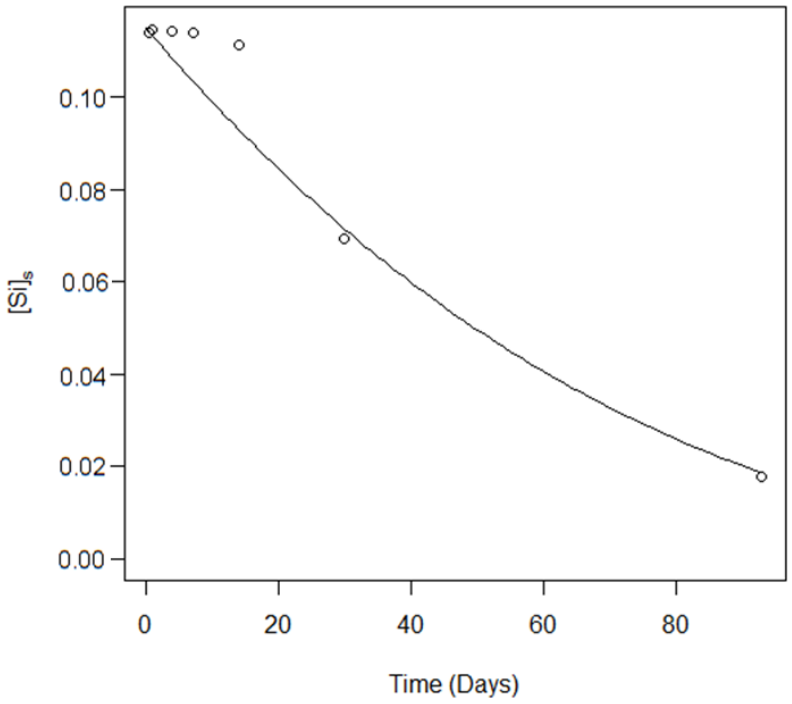

Figure 5.10: Silica Dissolution; $[Ca(OH)_2]_0$=0.023, $[NaOH]_0$=0.30, $[SiO_2]_0$=0.115

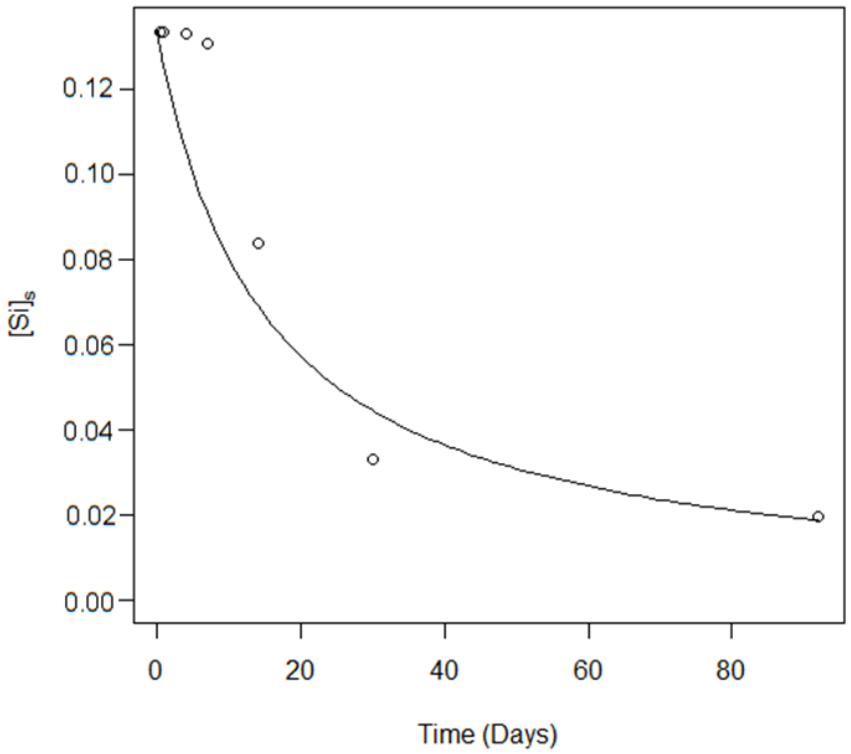

Figure 5.11: Silica Dissolution; $[Ca(OH)_2]_0$=0.023, $[NaOH]_0$=0.30, $[SiO_2]_0$=0.134

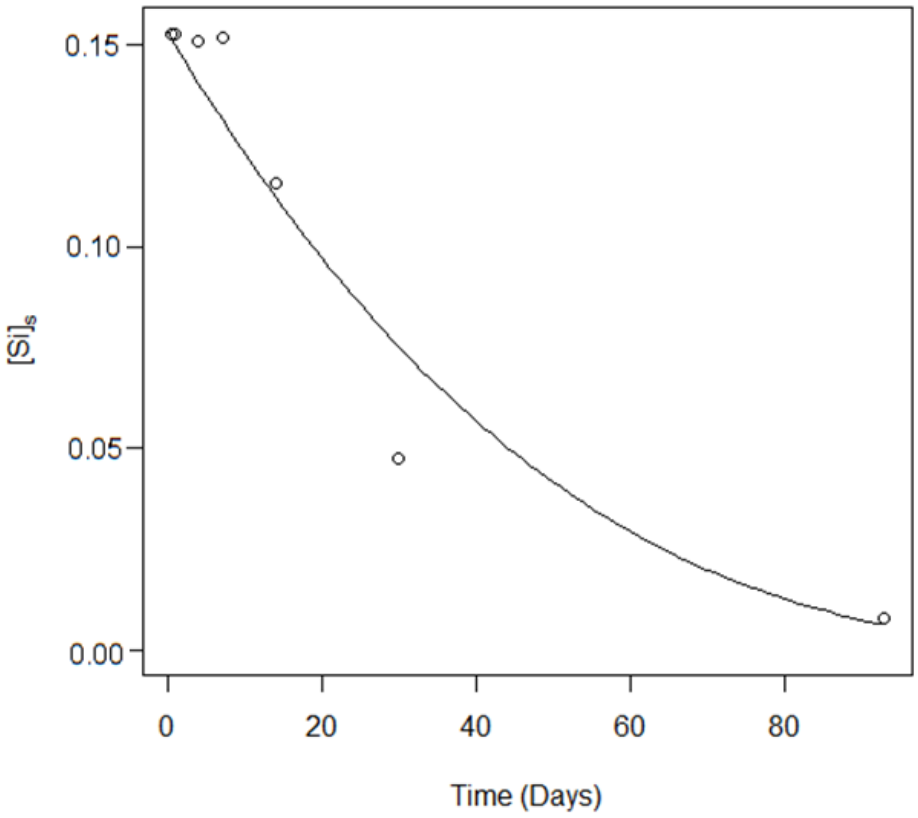

Figure 5.12: Silica Dissolution; $[Ca(OH)_2]_0$=0.023, $[NaOH]_0$=0.30, $[SiO_2]_0$=0.153

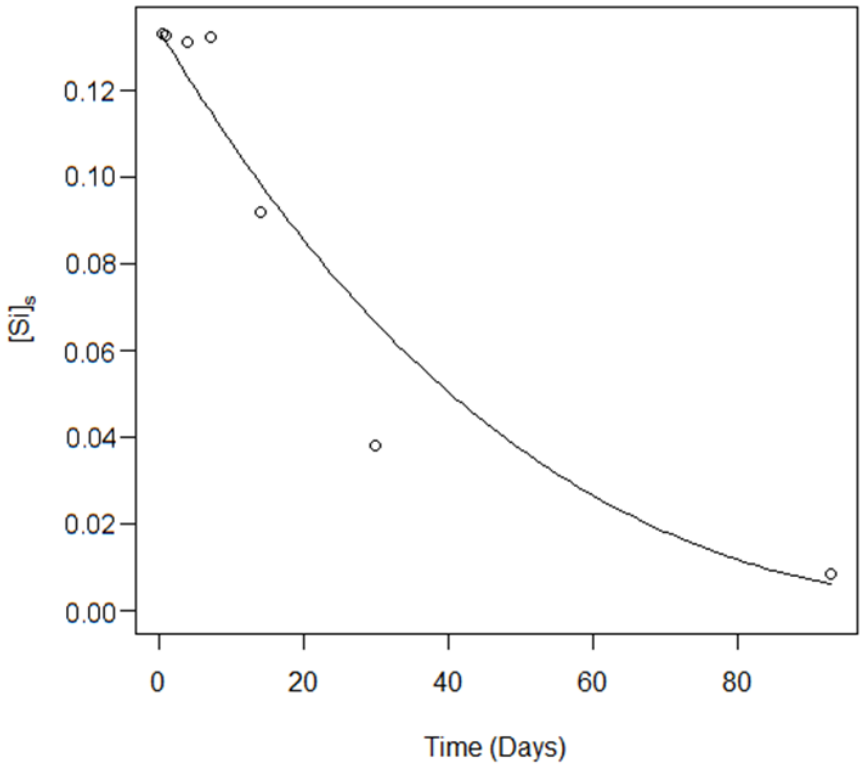

Figure 5.13: Silica Dissolution; $[Ca(OH)_2]_0$=0.023, $[NaOH]_0$=0.42, $[SiO_2]_0$=0.134

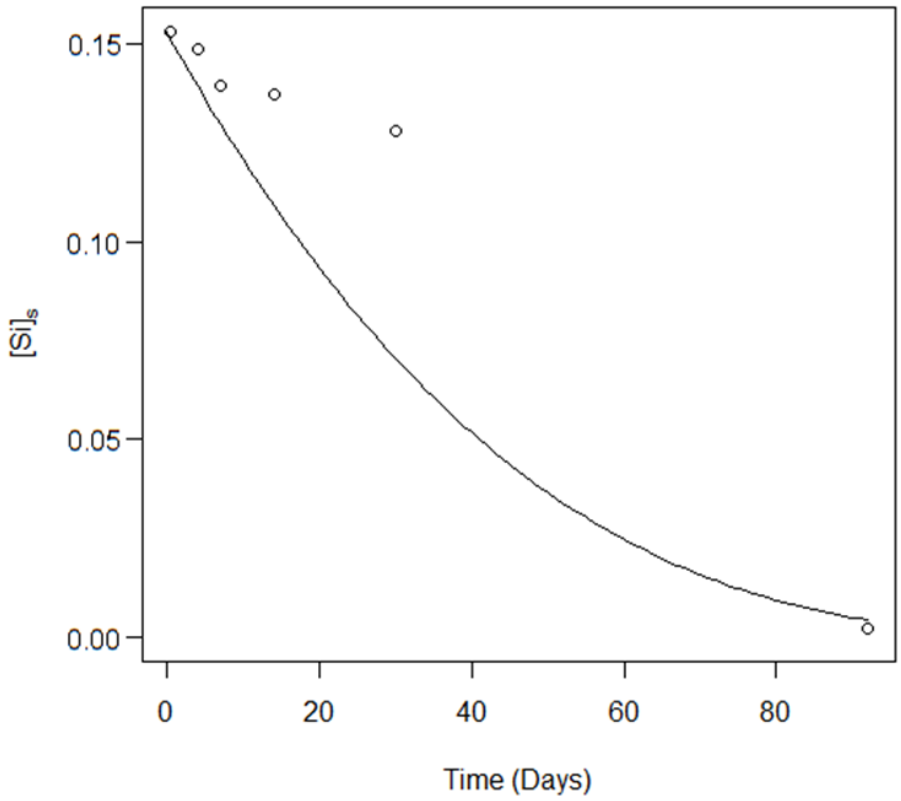

Figure 5.14: Silica Dissolution; $[Ca(OH)_2]_0$=0.023, $[NaOH]_0$=0.42, $[SiO_2]_0$=0.153

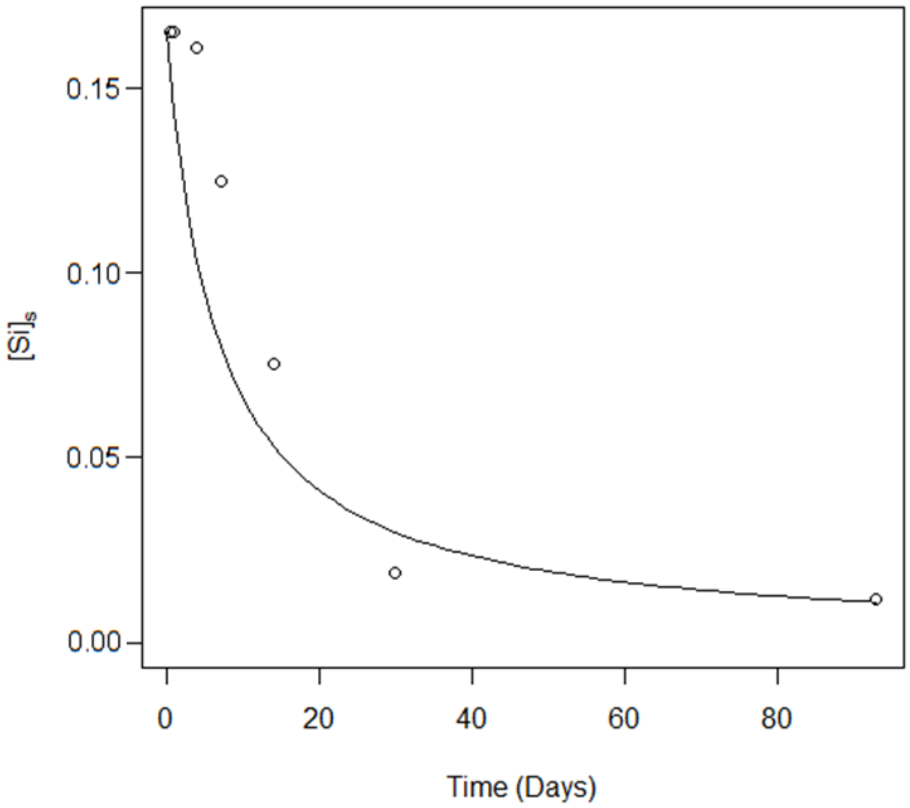

Figure 5.15: Silica Dissolution; $[Ca(OH)_2]_0$=0.023, $[NaOH]_0$=0.42, $[SiO_2]_0$=0.165

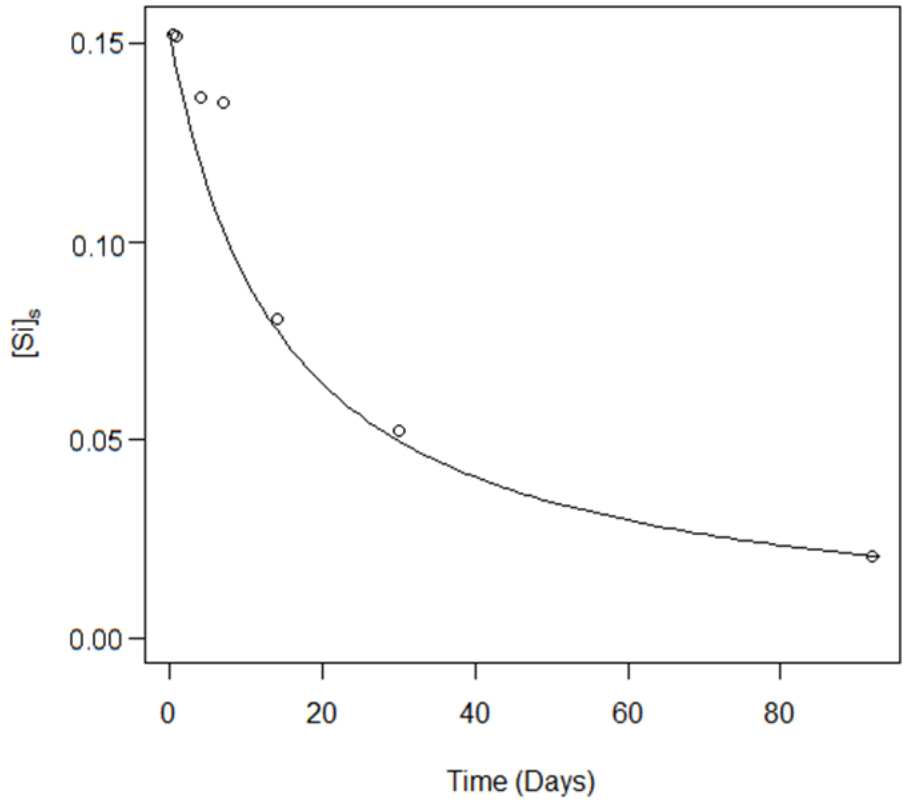

Figure 5.16: Silica Dissolution; $[Ca(OH)_2]_0$=0.023, $[NaOH]_0$=0.53, $[SiO_2]_0$=0.153

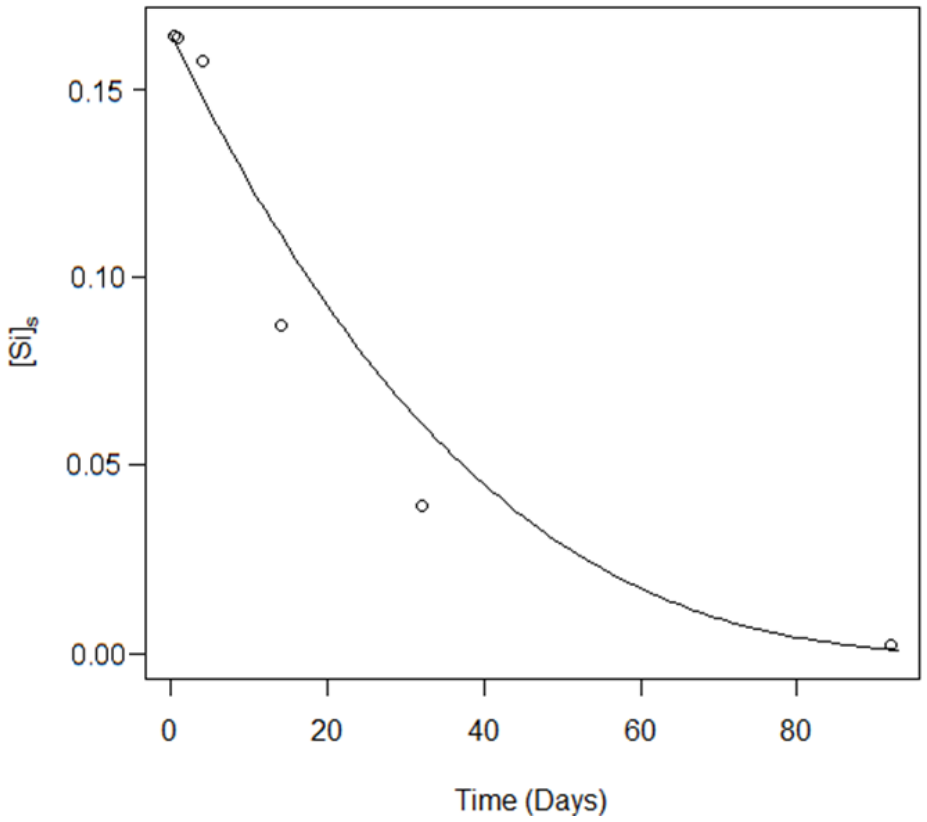

Figure 5.17: Silica Dissolution; $[Ca(OH)_2]_0$=0.023, $[NaOH]_0$=0.53, $[SiO_2]_0$=0.165

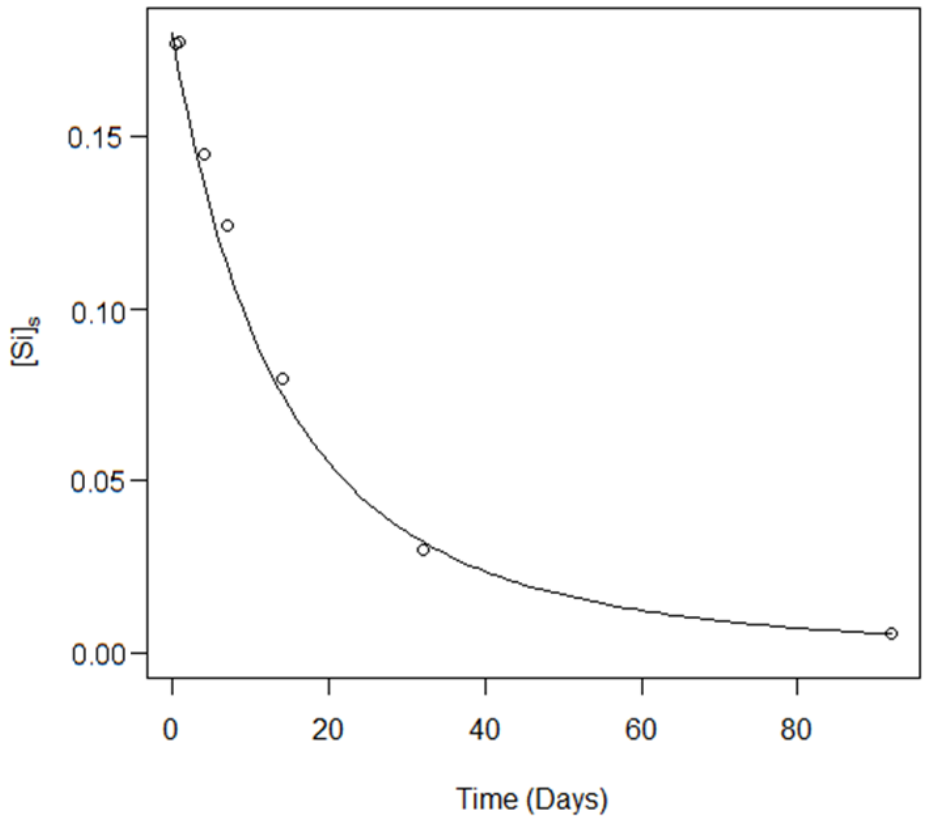

Figure 5.18: Silica Dissolution; $[Ca(OH)_2]_0$=0.023, $[NaOH]_0$=0.53, $[SiO_2]_0$=0.180

5.2.3 Discussion

The dissolution of silica has been fit to the Hixson-Crowell dissolution law. The solutions containing only silica and sodium hydroxide show dissolution curves that are steeper than those that would be expected from the Hixson-Crowell dissolution law. This indicates that the silica has a higher initial rate of dissolution than expected.

The fitted dissolution curves for the sodium hydroxide and silica solutions demonstrate how the dissolution is affected by the concentrations of the two components. The dissolution of the silica in the solution NLSL, as shown in Table 5.1, is the only dissolution curve that has an exponential curve of 1/3, fitting the Hixson-Crowell dissolution law. The rest of the solutions dissolve faster, necessitating the use of different exponents. In general, when the initial concentration of sodium hydroxide is held constant, the dissolution rate increases as the quantity of silica increases. This is the same conclusion as found by Greenberg (1957). The only sample that did not follow this trend was NMSH, see Table 5.1. This sample contained the highest amount of silica

among the solutions with an initial sodium hydroxide concentration of 0.42M, yet it experienced the slowest dissolution rate.

The dissolution rate of silica in the solution when the quantity of silica is held constant led to contradicting results. The samples that initially contained 0.134M of silica demonstrated that as the sodium hydroxide concentration increased, the dissolution rate also increased. The same trend was displayed in the samples that initially contained 0.165M of silica. The samples that contained 0.153M of silica behaved in the opposite manner; when the solution's sodium hydroxide concentration increased, the dissolution rate decreased.

The solutions containing silica, calcium hydroxide and sodium hydroxide dissolved closer to the Hixson-Crowell cubic root law than the ones without the calcium hydroxide. The addition of calcium hydroxide has slowed the dissolution rate of the silica, indicating a reacted layer has formed; similar to those modeled by Ichikawa (2009). In order to use Ichikawa's model, the experiment would need to be repeated with larger spherical silica particles. The thickness of the reaction layer would be measured and particles would require observation for cracking.

The fitted dissolution equations demonstrate the quantity of silica that is present in the solution. When the concentration of sodium hydroxide is held constant, the solutions with the smallest initial concentration of silica dissolve at the slowest rate. The solutions with initial sodium hydroxide concentrations of 0.42M and 0.53M dissolved at rates proportional to their concentration of silica. This trend also appeared in the solutions without the calcium hydroxide. The solutions with an initial sodium hydroxide concentration of 0.30M behave differently than the other solutions; the solution with the medium level of silica dissolved the fastest. When the initial concentration of silica is held constant, the solutions with the higher levels of sodium dissolve most rapidly.

While the rate of dissolution predominantly followed the cubic root law, the initial dissolution rate was slow; similar to the experiment by Dron and Brivot (1993). The modeled dissolution does not include this initial portion of the curve. Since this is not observed in the solutions without calcium hydroxide, the calcium is causing this initial retardation. This phenomenon is more evident in the solutions containing lower initial sodium concentrations.

The dissolution of silica in this experimental program is similar to what is expected when using glass particles instead of pure silica. Kouassi et al. found that when the pH

of the solution is increased, the dissolution rate increased. The three stages of dissolution would not have occured as identified by Kouassi since the silicon remained unsaturated in the solution. Had the pH of the solution been below 10.7, the silica would have reached saturation and these stages could have occured. Since concrete has a higher pH, this is not expected to occur in a concrete-glass system.

5.3 Reaction Progression

5.3.1 Calcium and Silica

The solutions composed of calcium and silica showed the level of calcium in the solution slowly lowering and the quantity of silica in the solution remaining negligible or increasing slightly. The samples that contained low initial silica and calcium concentrations often did not produce enough precipitate to test with the TGA so the calcium to silica ratio in the reacted product is unknown. These solutions would need to be repeated with a larger volume in order to produce more precipitate to find this data.

There are some large jumps in the concentration measurements of the calcium in the solutions. It is possible that these were caused by differences in handling the solutions before they were filtered. If some of the solutions were jostled more than others, some of the calcium hydroxide in precipitate form could have entered the solution. This would cause a measurement that is unnaturally high.

The calcium to silica ratio in the precipitate remained low at approximately 0.1 for most of the solutions. The calcium bonded to the silica very slowly over the course of the testing. The only abnormal sample was the one with high initial concentrations of calcium hydroxide and very low concentrations of silica. As seen in Figure 4.15, C/S ratios started around 5.5 and increased to approximately 7. The other two solutions with the low initial concentration of silica did not produce enough precipitate to measure, so it is unknown whether they displayed the same trend.

Barret et al. found that the silica in their samples dissolved faster than it could react with the lime in the solution (1977). The opposite occurred in this experiment; the calcium is exiting the solution more rapidly than the silica is entering. This indicates that the rate determining step is the dissolution of the silica; whereas it was the precipitation in Barret et al.'s observations.

As observed by Greenberg, the rate of reaction is proportional to the quantity of silica in the solution (1961). This can also be seen in Figure 4.8, Figure 4.10 and Figure

4.12. In these plots, the initial level of calcium hydroxide is held constant and the concentration of silica was varied. The solution containing the lower level of silica is the slowest to reach equilibrium and the solution with the highest concentration reaches equilibrium much more rapidly.

5.3.2 Sodium and Silica

The samples containing silica and sodium hydroxide have the silica dissolving and a small amount of the sodium reacting with the silica. In comparison with the solutions without the sodium, the silica has dissolved much more rapidly. This is due to the higher pH in the solutions and because alkalis act as a catalyst in the dissolution process.

The sodium levels remained high throughout the testing; indicating that not much had reacted with the silica. Additionally, the pH values dropped only slightly. The silica dissolved and reacted with the hydroxide ions forming various reaction products, some being $Si(OH)_4$, $Si(OH)_3^-$, $SiO_2(OH)_2^2$, $Si_4O_4(OH)_6^{2-}$ and $Si_4O_4(OH)_4^{4-}$. These products are in equilibrium according to Equation 2-1 to Equation 2-5. While these products could not be identified through the testing methods performed, they are known to exist in the solutions due to the high pH.

5.3.3 Calcium, Sodium and Silica

The samples containing calcium hydroxide, sodium hydroxide and silica showed behaviours evident in the solutions with just two components. The dissolution of the silica in the sodium hydroxide competed with the reaction of the calcium on the surface of the silica. As can be observed, the silica dissolves rapidly into the solution while the calcium concentration remains very low and the sodium slowly exits the solution. The pH level also decreases slightly, similar to the solutions with the sodium hydroxide and silica.

The level of calcium ions in the solution remained low throughout the entire testing period due to the common ion effect. The high concentration of sodium hydroxide in the solution caused the solubility of the calcium hydroxide to be suppressed according to Figure 2.5. When some hydroxide from the solution reacted with the silica, more calcium hydroxide was able to enter the solution and react with the silicate ions. From the TGA testing, it was observed that the solutions remained saturated in calcium hydroxide throughout the entire testing period.

The reacted precipitate started as mostly silica and progressed to a combination of silica, sodium and calcium. The composition of the precipitate over the course of the

experiment can be seen in Figure 4.46 to Figure 4.52. At twelve hours, the precipitate was extremely similar for all of the samples. Since the reaction had just commenced, the product is mostly silica. The solutions containing the highest initial concentration of sodium have the highest levels of sodium in the precipitate. At one day, the composition of the reaction product is extremely similar as at twelve hours. It can be seen in the concentration and pH versus time plots for the three component systems in section 4.4 that the silica has not dissolved much into the solution while the sodium and calcium concentrations have not altered much. Therefore not much change in the precipitate was expected.

At four days, the samples were still essentially silica. As seen in the concentration and pH versus time plots, the silica dissolution is in its initial stagnant phase. The level of calcium in the precipitate had risen to approximately 10 percent for all the samples. The sample CNMSL contained the most sodium at approximately 22 percent. At the seven day mark, many of the results were unable to be measured due to the quantity of precipitate gathered being too low to analyze with the TGA. The samples that were measured did not differ greatly from the composition at four days.

At fourteen days, the level of sodium in the reaction product had increased. A distinction can be seen between the products with different initial levels of sodium. The concentration in the products was proportional to the initial concentration. At this point, the level of calcium has increased very slightly up to approximately 10 percent of the sample.

At thirty days, a drastic change has occurred in the composition of the reaction product. A significant increase in the quantity of calcium can be observed. The mixes with the highest initial concentration of sodium now have from 20 to 25% calcium in the reaction product. The mixes with the medium level of initial sodium are extremely varied in terms of the quantity of calcium and silica. The mix CNMSM contains approximately 5% calcium, 12% sodium and 83% silica, and the mix CNMSH contains approximately 35% calcium, 30% sodium and 35% silica. The composition of these reaction products do not correlate with the initial concentration of silica. The products at this point contain concentrations of silica and calcium that would be found in ASR. The composition of ASR from field samples is seen in Figure 2.1, the reaction products from the samples CNMSM, CNMSL, CNLSM, CNLSH and CNLSL would fit well with those found by Thaulow, Hjorth Jakobsen and Clark. The other samples have a similar C/S ratio but contain more sodium.

The samples at ninety two days have evolved to contain more sodium and less silica. The products that could have been considered ASR at 30 days now contain very little silica. It can be seen in the concentration and pH versus time plots that the silica has mostly dissolved and reaction rims have not prevented dissolution. The reaction product at this point has progressed past what would be considered ASR and C-S-H and now has extremely large concentration of sodium. However, two of the samples, CNLSL and CNLSM, contain low amounts of sodium. Those samples contained low initial concentrations of sodium and silica. The final composition of these samples were similar to C-S-H. It is possible that these solutions developed reaction rims that were unable to be dissolved because the pH was lower.

Similarly to Kalousek, the samples did not undergo any visual changes throughout the experiment. Over time, more of the precipitate would get stuck to the sides of the bottle, however when it was filtered, the consistency was still the same. The equilibrium of the solutions differed between these experiments. Kalousek's ratio of sodium to silica was approximately 0.5 and was significantly lower than what was measured in this experiment. The ratio of calcium to silica was between 1.0 and 1.5, which was also lower than what was measured at the end of the experiment. The precipitate was closest to Kaolusek's values at thirty days. After this time, the silica continued to dissolve causing the ratios to increase. Kalousek did not have his samples being mixed continuously as in this experiment. They were mixed initially and then once per day. Therefore, the dissolution rate would have been slower and more silica would still be in the precipitate. The two samples that formed reaction product similar to C-S-H, CNLSL and CNLSM, displayed equilibrium compositions similar to those in Kalousek's experiment. These solutions did not dissolve to the extent of the others and thus had higher silica contents.

Macphee et al. studied systems similar to those in this experiment. Their range of concentrations was larger and their time frame was longer. The calcium to silica ratios at equilibrium for the samples in this experiment were between 0.6 and 9.0 with the median value of 2.2, which were higher than those by Macphee et al. with an 0.8M initial sodium hydroxide concentration. As seen in Figure 2.11, their samples reached their equilibrium concentrations much faster than the ones in this experiment. It is possible that those samples were mixed more rapidly, causing them to react faster. Macphee et al. reported their calcium to silica ratios having a maximum at approximately fifty days for their samples with 0.2M initial sodium hydroxide. The

samples with low sodium hydroxide in this experiment did not have this maximum. The ratio of calcium to silica rose and reached a maximum at the end of the testing period.

The trends in Macphee et al.'s solutions matched the ones in this work. Figure 2.8 and Figure 2.9 demonstrate that as the sodium concentration increased, the calcium concentration decreased and the silica concentration increased. This can be seen in the plot of CNLSH, Figure 4.32, and CNMSM, Figure 4.36. The initial concentrations of silica and calcium hydroxide are then same for these two mixes, but the initial sodium hydroxide concentration was changed from 0.30M to 0.42M. The silicon ion concentration in the solution was higher when there was a higher sodium concentration. At six months, Macphee et al. experienced the calcium and silicon ion concentrations lowering. This experimental program had a shorter testing period and thus it is unknown if the solutions would eventually experience lowering concentrations in the solution.

In this study, the silica dissolved faster than it reacted with the calcium and sodium. Leeman et al. encountered the opposite effect. They found that the silica concentration increased considerably once all of the calcium was consumed; indicating that the rate determining step was the dissolution. It is possible that this difference was caused by the ratio of solids to liquids in the experiments. Leeman et al. had a mass ratio of 1:2 between the solids and the solution, this experiment was close 1:200.

6 Conclusions and Recommendations

6.1 Conclusions

6.1.1 Dissolution of Silica

There are several conclusions that can be drawn from studying the dissolution of silica in the alkaline solutions.

1. The rate of dissolution is proportional to the pH level and the quantity of sodium in the solution. These conclusions cannot be separated because the two are coupled.
2. Adding calcium hydroxide to a solution causes the rate that silicon is entering the solution to decrease. This was caused by the calcium ions reacting with the silicate ions in the solution, which decreased the concentration.
3. The dissolution of silica first has a stagnant period that lasted approximately one week when there were calcium ions in the solution. This period was shorter for solutions containing higher sodium ion concentrations.
4. Silica powder dissolves at a faster rate in a sodium hydroxide solution than the Hixson-Crowell cubic root law predicts. The alkali ions act as additional catalysts for the dissolution process.
5. For most of the solutions studied, the dissolution rate is proportional to the quantity of silica that was added to the solution. This is due to a higher surface area of silica being attacked by the hydroxide and alkali ions.

6.1.2 Reaction of Silica with Calcium Hydroxide and Sodium Hydroxide

The following conclusions can be made concerning the reaction products that are formed in the reaction between silica and calcium hydroxide and sodium hydroxide.

1. The rate of the reaction between calcium and silica is determined by the rate of silica dissolution. This is observed in the concentration vs. time plots when the calcium ions are exiting the solution faster than the silica is entering the solution.
2. When the pH is sufficiently low and the concentration of silica is low, reaction rims are able to form causing C-S-H products. The solutions that produced C-S-H had a pH of 13.48, and initial silica concentrations of

0.115M and 0.134M. Solutions with lower pH levels were not tested for the three component systems.

3. The solutions containing pH levels higher than 13.48 formed products similar in composition to ASR, however the silica continued to dissolve. The silica was able to dissolve readily, forming products with extremely low silica concentrations and very high sodium concentrations. Therefore, if ASR is to be prevented, the pH of the pore solution should be kept below this level.
4. Sodium hydroxide and silica do not react as readily as calcium hydroxide and silica solutions. The calcium ions can be seen to exit the solution rapidly while the sodium ions remain high for the duration of the experiment.

6.2 Future Research

To continue this research, the following recommendations can be identified for future work:

1. This experiment should be repeated with larger size particles to study the impact of the size of particle on the dissolution rate and the products formed. When the concentration is held constant and the size of particle increases, the surface area will decrease. It is expected that the dissolution rate would decrease with increasing particle size.
2. The use of glass particles instead of pure silica should be studied to understand the impact of chemical impurities on the dissolution rate of the particles. It is known that the impurities decrease the resistance to chemical attack, thus it is expected that the dissolution rate will be higher.
3. It is necessary to study the impact of different colours of glass on the products formed. In past studies, the colour of glass has greatly impacted whether a concrete mix has expanded past ASTM limits. The colours are created from different chemical impurities and they will alter the composition of the final reaction products.
4. A model should be created that relates the size of particle, the initial composition of the pore solution and the composition of the glass to the final reaction products. This should be able to predict whether the

ground recycled glass particles will form an ASR or C-S-H type product in a specific concrete mix.

7 References

Alexander, G., Heston, W., & Iler, R. (1954). The Solubility of Amorphous Silica in Water. *The Journal of Physical Chemistry , 58* (6), 453-455.

Alfa Aesar. (2013). *Silicon (IV) Oxide, 99.5%*. Retrieved September 2013, from Alfa Aesar: http://www.alfa.com/en/gp100w.pgm?dsstk=013024

Barret, P., Ménétrier, D., & Cottin, B. (1977). Study of silica-lime solution reactions. *Cement and Concrete Research , 7*, 61-68.

Box, G. E., Hunter, J. S., & Hunter, W. G. (2005). *Statistics for Experimenters; Design, Innovation and Discovery* (2nd ed.). John Wiley & Sons Inc.

Bray, C. (2001). *Dictionary of Glass: Materials and Techniques* (2nd ed.). London: A & C Black.

Chatterji, S. (2005). Chemistry of alkali-silica reaction and testing of aggregates. *Cement & Concrete Composites , 27* (7-8), 788-795.

Chen, C., Habert, G., Bouzidi, Y., & Jullien, A. (2010). Environmental impact of cement production: detail of the different processes and cement plant variability evaluation. *Journal of Cleaner Production , 18* (5), 478-485.

Chidiac, S. E., & Mihaljevic, S. N. (2011). Performance of dry cast concrete blocks containing waste glass powder or polyethylene aggregates. *Cement and Concrete Composites , 33* (8), 855-863.

Cole-Parmer Canada Inc. (2012). *pH Electrode Selection Guide.* Retrieved June 2012, from Cole Parmer: http://www.coleparmer.ca/TechLibraryArticle/684

Cole-Parmer Canada Inc. (2012). *Thermo Scientific Orion Star A211 pH Benchtop Meter Only*. Retrieved June 2012, from Cole-Parmer: http://www.coleparmer.com/Product/Thermo_Scientific_Orion_Star_A211_pH_Benchtop_Meter_Only/EW-58825-22

De Jong, B. H., Beerkens, R. G., van Nijnatten, P. A., & Le Bourhis, E. (2011). Glass, 1. Fundamentals. In *Ullmann's Encyclopedia of Industrial Chemistry.*

Dhir, R. K., Dyer, T. D., & Tang, M. C. (2009). Alkali-silica reaction in concrete containing glass. *Materials and Structures , 2009*, 1451-1462.

Diamond, S. (1975). Long-Term Status of Calcium Hydroxide Saturation of Pore Solutions in Hardened Cements. *Cement and Concrete Research , 5*, 607-616.

Dove, P. M., & Rimstidt, J. D. (1994). Silica-Water Interactions. In P. J. Heaney, C. T. Prewitt, & G. V. Gibbs (Eds.), *Silica: Physical Behaviour, Geochemistry and Materials Applications* (Vol. 29, pp. 259-308). Washington, D.C.: Mineralogical Society of America.

Dron, R., & Brivot, F. (1993). Thermodynamic and Kinetic Approach to the Alkali-Silica Reaction. Part 2: Experiment. *Cement and Concrete Research , 23*, 93-103.

EDM Millipore. (2013). *Calcium hydroxide.* Retrieved September 2013, from EDM Millipore: http://www.emdmillipore.com/is-bin/INTERSHOP.enfinity/WFS/Merck-CA-Site/en_CA/-/USD/ViewPDF-Print.pdf?RenderPageType=ProductDetail&CatalogCategoryID=&ProductUUID=J0CsHfETFiMAAAE2JilwtCIm&PortalCatalogUUID=KvSb.s1Ob48AAAEgr9B6cjOt

EDM Millipore. (2013). *Sodium hydroxide solution.* Retrieved September 2013, from EDM Millipore: http://www.emdmillipore.com/is-bin/INTERSHOP.enfinity/WFS/Merck-CA-Site/en_CA/-/USD/ViewPDF-Print.pdf;sid=qDiZk-eYl3-ek7Xf6Dn0xE9YL7uLY40_kBaHxVQ1ikwn8GkWhNj6OeGmv2MULszhKEuJj-RBVQCwlG5RCrwseEjSicyA1ytIm6Ihsl-B4wYVmY0_kBYhsl-B?RenderPageType=ProductDetail

El-Shimy, E., Abo-El-Enein, S. A., El-Didamony, H., & Osman, T. A. (2000). Physico-Chemical and Thermal Characteristics of Lime-Silica Fume Pastes. *Journal of Thermal Analysis and Calorimetry , 60*, 549-556.

Federico, L. M., & Chidiac, S. E. (2009). Waste glass as a supplementary cementitious material in concrete – Critical review of treatment methods. *Cement and Concrete Composites , 31* (8), 606-610.

Federico, L. M., Chidiac, S. E., & Raki, L. (2011). Reactivity of cement mixtures containing waste glass using thermal analysis. *Journal of Thermal Analysis and Calorimetry , 104* (3), 849-858.

Fertani-Gmati, M., & Jemal, M. (2011). Thermochemistry and kinetics of silica dissolution in NaOH aqueous solution. *Thermochemica Acta , 513*, 43-48.

Greenberg, S. (1961). Reaction Between Silica and Calcium Hydroxide Solutions: I. Kinetics in the Temperature Range 30 to 85°. *The Journal of Physical Chemistry , 65* (1), 12-16.

Greenberg, S. (1957). The Depolymerization of Silica in Sodium Hydroxide Solutions. *The Journal of Physical Chemistry , 61* (7), 960-965.

Greenberg, S., & Copeland, L. (1960). The Thermodynamic Functions for the Soltuion of Calcium Hydroxide in Water. *The Journal of Physical Chemistry , 64* (8), 1057-1059.

Hixson, A. W., & Crowell, J. H. (1931). Dependence of Reaction Velocity upon Surface and Agitation. *Industrial & Engineering Chemistry , 23* (8), 923-931.

Ichikawa, T. (2009). Alkali-silica reaction, pessimum effects and pozzolanic effect. *Cement and Concrete Research , 39*, 716-726.

Ichikawa, T., & Miura, M. (2007). Modified model of alkali-silica reaction. *Cement and Concrete Research , 37*, 1291-1297.

Idir, R., Cyr, M., & Tagnit-Hamou, A. (2011). Pozzolanic properties of fine and coarse color-mixed glass cullet. *Cement & Concrete Composites , 33* (1), 19-29.

Idir, R., Cyr, M., & Tagnit-Hamou, A. (2010). Use of fine glass as ASR inhibitor in glass aggregate mortars. *Construction and Building Materials , 24*, 1309-1312.

Iler, R. K. (1979). *The Chemistry of Silica.* Toronto: John Wiley & Sons.

International Energy Agency. (2006). *Energy Technology Perspectives 2006.*

Ismail, Z. Z., & Al-Hashmi, E. A. (2009). Recycling of waste glass as a partial replacement for fine aggregate in concrete. *Waste Management , 29*, 655-659.

Jain, J., & Neithalath, N. (2009). Physico-chemical changes in nano-silica and silica fume modified cement pastes in response to leaching. *International Journal of Materials and Structural Integrity* , 114-133.

Kalousek, G. L. (1944). Studies of Portions of the Quaternary System Soda-Lime-Silica-Water at 25°C. *Journal of Research of the National Bureau of Standards , 32*, 285-302.

Kawamura, M., & Fuwa, H. (2003). Effects of lithium salts on ASR gel composition and expansion of mortars. *Cement and Concrete Research , 33* (6), 913-919.

Kim, J. J., Foley, E. M., & Reda Taha, M. M. (2013). Nano-mechanical characterization of synthetic calcium-silicate-hydrate (C-S-H). *Cement & Concrete Composites , 36*, 65-70.

Kouassi, S. S., Andji, J., Bonnet, J.-P., & Rossignol, S. (2010). Dissolution of waste glass in highly alkaline solutions. *Ceramics-Silikáty , 54* (3), 235-240.

Leemann, A., Le Saout, G., Winnefeld, F., Rentsch, D., & Lothenbach, B. (2011). Alkali-Silica Reaction: the Influence of Calcium on Silica Dissolution and the Formation of Reaction Products. *Journal of the American Ceramic Society , 94* (4), 1243-1249.

Macphee, D. E., Luke, K., Glasser, F. P., & Lachowski, E. E. (1989). Solubility and Aging of Calcium Silicate Hydrates in Alkaline Solutions at 25°C. *Journal of the American Ceramic Society , 72* (4), 646-654.

Maraghechi, H., Shafaatian, S.-M.-H., Fischer, G., & Rajabipour, F. (2012). The role of residual cracks on alkali-silica reactivity of recycled glass aggregates. *Cement & Concrete Composites , 34* (1), 41-47.

Mehta, P. K., & Monteiro, P. J. (2006). *Concrete: Microstructure, Properties, and Materials* (3rd ed.). New York: McGraw-Hill.

Niibori, Y., Kunita, M., Tochiyama, O., & Chida, T. (2000). Dissolution rates of amorphous silica in highly alkaline solution. *Journal of Nuclear Science and Technology , 37* (4), 349-357.

O'Connor, T. L., & Greenberg, S. A. (1958). The Kinetics for the Solution of Silica in Aqueous Solutions. *The Journal of Physical Chemistry , 62* (10), 1195-1198.

Park, S. B., Lee, B. C., & Kim, J. H. (2004). Studies on mechanical properties of concrete containing waste glass aggregate. *Cement and Concrete Research , 34*, 2181-2189.

Park, S.-B., & Lee, B.-C. (2004). Studies on expansion properties in mortar containing waste glass and fibres. *Cement and Concrete Research , 34*, 1145-1152.

Paul, A. (1982). *Chemistry of Glasses.* New York: Chapman and Hall.

Rajabipour, F., Maraghechi, H., & Fisher, G. (2010). Investigating the Alkali-Silica Reaction of Recycled Glass Aggregates in Concrete Materials. *Journal of Materials in Civil Engineering , 22* (12), 1201-1208.

Romeo, L. M., Catalina, D., Lisbona, P., Lara, Y., & Martínez, A. (2011). Reduction of greenhouse gas emissions by integration of cement plants, power plants, and CO2 capture systems. *Greenhouse gases: science and technology , 1* (1), 72-82.

Schwarz, N., & Neithalath, N. (2008). Influence of a fine glass powder on cement hydration: Comparison to fly ash and modeling the degree of hydration. *Cement and Concrete Research , 38*, 429-436.

Shao, Y., Lefort, T., Moras, S., & Rodriguez, D. (2000). Studies on concrete containing ground waste glass. *Cement and Concrete Research , 30*, 91-100.

Shaw, W. M., & MacIntire, W. H. (1930). The Nature of Calcium Hydroxide Absorption by Hydrated Silica. *Soil Science , 29* (6), 429-456.

Shi, C., Wu, Y., Riefler, C., & Wang, H. (2005). Characteristics and pozzolanic reactivity of glass powders. *Cement and Concrete Research , 35*, 987-993.

Sjöberg, S. (1996). Silica in aqueous environments. *Journal of Non-Crystalline Solids , 196*, 51-57.

Stanton, T. E. (1940). Expansion of Concrete Through Reaction Between Cement and Aggregate. *Proceedings of the ASCE , 66* (10), 1781-1811.

TA Instruments. (2013). *Advantage Software*. Retrieved August 27, 2013, from TA Instruments: http://www.tainstruments.com/main.aspx?id=292&n=2&siteid=11

TA Instruments. (2013). *Q600*. Retrieved August 27, 2013, from TA Instruments: http://www.tainstruments.com/product.aspx?id=22&n=1&siteid=11

Thaulow, N., Hjorth Jakobsen, U., & Clark, B. (1996). Composition of Alkali Silica Gel and Ettringite in Concrete Railroad Ties: SEM-EDX and X-Ray Diffraction Analysis. *Cement and Concrete Research , 26* (2), 309-318.

Thornton, S. D., & Radke, C. J. (1988). Dissolution and Condensation Kinetics of Silica in Alkaline Solution. *SPE Reservoir Engineering , 3* (2), 743-752.

Varian. (2013). *ICP-OES.* Retrieved August 27, 2013, from Varian Vista-MPX CCD Simultaneous ICP-OES: http://www.colloidalsciencelab.com/fact_pages/Varian-MPX.pdf

Way, S., & Shayan, A. (1992). Study of Some Synthetically Prepared Hydrous Alkali Calcium Silicates. *Cement and Concrete Research , 22*, 915-926.

Wirth, G. S., & Gieskes, J. M. (1978). The Initial Kinetics of the Dissolution of Vitreous Silica in Aqueous Media. *Journal of Colloid and Interface Science , 68* (3), 492-500.

World Business Council for Sustainable Development. (2002). *Toward a Sustainable Cement Industry.*

Wright, M. R. (2007). *An Introduction to Aqueous Electrolyte Solutions.* Chichester, England: John Wiley & Sons Ltd.

Zhang, Q., & Ye, G. (2012). Dehydration kinetics of Portland cement paste at high temperature. *Journal of Thermal Analysis and Calorimetry , 110*, 153-158.